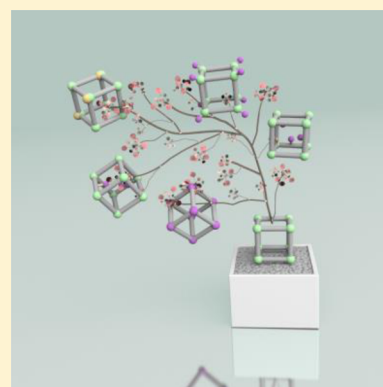


Metal–Organic Frameworks for Heterogeneous Basic Catalysis

Li Zhu,[†] Xiao-Qin Liu,[†] Hai-Long Jiang,[‡] and Lin-Bing Sun^{*,†}[†]State Key Laboratory of Materials-Oriented Chemical Engineering, Jiangsu National Synergetic Innovation Center for Advanced Materials (SICAM), College of Chemistry and Chemical Engineering, Nanjing Tech University, Nanjing 210009, China[‡]Department of Chemistry, Hefei National Laboratory for Physical Sciences at the Microscale, University of Science and Technology of China, Hefei, Anhui 230026, China

ABSTRACT: Great attention has been given to metal–organic frameworks (MOFs)-derived solid bases because of their attractive structure and catalytic performance in various organic reactions. The extraordinary skeleton structure of MOFs provides many possibilities for incorporation of diverse basic functionalities, which is unachievable for conventional solid bases. The past decade has witnessed remarkable advances in this vibrant research area; however, MOFs for heterogeneous basic catalysis have never been reviewed until now. Therefore, a review summarizing MOFs-derived base catalysts is highly expected. In this review, we present an overview of the recent progress in MOFs-derived solid bases covering preparation, characterization, and catalytic applications. In the preparation section, the solid bases are divided into two categories, namely, MOFs with intrinsic basicity and MOFs with modified basicity. The basicity can originate from either metal sites or organic ligands. Different approaches used for generation of basic sites are included, and each approach is described with representative examples. The fundamental principles for the design and fabrication of MOFs with basic functionalities are featured. In the characterization section, experimental techniques and theoretical calculations employed for characterization of basic MOFs are summarized. Some representative experimental techniques, such as temperature-programmed desorption of CO₂ (CO₂-TPD) and infrared (IR) spectra of different probing molecules, are covered. Following preparation and characterization, the catalytic applications of MOFs-derived solid bases are dealt with. These solid bases have potential to catalyze some well-known “base-catalyzed reactions” like Knoevenagel condensation, aldol condensation, and Michael addition. Meanwhile, in contrast to conventional solid bases, MOFs show some different catalytic properties due to their special structural and surface properties. Remarkably, characteristic features of MOFs-derived solid bases are described by comparing with conventional inorganic counterparts, keeping in mind the current opportunities and challenges in this field.



CONTENTS

1. Introduction	8130	4.5. Transesterification Reaction	8159
2. Generation of Basic Sites	8131	4.6. Cycloaddition Reaction	8160
2.1. MOFs with Intrinsic Basicity	8131	4.7. One-Pot Cascade Reaction	8163
2.1.1. Basicity from Alkaline Earth Metal Sites	8131	5. Characteristic Features of MOFs-Derived Solid Bases	8164
2.1.2. Basicity from Hybrid Metal Nodes	8133	5.1. Preparation	8164
2.1.3. Basicity from N-Containing Ligands	8134	5.2. Activation	8164
2.1.4. Basicity from Structural Phenolates	8138	5.3. Basic Properties	8164
2.2. MOFs with Modified Basicity	8139	6. Summary and Perspectives	8165
2.2.1. Functionalization of Metal Sites	8139	Author Information	8166
2.2.2. Functionalization of Ligands	8142	Corresponding Author	8166
3. Characterization of Basic Sites	8145	ORCID	8166
3.1. Experimental Techniques	8145	Notes	8166
3.1.1. CO ₂ -TPD	8145	Biographies	8166
3.1.2. IR of Adsorbed CO ₂	8146	Acknowledgments	8166
3.1.3. IR of Adsorbed Pyrrole	8146	Abbreviations	8166
3.1.4. Propyne Adsorption	8147	Chemicals Including Ligands	8166
3.2. Theoretical Calculations	8148	Common Terminology	8167
4. Catalytic Applications	8149	References	8167
4.1. Knoevenagel Condensation	8149		
4.2. Aldol Condensation	8153		
4.3. Michael Addition	8156		
4.4. Henry Reaction	8157		

Received: February 10, 2017

Published: May 25, 2017

1. INTRODUCTION

Interest in the development of heterogeneous catalysts has undergone a marked increase in recent years.^{1–3} As an important group of heterogeneous catalysts, solid bases have attracted great attention because they possess a series of merits over their liquid analogues.^{4–6} By using solid bases, instead of stoichiometric amounts of liquid bases, the overall atom efficiency of reactions is improved and the turnover number (TON) of catalysts is enhanced. Solid bases are far less corrosive and lead to scarcer treatment problems. Moreover, the recovery of products and the separation of catalysts after reactions become easy, and thus, it is convenient to reuse the catalysts.^{7–10} Therefore, solid bases provide an economic and environmentally friendly approach to synthesize chemicals, which is extremely desirable for green chemistry and sustainable development but difficult to realize by use of conventional liquid base catalysts.

In comparison with their counterparts, solid acids, relatively less attention has been given to solid bases. Nevertheless, solid bases play an important role in many organic reactions, which vary from Knoevenagel condensation and aldol condensation to Michael addition and transesterification reaction, to name just a few. Some of these reactions are crucial for the synthesis of organic intermediates and fine chemicals.^{7,8,11–13} For the effective utilization of solid bases as heterogeneous catalysts, a case in point is the preparation of 4-methylthiazole (4-MT). 4-MT is an important starting material for the synthesis of the fungicide thiabendazole. Traditionally, the preparative route involves five-step reactions, and several hazardous chemicals are employed.¹⁴ The multistep process initiates from the reaction of chlorine with acetone (to yield the intermediate chloropropanone) and the reaction of carbon disulfide with ammonia (to yield the intermediate ammonium dithiocarbamate). The reaction of two intermediates gives 4-methylthiazole-2-thiol, which then reacts with NaOH followed by oxidation to form the target product 4-MT. It is worth noting that the preparative route can be diminished from traditional five steps to two steps in the presence of a solid base (namely, the Cs-containing zeolite). The most important part of this new route is the preparation of 4-MT through the reaction between the imine and the sulfur dioxide catalyzed by the solid base. Apparently, the preparative route is greatly shortened, and some hazardous chemicals (such as chlorine and carbon disulfide) are evaded by utilizing the solid base as a catalyst. Dating back to the 1950s, Pines et al. prepared a material by depositing metallic sodium on alumina, which is the first report of solid bases and initiates the investigation of this kind of material.¹⁵ With the development of synthetic methods and characterization techniques, a huge amount of solid bases have been reported from then on. Introduction of basic species to porous supports is a regular method for the preparation of solid bases. Thus far, various materials have been employed as supports for solid bases, and the supports range from inorganic materials (such as alumina, zeolites, and mesoporous silicas)^{16–21} to organic ones (such as porous organic polymers).^{22–28} Apparently, supports have a significant effect on the surface properties and the catalytic activity of resultant solid bases.

Metal–organic frameworks (MOFs),^{29–32} also called porous coordination polymers (PCPs)^{33–35} or porous coordination networks (PCNs),^{36–38} are organic–inorganic hybrids assembled from metal ions (or clusters) and organic ligands.

MOFs not only combine the respective beneficial characteristics of inorganic and organic components but also often exhibit unique properties that exceed the expectations for a simple mixture of the components.^{39–48} Early efforts in this research area were mainly devoted to the synthesis of new materials;^{49–56} however, in recent years the search for potential applications has been a topic of much interest.^{57–61} Owing to their special characteristics such as hybrid compositions, adjustable functionality, and diverse structure, MOFs are of pronounced interest for various applications such as separation, sensing, and catalysis.^{62–72} The occurrence of MOFs opens up new opportunities for the development of solid bases. MOF-derived solid bases are of great significance from both fundamental and practical points of view. In contrast to the traditional solid bases, MOFs can incorporate different types of basic sites into both metal nodes and organic ligands, leading to the fabrication of a range of base catalysts with special characteristics. To date, various MOF-derived solid bases have been reported. The origin of basicity varies from inorganic species to organic ones, and the basic functionalities can be introduced by either direct synthesis or postsynthetic modification.^{73–75} The structure of basic MOFs is tunable through the judicious selection of metal centers and organic ligands, which shows almost infinite variations theoretically. Both metal centers and organic ligands in MOFs are facile for introduction of basic functionalities; moreover, these connections are plentiful, site isolated, and periodically organized. As a result, MOFs bring a great deal of opportunities for the development of new solid bases with characteristic features which are unachievable by traditional porous materials. The obtained MOFs with basic functionalities are able to catalyze an assortment of organic reactions including Michael addition, Knoevenagel condensation, transesterification, etc. Recent studies also show that MOF-derived solid bases can be applied in the field of energy and environment such as preparation of biodiesel⁷⁶ and chemical fixation of CO₂.^{77,78} The past decade has witnessed rapid progress in MOF-derived solid bases. MOFs with various functionalities for applications including separation,⁷⁹ sensing,⁸⁰ photochemistry,⁸¹ and energy storage^{82,83} have been summarized recently. Very recently, a review on Brønsted acidity in MOFs was published in *Chemical Reviews*.⁸⁴ To the best of our knowledge, however, MOFs for heterogeneous basic catalysis have never been reviewed to date. Therefore, a review summarizing MOF-derived base catalysts is highly expected.

In this paper, we provide a comprehensive review of MOF-derived solid bases, summarizing recent advances from various research groups and ours. Different methods that were utilized to incorporate basic sites into MOFs are covered, and each method is described with representative examples. The fundamental principles for the design and synthesis of basic MOFs are featured. The generation mechanism of basic sites on MOFs is discussed. Different approaches, including experimental techniques and theoretical calculations, applied to characterize the basicity of MOFs are presented. Afterward, applications of MOFs in heterogeneous basic catalysis are given. Noteworthily, characteristic features of basic MOFs are discussed and compared with that of traditional solid bases, bearing in mind the current opportunities and challenges in MOF-derived solid bases. It is expected that this review would raise interest in gaining fundamental understanding of MOF-derived solid bases and assist in the judicious design and construction of novel heterogeneous basic catalysts.

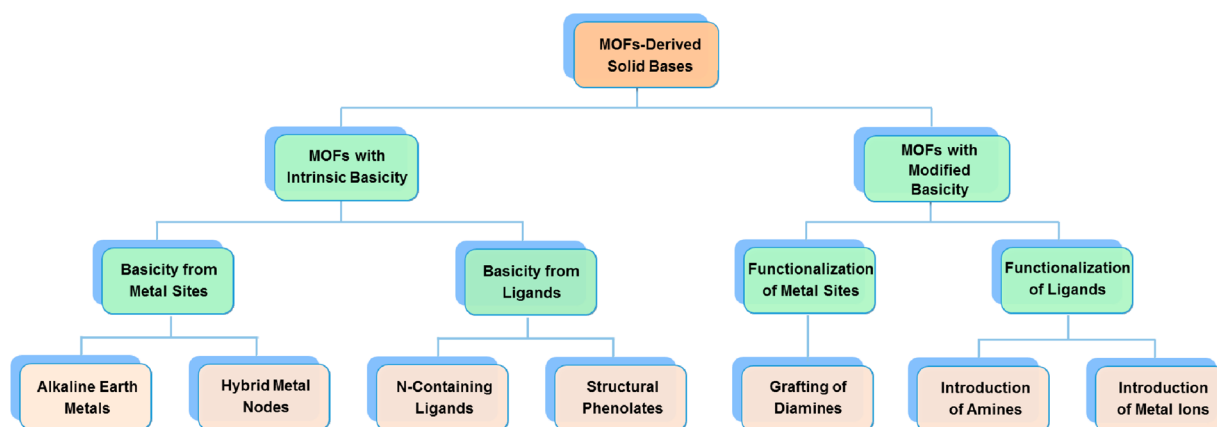


Figure 1. Classification of basic MOFs and typical methods for generation of basicity on MOFs.

2. GENERATION OF BASIC SITES

Thus far, various approaches have been developed for the generation of basic sites on MOFs, leading to the production of a series of MOFs-derived solid bases. These solid bases can be generally divided into two classes, namely, (i) MOFs with intrinsic basicity and (ii) MOFs with modified basicity (Figure 1). For the first class, MOFs are obtained from the self-assembly of special metal ions and/or functional ligands, and the resultant MOFs possess intrinsically basic frameworks. A well-known example is IRMOF-3, $\text{Zn}_4\text{O}(\text{NH}_2\text{-BDC})_3$, that assembled from $\text{Zn}(\text{NO}_3)_2$ and 2-aminoterephthalic acid ($\text{NH}_2\text{-BDC}$);⁸⁵ the ligands containing amino groups endow the frameworks with basicity.⁸⁶ For the second class, the synthetic MOFs are not basic in nature and further modification is required. For example, basic species ethylenediamine (ED) can be grafted onto the coordinatively unsaturated metal sites (CUSs) of MIL-101(Cr), $\text{Cr}_2(\text{F},\text{OH})(\text{H}_2\text{O})_2\text{O}(\text{BDC})_3$; this leads to the fabrication of solid base MIL-101(Cr)-ED, and the pendent groups play the role of immobilized basic sites.⁸⁷ For clarity, a MOF functionalized through CUSs with R groups is denoted as MOF-R in this review, while that functionalized through ligands is denoted as R-MOF. This section covers two categories for the fabrication of basic MOFs, that is, MOFs with intrinsic basicity due to special metal ions and/or functional ligands as well as MOFs functionalized with basic species after synthesis.

2.1. MOFs with Intrinsic Basicity

According to the composition of MOFs, basicity may originate from either metal ions or ligands. Metal ions that act as the catalytically active sites become the first consideration. The metal centers can not only perform as Lewis acid sites but also act as basic sites, which depends on their type. For metal centers, two main aspects should be taken into account. The first one is the alkaline earth metal, such as Mg, Ca, Sr, and Ba. Certain alkaline earth metal MOFs, which possess high dispersion of metal–oxygen or metal–hydroxide strands, may provide a starting point for imparting basic catalytic activity to these MOFs. The second one is the hybrid metal node. Because a charge polarization will be induced on the hybrid metal nodes, the activity of the unsaturated metal sites may be enhanced. Apart from the intrinsic basicity from metal sites, the basicity can also come from organic ligands. There are generally two kinds of ligands that can create basicity. The first one is N-containing ligands (for instance, $\text{NH}_2\text{-BDC}$), which is the broadest selection for the formation of basic sites. The other

one exhibits the potentially available basic sites arising from structural phenolates. In this subsection, various explorations of basicity on MOFs stemmed from metal ions and ligands are dealt with. In the case of metal ions, alkaline earth metals and hybrid metal nodes are covered. For organic ligands, N-containing ligands and structural phenolates are described in sequence.

2.1.1. Basicity from Alkaline Earth Metal Sites. In MOFs the high density of exposed metal sites has been widely used in the catalytic field as Lewis acid centers. Compared with the acidity of metal sites, research on the basicity comes out somewhat later. Taking into account that alkali metal oxides^{88–93} and alkaline earth metal oxides^{94–102} are well-known basic species, attention has been given to the fabrication of basic MOFs by using these metal ions as nodes. In general, MOFs assembled from alkali metal ions are limited, due to the stability issue (see ref 103 and literature cited therein). MOFs based on various alkaline earth metal ions has been successfully fabricated, which include Mg,^{104–106} Ca,^{107–110} Sr,^{108,109,111,112} and Ba.^{108,110,113,114}

MgO is a benchmark solid base, and the synthesis of Mg-based MOFs is thus attempted. An Mg-based carboxylate framework, $\text{Mg}_3(\text{PDC})(\text{OH})_3(\text{H}_2\text{O})_2$, was constructed from $\text{Mg}(\text{NO}_3)_2$ and 3,5-pyrazoledicarboxylic acid (H_3PDC) in water at 170 °C for 3 days.¹⁰⁶ The structure shows three Mg centers in the asymmetric unit, and all Mg centers have distorted octahedral geometry. A secondary building unit (SBU) is the Mg_3 triad (Figure 2). An edge is shared by the Mg_3 centers and the Mg_1 centers, and the Mg_3 centers are bonded with the Mg_2 centers as well, leading to the formation of a three-dimensional (3D) framework. This MOF can be represented as I^0O^3 in terms of its connectivity. The result of N_2 adsorption demonstrates the microporosity of $\text{Mg}_3(\text{PDC})(\text{OH})_3(\text{H}_2\text{O})_2$, and the Brunauer–Emmett–Teller (BET) surface area is $450 \text{ m}^2\text{g}^{-1}$.¹⁰⁶ To examine the basicity of $\text{Mg}_3(\text{PDC})(\text{OH})_3(\text{H}_2\text{O})_2$, the aldol condensation reactions of aromatic aldehydes with acetone were employed.¹⁰⁶ At temperatures between 5 and 10 °C, the product benzylideneacetone can be obtained. For example, the reaction of *p*-, *o*-, and *m*-nitrobenzaldehyde with acetone gave the corresponding β -aldol products with 94, 82, and 76 wt % of the isolated yield, respectively. To confirm the heterogeneous process, a hot filtration exam was conducted when the reaction was 30–40% completed.¹⁰⁶ No product was yielded after further reaction under the same conditions, which implies no leaching of basic species from the MOF catalyst. In addition, the stability of this

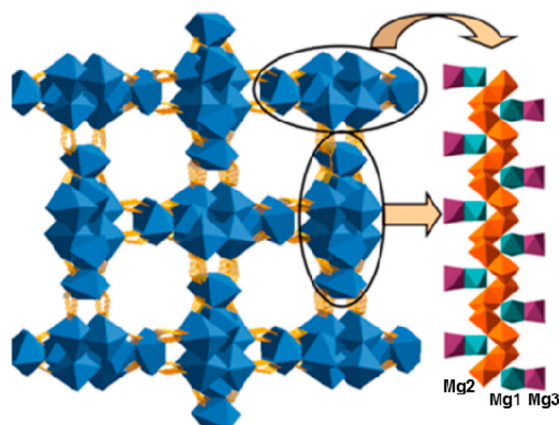


Figure 2. Schematic structure of $\text{Mg}_3(\text{PDC})(\text{OH})_3(\text{H}_2\text{O})_2$, depicting the fabrication of the Mg_3 triad SBU and a one-dimensional (1D) helical chain produced by the edge sharing of Mg_2 centers. Reproduced with permission from ref 106. Copyright 2012 Wiley-VCH.

Mg-based MOF was quite good, and the catalyst could be recovered by simple filtration and reused a couple of times with good maintenance of activity.

In addition to Mg, Ba is also able to assemble with the same ligand, H_3PDC , affording a new 3D alkaline earth MOF, $\text{Ba}(\text{PDC})\text{H}_2\text{O}$.¹¹⁵ In this Ba-based MOF, each alkaline earth metal ion is coordinated with one N atom and eight O atoms. Each ligand coordinates to six metal centers via two carboxylate groups, each of which adopts a $\mu_3\text{-}\eta_2\text{:}\eta_1$ -bridging coordination mode to give a 3D framework. Aldol condensation reactions were also used to evaluate the basicity of the Ba-based MOF.¹¹⁵ In contrast to its Mg-based counterpart, the Ba-based MOF showed superior catalytic activity under similar reaction conditions. The respective isolated yield of β -aldol product is 96, 90, and 80 wt % for the reaction of *p*-, *o*-, and *m*-nitrobenzaldehyde with acetone over the Ba-based MOF, which is higher than that over the Mg-based MOF (82, 77, and 70 wt %, respectively).¹¹⁵ It is known that the base strength of alkaline earth metal oxides decreases in the order $\text{BaO} > \text{SrO} > \text{CaO} > \text{MgO}$. The identical sequence of activity for Mg- and Ba-based MOFs indicates that alkaline earth metals are involved in the heterogeneous basic catalysis.

A systematic study on the formation of basic sites in alkaline earth MOFs was carried out by De Vos's group.⁴ The investigation concentrated on the Ba-based MOF possessing the structure $\text{Ba}_2(\text{BTC})(\text{NO}_3)(\text{DMF})$,¹¹³ where the ligand H_3BTC is 1,3,5-benzenetricarboxylic acid and the solvent DMF is *N,N'*-dimethylformamide. The Ba–O–Ba bonds in $\text{Ba}_2(\text{BTC})(\text{NO}_3)(\text{DMF})$ outspread in three dimensions, and the framework is symbolized as I^3O^0 . The inorganic SBUs and the organic ligands generate hexagonal prism-shaped crystals possessing three-leaf-clover-shaped pore channels running lengthwise through the crystals in the [001] direction (Figure 3A). The size of the broadest part of each pore is about 13 Å, while the size of the narrowest point is 6.5 Å. It is worthy of note that nitrate anions that keep charge neutrality exist in the structure (Figure 3B). Upon thermal activation, decomposition of nitrate anions leads to the formation of basic $\text{Ba}^{2+}\text{-O}^{2-}\text{-Ba}^{2+}$ species within the pores.

In order to obtain the most catalytically active state of the material, activation of $\text{Ba}_2(\text{BTC})(\text{NO}_3)$ was attempted at different temperatures.⁴ An elevated activation temperature

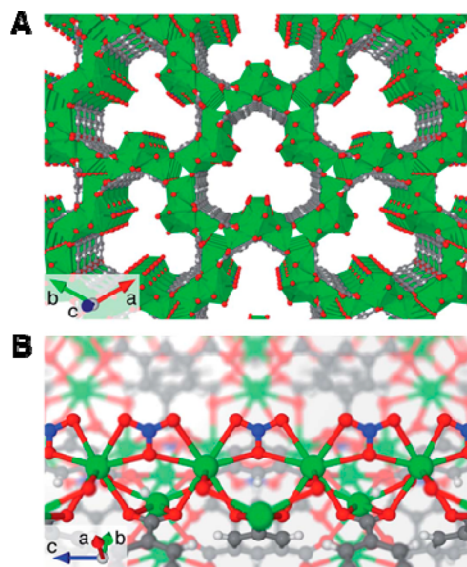


Figure 3. (A) Schematic structure of $\text{Ba}_2(\text{BTC})(\text{NO}_3)$, and (B) close view of the nitrate chain running along the MOF pores. Color scheme: for Ba atoms, green; for N atoms, blue; for O atoms, red; for C atoms, gray; for H atoms, white. Reproduced with permission from ref 4. Copyright 2014 Royal Society of Chemistry.

played a remarkable role in enhancing its basicity. By thermal treatment of the MOF overnight at 320 °C, the nitrate anions were well decomposed and resulted in replacement of two nitrate anions by one single O^{2-} anion (Figure 4A). In the

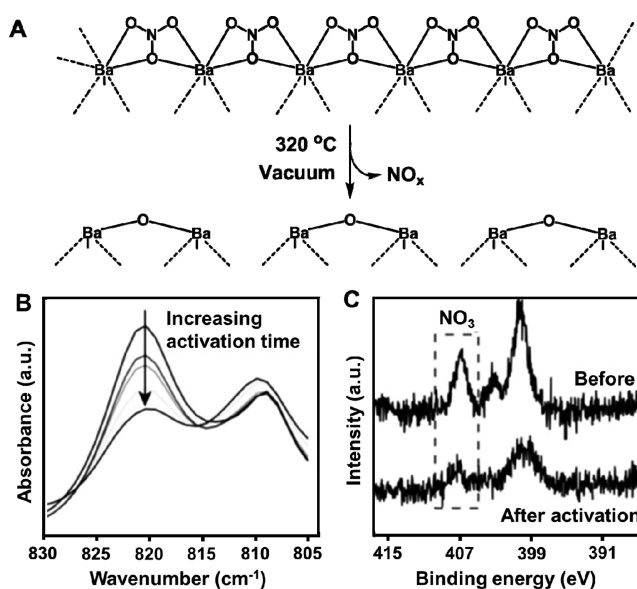


Figure 4. (A) Proposed pathway for generation of basic sites on the MOF $\text{Ba}_2(\text{BTC})(\text{NO}_3)$ after thermal treatment. (B) IR and (C) XPS of the nitrate anions upon thermal treatment. Adapted with permission from ref 4. Copyright 2014 Royal Society of Chemistry.

meanwhile, multiple low-coordination metal sites, $\text{Ba}^{2+}\text{-O}^{2-}\text{-Ba}^{2+}$ motifs, were produced as a new type of basic active sites. A comparison of the electron paramagnetic resonance (EPR) spectra before and after activation demonstrated the formation of new electron-rich active sites during activation. The results of fluorescence microscopy (FM) suggested that the basic sites were located in the pore channels of the MOF. The entire

activation process of $\text{Ba}_2(\text{BTC})(\text{NO}_3)$ was investigated by thermal gravimetric (TG) analysis equipped with a mass spectrometer (MS) detector.⁴ Physisorbed and chemisorbed DMF molecules were gradually released when the temperature was lower than 300 °C. As the temperature rose to 320 °C, NO_x species including NO, NO_2 , and N_2O were detected, which indicates the decomposition of nitrate in the pores.^{116,117} By combing the results of Fourier transform infrared (IR, Figure 4B) spectroscopy and X-ray photoelectron spectroscopy (XPS, Figure 4C), the loss of at least 70% of nitrate from the framework was observed. In terms of the results from colorimetric assay and inductively coupled plasma (ICP), an even higher nitrate loss (~85%) was detected. It should be stated that after activation, the loss of long-range order and the decrease of crystallinity of the material was reflected by the X-ray diffraction (XRD) data. The decomposition of structure-embedded nitrate may cause stress in the structure, and relaxation of the material leads to partial degradation of the framework. Similarly, basic sites can also be formed through thermal treatment of the Sr-variant $\text{Sr}_2(\text{BTC})(\text{NO}_3)$.^{4,111} Both Sr- and Ba-MOFs were active in the typical heterogeneous base-catalyzed reactions including Knoevenagel condensation and Michael addition.⁴ The order of activity for the activated Sr- vs Ba-MOFs was in line with the order of base strength for corresponding oxides (i.e., $\text{SrO} < \text{BaO}$).

In summary, the assembly of alkaline earth metals with proper ligands is a good approach to fabricate basic MOFs, considering that alkaline earth metal oxides are classic solid bases. The basicity of oxides is derived from low-coordination sites located at the corner and edge as well as on the surface. In the case of alkaline earth MOFs, the structural anions can be transformed to create defect sites, leading to the formation of a new type of basic sites which are uniformly dispersed in the structure. In comparison with the coordination chemistry of transition metals with ligands, less attention has been paid to the alkaline earth metal coordination frameworks and even less for alkali metals-based MOFs. This hinders the development of this kind of MOF-derived solid base. Although a certain amount of alkaline earth MOFs are constructed, the reports concerning their basicity are relatively scarce. One reason is that early studies are mainly focused on the preparation of materials rather than their applications. Another reason is that the basicity of MOFs is strongly dependent on the activation conditions. Typically one needs to pretreat the MOFs at relatively high temperatures aiming to expose the basic sites, which is different from the removal of solvents used for the traditional MOFs. Structural destruction is also possible if these MOFs are activated improperly. Further growth of this category of basic MOF relies on the development of synthetic techniques as well as appropriate activation methods.

2.1.2. Basicity from Hybrid Metal Nodes. With the purpose of producing catalytically active sites in MOFs, hybridization has been employed during the past decades. It is noticeable that most studies are focused on hybrid ligands.^{118–122} Very recently, some pioneering studies started to examine the possibility of hybrid metal nodes in MOFs.^{123–125} The employment of hybrid metal nodes during the self-assembly process has gradually become an effective approach, which is expected to obtain frameworks with more diverse performance compared to the use of only one type of metal.

To generate basicity on Cu–BTC, also recognized as HKUST-1 or $\text{Cu}_3(\text{BTC})_2(\text{H}_2\text{O})_3$, through hybridization,

tungsten (W) ions were selected due to the reasons that follows.¹²⁶ On one hand, W is active in CO_2 activation and inexpensive; on the other hand, incorporation of W into Cu–BTC should occur readily since W is in an identical group to Mo and Cr, and the synthesis of Mo–BTC¹²⁷ and Cr–BTC¹²⁸ with the same topology have been reported. A hybrid MOF, W–Cu–BTC, was designed by incorporating W ions into the frameworks of Cu–BTC on the basis of density functional theory (DFT) calculations.¹²⁶ When 50% of Cu ions were replaced by W ions, the triclinic crystalline structure slightly expanded because the W–Cu bond (2.74 Å) is longer than the Cu–Cu bond (2.57 Å). Simultaneously, the atomic binding energy rose from 6.69 (Cu) to 10.78 eV (W) on the basis of a cluster model, reflecting that the stability was enhanced. In order to create open W ions in W–Cu–BTC, the framework was heated at about 500 K; the six coordination of each W cation was reduced to five coordination. This means that the unsaturated W ions may be potential catalytically active sites. The data of CO adsorption show that CO molecules attract a small number of electrons from the exposed W ions, indicating that W ions function as Lewis base. This is different from the parent Cu–BTC and some other MOFs which lose electrons in CO adsorption.

To further reveal the basicity, the adsorption mode of the acidic molecule CO_2 on W–Cu–BTC was studied by calculating the electron density difference (EDD).¹²⁶ Five modes were considered as shown in Figure 5. The area around the open W ion was depleted of electrons, in contrast to the electron accumulation region surrounding the interacted O atom. In addition, the electron depletion around W and electron accumulation around C or O virtually overlapped in the activated complexes $\eta^1(\text{C})$, $\eta^2(\text{CO})$, and $\eta^2(\text{OO})$, which indicates that charge transfer occurs from W to CO_2 . This suggests that the exposed W ions in W–Cu–BTC act as strong Lewis bases in the activation process of CO_2 by transferring electrons from W ion to CO_2 . The frontier molecular orbital theory was employed to illustrate the interaction between CO_2 and the open metal ions in W–Cu–BTC.¹²⁶ The highest occupied molecular orbital (HOMO) of W–Cu–BTC is remarkably localized on the W $5d_z^2$ orbital along the W–Cu axis. On the basis of the principle of orbital symmetry matching, the lowest unoccupied molecular orbital (LUMO) of CO_2 interacts with the W $5d_z^2$ orbital between one C=O bond and the W ion in W–Cu–BTC by maximum overlapping. These results show that W–Cu–BTC is capable of activating CO_2 . Further studies according to the calculated IR and XPS results exhibit vibrational frequency and ionization energy shift of the adsorbed CO_2 as well. It should be stated that the parent Cu–BTC and 100% W-substituted Cu–BTC (namely, W–BTC) show no basic catalytic activity. The asymmetric W–Cu dimer in the hybrid node plays a vital role in the formation of basic sites owing to the unequal electron negativity.

In conclusion, the synthesis of hybrid MOFs with mixed metals is relatively infrequent in contrast to single metals. The parent MOFs with one type of metal usually reveal the Lewis acid nature of metal cations. Due to a charge polarization, Lewis base sites can be generated on the hybridizing metal nodes subjected to heat treatment. Obviously, such a mechanism is different from that of basicity derived from alkaline earth MOFs. It should be stated that the metals used for hybridization are crucial. For instance, Mo and Cr were also employed for hybridization, and Mo–Cu–BTC and Cr–Cu–BTC were formed, respectively.¹²⁶ The capacity on CO_2

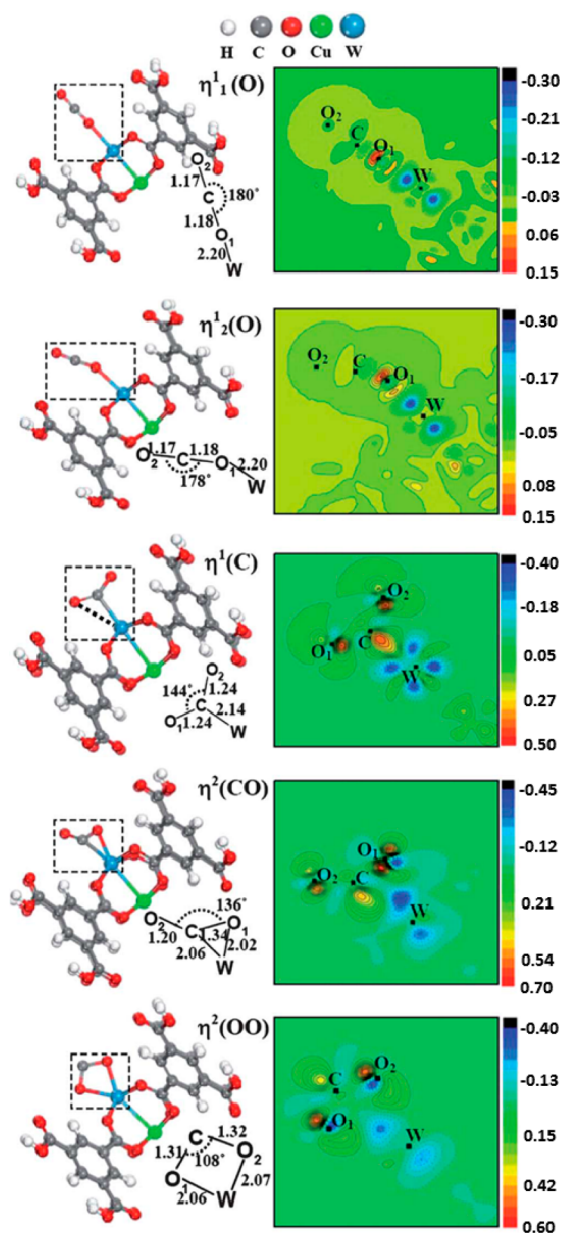


Figure 5. Structure and corresponding EDD of the five interaction modes between CO_2 and W-Cu-BTC . Geometry parameters in the dashed areas are given in the right corner of each mode. Selected plane of EDD consists of C, O, and W atoms (distances in Angstroms). Adapted with permission from ref 126. Copyright 2012 Royal Society of Chemistry.

activation of Mo-Cu-BTC and Cr-Cu-BTC is much weaker as compared with W-Cu-BTC . A significant increase or decrease in the amount of hybrid metals has an effect on basic properties because of the unequal electron negativity. A collection of recent reports demonstrates that the synthesis of hybrid MOFs can be achieved by utilizing either mixed substrates or postsynthetic exchange of metal ions. The development of synthetic techniques, in combination with the judicious choice of hybrid metals, makes it possible to fabricate a series of hybrid MOFs possessing basicity.

2.1.3. Basicity from N-Containing Ligands. One of the most attractive advantages of MOFs is the tunable functionality of organic ligands. Basicity can be introduced to MOFs by using basic N-containing ligands as building blocks.^{129–132} On one

hand, N-containing ligands can be employed, instead of their nonfunctional counterparts, for construction of MOFs. For example, IRMOF-1 (commonly known as MOF-5) is constructed from the ligand BDC, while replacement of BDC with $\text{NH}_2\text{-BDC}$ yields IRMOF-3, which shows basic properties.¹²⁰ On the other hand, partial substitution of original ligands with functional N-containing ones is an interesting alternative. For instance, the synthesis using mixed ligands consisting of both BDC and $\text{NH}_2\text{-BDC}$ leads to the formation of MIXMOFs (Table 1).^{133–139} This subsection describes the fabrication of basic MOFs via two ways, namely, complete utilization of N-containing ligands as well as partial substitution with N-containing ligands.

For the direct synthesis of basic MOFs, the most frequently used N-containing ligand is $\text{NH}_2\text{-BDC}$. Thus far, a range of metals (e.g., Zn,⁸⁶ Zr,¹³⁸ Al,¹⁴⁰ Fe,¹⁴² Ti,¹⁴⁸ and Cu¹⁵⁶) has been employed to assemble with $\text{NH}_2\text{-BDC}$, resulting in the formation of various MOFs as listed in Table 1. Due to the similarity of $\text{NH}_2\text{-BDC}$ with BDC, these basic MOFs show identical crystal structure to their nonsubstituted analogues (Figure 6). A detailed comparison of $\text{NH}_2\text{-UiO-66}$ with UiO-66 was made by De Vos's group.¹³⁶ The basic MOF $\text{NH}_2\text{-UiO-66}$ can be synthesized from ZrCl_4 and $\text{NH}_2\text{-BDC}$ under solvothermal conditions at 120 °C in DMF.¹³⁶ The synthetic conditions are the same as the preparation of UiO-66 except the simple substitution of BDC with $\text{NH}_2\text{-BDC}$ (Figure 7). In the XRD patterns, $\text{NH}_2\text{-UiO-66}$ presents quite similar diffraction peaks to UiO-66, indicating preservation of the original crystal structure (Figure 8).¹³⁶ The existence of amino groups does not lead to an obvious decrease in BET surface area, suggesting the highly accessible surface of both $\text{NH}_2\text{-UiO-66}$ and UiO-66. The scanning electron microscopy (SEM) images indicated that both $\text{NH}_2\text{-UiO-66}$ and UiO-66 showed small cubic crystals of around 100 nm. TG results indicated that $\text{NH}_2\text{-UiO-66}$ collapsed at 275 °C, which is lower than UiO-66 at temperatures above 450 °C. What is pleasantly surprising, the structure of $\text{NH}_2\text{-UiO-66}$ can be maintained for 3 months at 160 °C, which suggests that the material has long-term thermal stability. In terms of TG analysis of DMF-free $\text{NH}_2\text{-UiO-66}$ and UiO-66, they were moisture stable. Thus, a mild dehydration is necessary before initiating reactions with adsorbed organic compounds. The dehydration processes of these samples were examined by in situ IR. In the case of both $\text{NH}_2\text{-UiO-66}$ and UiO-66, the original IR spectra can be restored. These results, in combination with XRD follow-up, demonstrate that both materials keep intact during dehydration treatment.¹³⁶ In the heterogeneous catalytic synthesis of jasminaldehyde through condensation of heptanal and benzaldehyde, $\text{NH}_2\text{-UiO-66}$ exhibited higher activity with higher selectivity than UiO-66.¹³⁶ The examination of hot filtration confirmed that the catalytic activity was related to the solid exclusively and not to the liquid phase.

Similar to $\text{NH}_2\text{-UiO-66}$, IRMOF-3 can be synthesized by replacement of BDC with $\text{NH}_2\text{-BDC}$.⁸⁵ The amino-containing MOF shows interesting basic properties. The basicity of the aniline-like amino group is enhanced upon incorporation into the framework, which increases the $\text{p}K_a$ of basic catalyst and is more active than pure aniline.⁸⁶ For instance, in the Knoevenagel condensation, the conversion of benzaldehyde was almost double that of pure aniline after 2 h of reaction. In the optimized geometry, the benzene rings in IRMOF-3 lie in-plane with the zincocoxycarboxylate rings and are stabilized by an intramolecular hydrogen bond between the amino group and a

Table 1. Summary of Basic MOFs Constructed Directly from Various N-Containing Ligands

No.	MOF name and/or formula	metal salt	ligand	ligand structure	ref
1	IRMOF-3	Zn(NO ₃) ₂	2-aminoterephthalic acid (NH ₂ -BDC)		85,86
2	NH ₂ -UiO-66	ZrCl ₄	2-aminoterephthalic acid (NH ₂ -BDC)		77,134-139
3	NH ₂ -MIL-101(Al)	AlCl ₃	2-aminoterephthalic acid (NH ₂ -BDC)		140,141
4	NH ₂ -MIL-101(Fe)	FeCl ₃	2-aminoterephthalic acid (NH ₂ -BDC)		141-143
5	NH ₂ -MIL-53(Al)	AlCl ₃	2-aminoterephthalic acid (NH ₂ -BDC)		86,144-147
6	NH ₂ -MIL-53(Fe)	FeCl ₃	2-aminoterephthalic acid (NH ₂ -BDC)		142
7	NH ₂ -MIL-125(Ti)	Ti(OC ₄ H ₉) ₄	2-aminoterephthalic acid (NH ₂ -BDC)		143,148,149
8	ZIF-8	Zn(NO ₃) ₂	2-methylimidazole (H-MeIm)		76,150,151
9	Tb-TCA	Tb(NO ₃) ₃	4,4',4''-tricarboxytriphénylamine (H ₃ TCA)		152
10	[Cd(4-BTAPA) ₂ (NO ₃) ₂]·6H ₂ O·2DMF	Cd(NO ₃) ₂	1,3,5-benzene tricarboxylic acid tris[N-(4-pyridyl)amide] (4-BTAPA)		153

Table 1. continued

No.	MOF name and/or formula	metal salt	ligand	ligand structure	ref
11	[Cd(BPDB)(SCN) ₂] \cdot CH ₂ Cl ₂	Cd(SCN) ₂	1,4-bis(3-phenol)-2,3-diaza-1,3-butadiene (BPDB)		154
12	PCN-100	Zn(NO ₃) ₂	4,4',4''-s-triazine-1,3,5-triyltri- <i>p</i> -aminobenzoate (H ₃ TATAB)		155
13	PCN-101	Zn(NO ₃) ₂	4,4',4''-(benzene-1,3,5-triyltris(azanediyl))tribenzoate (H ₃ BTATB)		155
14	PCN-124	Cu(NO ₃) ₂	5,5'-(pyridine-3,5-dicarbonyl)bis(azanediyl)diisophthalate (H ₄ PDAI)		156
15	MIXMOF	Zn(NO ₃) ₂	benzene-1,4-dicarboxylate (H ₂ BDC) and NH ₂ -BDC		133
16	Zn ₂ (OA)(ATZ) ₂ \cdot (H ₂ O) _{0.5}	ZnCO ₃	oxalic acid (H ₂ OA) and 3-amino-1,2,4-triazole (ATZ)		157

carboxylate oxygen (Figure 9).¹⁴⁰ The formation of intraframework hydrogen bonding with an electron-donating oxygen from the carboxylic group increases the base strength of the MOF. As a result, the basic catalytic activity of IRMOF-3 is obviously better than that of pure aniline.

The same N-containing ligand, NH₂-BDC, can also be used to fabricate basic MOFs with mesoporosity such as NH₂-MIL-101(Al)^{124,125} and NH₂-MIL-101(Fe).^{142,143} These mesoporous MOFs are able to catalyze reactions involving bulky molecules, which is difficult for microporous MOFs such as NH₂-UiO-66.¹⁵⁸ Alternatively, construction of mesoporous MOFs can be realized using elongated ligands. By using Zn₄O(CO₂)₆ as SBUs and two extended linkers containing amino functional groups, 4,4',4''-s-triazine-1,3,5-triyltri-*p*-aminobenzoate (TATAB) and 4,4',4''-(benzene-1,3,5-triyltris(azanediyl))tribenzoate (BTATB), two isostructural mesopo-

rous MOFs with cavities up to 2.73 nm were prepared and represented as PCN-100 and PCN-101, respectively (Figure 10).¹⁵⁵ Both of the ligands have free amines which are not coordinated with metals. As a result, the basic functionalities are preserved in the frameworks and function as active sites for catalysis. For PCN-100, the mesoporous cavity (with an internal diameter of about 2.73 nm) is constructed from eight TATAB ligands and six Zn₄O(CO₂)₆ clusters; the size of windows is approximately 1.32 nm \times 1.82 nm (Figure 10). Further connection of these mesoporous cavities via TATAB results in the formation of a 3D network. The obtained mesoporous MOFs PCN-100 and PCN-101 were applied to catalyze Knoevenagel condensation between butyl cyanoacetate and three aldehydes possessing different molecular dimensions, i.e., benzaldehyde (linear; 0.61 nm \times 0.87 nm), 4-phenylbenzaldehyde (linear; 0.61 nm \times 1.33 nm), and benzophenone

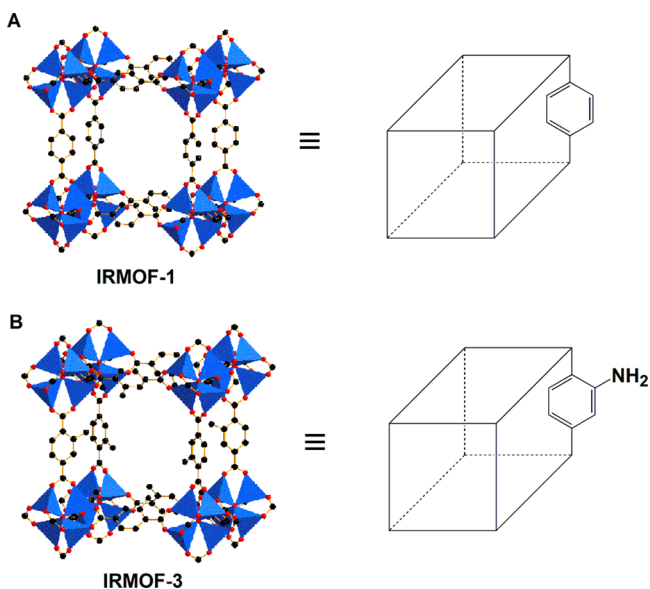


Figure 6. Structure of (A) IRMOF-1 and (B) IRMOF-3 derived from the nonfunctionalized ligand BDC and N-containing ligand $\text{NH}_2\text{-BDC}$, respectively. Color scheme: for Zn atoms, blue; for O atoms, red; for C atoms, black; for N atoms, blue.

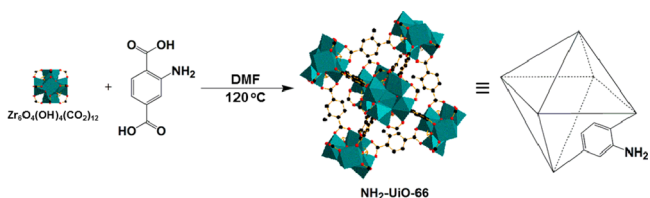


Figure 7. Synthesis of $\text{NH}_2\text{-UiO-66}$ from ZrCl_4 and $\text{NH}_2\text{-BDC}$. Color scheme: for Zr atoms, green; for O atoms, red; for N atoms, blue; for H atoms, white.

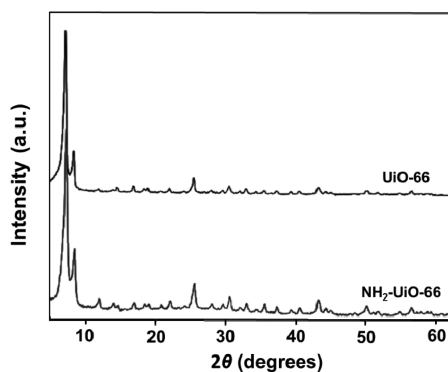


Figure 8. Powder XRD patterns UiO-66 and $\text{NH}_2\text{-UiO-66}$. Reproduced with permission from ref 136. Copyright 2011 Royal Society of Chemistry.

(angular; $0.66 \text{ nm} \times 1.14 \text{ nm}$).¹⁵⁵ In the case of benzaldehyde, the conversion reached 93% under the catalyst PCN-100. For 4-phenylbenzaldehyde with a slightly larger size, the conversion was declined to 58%. Remarkably, when benzophenone was used as the reactant, no conversion was observed over the same catalyst PCN-100. Under the catalysis of PCN-101, an identical trend of reactivity for different reactants was found as well. This indicates that PCN-100 and PCN-101 show size selectivity during catalysis and that the reactions proceed in the cavities of mesoporous MOFs.

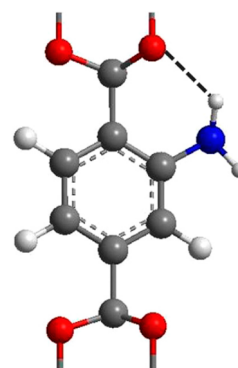


Figure 9. Intramolecular hydrogen bond formed inside IRMOF-3 in its minimum energy configuration. Color scheme: for O atoms, red; for carbon atoms, gray; for N atoms, blue; for H atoms, white.

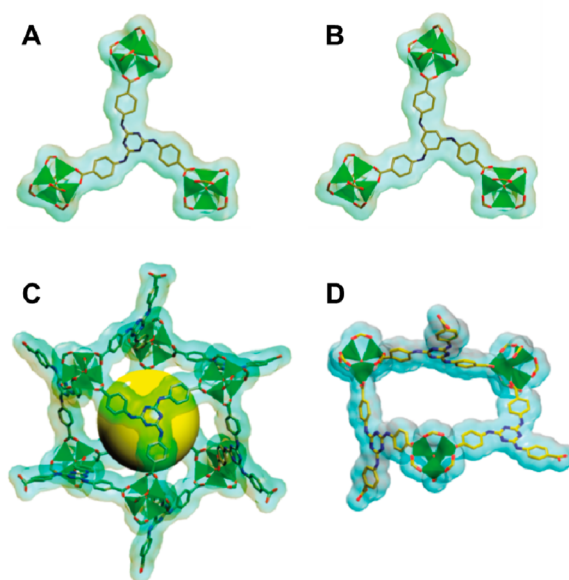


Figure 10. Elongated ligands (A) TATAB and (B) BTAB of PCN-100 and PCN-101 linked to three $\text{Zn}_4\text{O}(\text{CO}_2)_6$ SBUs. (C) Mesoporous cavity of PCN-100 with an internal size of 2.73 nm. (D) Window of the cavity with about $1.32 \text{ nm} \times 1.83 \text{ nm}$. Adapted with permission from ref 155. Copyright 2010 American Chemical Society.

Apparently, porous materials with sufficient pore sizes are important for the accessibility of active sites inside the pores, which makes the diffusion of reactants/products possible.^{159–162} It is worth noting that some unusual MOFs with N-containing ligands possess structure lacking the porosity required for intraporous catalysis, featuring basic sites mainly at lattice-terminating surface sites. The typical examples are zeolite imidazolate frameworks (ZIFs), which are an important family of MOFs with remarkable chemical stability.^{163,164} The assembly of tetrahedrally coordinated cations with organic imidazolate ligands affords the formation of tunable and chemically versatile structure, including similar topologies to those of zeolites.¹⁶⁵ The N-containing ligands endow some ZIFs with basicity. Taking ZIF-8 as an example, its synthesis is easy to realize from a zinc compound and 2-methylimidazole (H-MeIM) via a solvothermal process.¹⁶⁶ In the ZIF-8 structure, zinc atoms are connected through nitrogen atoms by MeIM ligands, producing nanosized pores formed by 4-, 6-,

8-, and 12-membered ring ZnN_4 tetrahedral clusters.^{164,167} The N_2 adsorption–desorption isotherm gives the characteristic shape of type I, which is the feature of microporous materials. Calculation from the isotherm data indicates that ZIF-8 possesses a BET surface area up to $\sim 1800 \text{ m}^2 \cdot \text{g}^{-1}$.¹⁵⁰ ZIF-8 presents an average pore diameter of 10.1 Å, which falls into the microporous regime. Nevertheless, the six-membered-ring pore windows of ZIF-8 are as narrow as 3.4 Å, which hinders the access of large molecules to the pores. Most reactions should take place on the external surface of ZIF-8 particles.⁷⁶ In this sense, smaller size crystals may exhibit higher catalytic activity because of the increased external surface. To demonstrate this point, Phan's group investigated the effect of the particle size of ZIF-8 on the catalytic activity.¹⁵⁰ ZIF-8 crystals with a different particle size of 143, 184, and 282 μm were employed to catalyze the Knoevenagel condensation of benzaldehyde with malononitrile. It was found that the increase of the particle sizes of the ZIF-8 catalyst resulted in a significant drop in the conversion. Further studies based on experimental results and DFT calculations indicate that N^- moieties and OH groups on the external surface act as the basic sites.⁷⁶

In addition to the use of N-containing ligands instead of nonfunctional ligands, partial substitution with N-containing ligands is also a good alternative to incorporate basic sites into MOFs.¹⁵⁷ A series of MIXMOF materials $Zn_4O(BDC)_x(NH_2\text{-BDC})_{3-x}$ was synthesized in which the BDC ligands were substituted partially by $NH_2\text{-BDC}$.¹³³ It is worthy of note that the synthetic conditions are of great importance for the formation of a phase-pure material. To allow for a random distribution of the two ligands, no additional base is added. Otherwise, slow addition of the base would most probably lead to a selective deprotonation of the stronger acid first, resulting finally in core–shell particles. At a reaction temperature of 150 °C up to 90% of $NH_2\text{-BDC}$ ligands could be introduced to the MIXMOFs. By using conventional XRD, identical patterns are expected for pure IRMOF-1, IRMOF-3, and MIXMOF materials; it is thus impossible to prove the presence of randomly distributed ligand molecules in the framework. Hence, high-resolution XRD experiments using synchrotron radiation were employed to characterize the materials.¹³³ The results show a clear linear shift of the peak positions from IRMOF-1 to the higher substituted MIXMOFs (Figure 11), which indicates a random distribution of the two ligand molecules in terms of Vegard's law. The basic catalytic activity of MIXMOFs were tested by the synthesis of propylene carbonate from propylene oxide and carbon dioxide.¹³³ A comparison of MIXMOFs from 0% to 40% of $NH_2\text{-BDC}$ revealed a dependence of activity on the number of amino groups.

In summary, MOFs with basicity can be constructed by using N-containing ligands as the building blocks. Direct functionalization shows the merits of a simple one-pot synthesis that enables straightforward introduction of the desirable functionality. The introduction of basic sites can be realized through the utilization of N-containing ligands instead of nonfunctional ligands as well as partial substitution with N-containing ligands (that is, mixed ligands). Note that for the direct synthesis, two issues should be considered. First, some ligands such as carboxylic acids produce protons in the process of MOFs synthesis, which may interact with N-containing ligands and compromise the basicity. Second, for MOFs that are synthesized at high temperatures such as MIL-101(Cr), amino groups cannot be incorporated due to the decom-

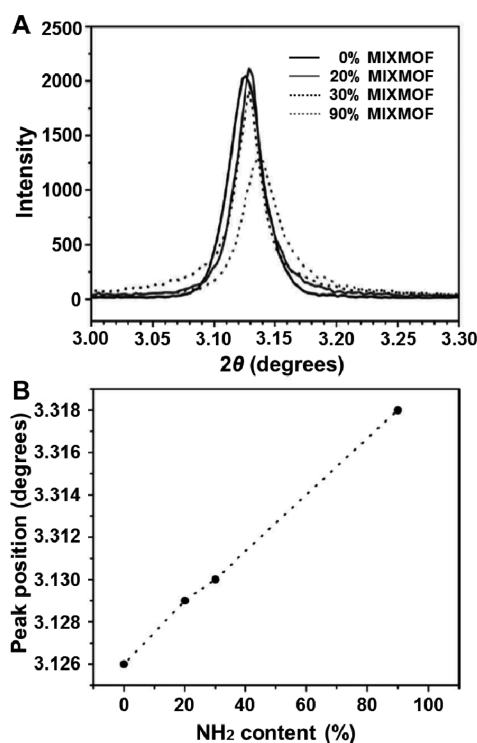


Figure 11. (A) Peak shift of the MIXMOF series with the increase of $NH_2\text{-BDC}$ ratio from 0% to 90% in high-resolution XRD. (B) Partial substitution of BDC by $NH_2\text{-BDC}$ leads to a slightly contracted unit cell, which is displayed by a linear correlation of $NH_2\text{-BDC}$ content and peak shift to higher 2θ values. Adapted with permission from ref 133. Copyright 2010 Wiley-VCH.

position of starting materials during synthesis.¹⁶⁸ In this regard, postsynthetic modification provides a good alternative, in which MOFs are first constructed followed by the attachment of functionality to organic ligands (as discussed later in section 2.2.2). Generally speaking, investigations concerning the fabrication of MOFs with prefunctionalized ligands are increasing, while more attention should be paid to their applications as base catalysts rather than to their synthesis and applications in gas adsorption.

2.1.4. Basicity from Structural Phenolates. The hybrid frameworks $M_2\text{DHTP}$ (DHTP = 2,5-dihydroxyterephthalate, $M^{2+} = Mg^{2+}, Co^{2+}, Ni^{2+}, Cu^{2+},$ and Zn^{2+}), also known as CPO-27 or MOF-74, are a kind of MOFs receiving much attention.^{169–172} The high density of exposed metal ions in these MOFs have sparked much interest in the field of adsorption and separation of various gases like $CO, CO_2, CH_4,$ ethane, acetylene, propane, and propylene.^{105,173–177} However, reports concerning the use of these materials as base catalysts are very scarce. Surprisingly, Valvekens et al. showed that these MOFs were active catalysts in typical base-catalyzed reactions such as Knoevenagel condensation recently.¹⁷⁸ The catalytic results indicated a distinct influence of the metal ion on the performance of the catalyst, with a clear preference for $Ni_2\text{DHTP}$ as the most active material in the reactions of malononitrile (or cyanoacetate) with benzaldehyde.

To understand the origin of basicity, the structure of $M_2\text{DHTP}$ materials is examined in detail. The structure comprises metal oxide chains connected by the DHTP ligands, generating a honeycomb-like structure possessing 1D hexagonal pores with a diameter of $\sim 1.2 \text{ nm}$ (Figure 12A).¹⁷⁸ As the linker molecule, DHTP is fully deprotonated in the framework,

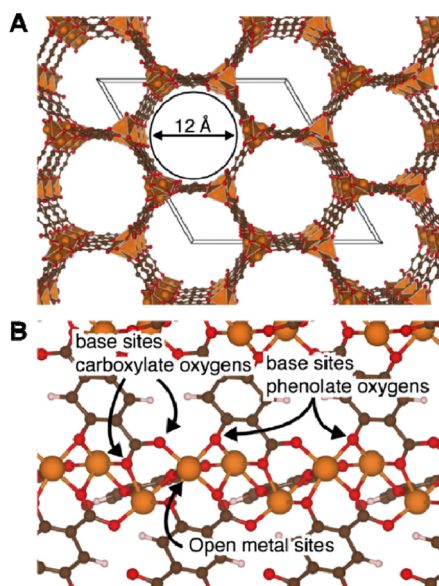


Figure 12. (A) Scheme showing the pores in M_2DHTP . (B) Representation of the potential basic sites in the framework. Color scheme: for O atoms, red; for carbon atoms, brown; for metal atoms, orange. Adapted with permission from ref 178. Copyright 2014 Elsevier.

and carboxylate oxygen atoms as well as phenolate oxygen atoms coordinate the metal centers (Figure 12B). The carboxylate oxygen atoms possess quite weak basicity, whereas a phenolate oxygen, which is a conjugate base to the weakly acidic phenol, should be far more basic. As is logical, the phenolate oxygen atoms function as basic sites in these MOFs, which deprotonate the acidic substrate such as malononitrile and subsequently activate the compound for further reaction. The CUS near the phenolate oxygen atom functions as a docking site for the deprotonated substrate molecule. The other substrate like benzaldehyde in the Knoevenagel reaction is able to be adsorbed on the protonated phenolate oxygen, followed by coupling of the substrates. This interplay of CUSs and phenolate oxygen atoms in the creation of active centers in catalysts is comparable to what occurred in alkaline earth metal binaphtholate catalysts.¹⁷⁹ The basic sites existing in M_2DHTP were also confirmed by the chemisorption of pyrrole observed with IR spectroscopy.¹⁷⁸

As described above, the basicity of M_2DHTP is dependent on the nature of metal ions (i.e., Mg^{2+} , Co^{2+} , Ni^{2+} , Cu^{2+} , and Zn^{2+}), since the coordination of the phenolate to the metal ion affects the electron density of the oxygen atom. Proton affinity (PA) is considered the first indication for the basicity of a material and was used to explain the experimental results.¹⁷⁸ PAs were calculated for both phenolate (denoted as PA1) and carboxylate oxygen atom (denoted as PA2). As shown in Table 2, the protonation is promoted on phenolate oxygen atoms, since PA1 is generally larger than PA2 for all metals. As a result, the deprotonation of donor molecules (e.g., malononitrile) will be preferred to occur on phenolate oxygen atoms. The high PA of the phenolate in Ni_2DHTP is in agreement with the high basicity, though it is unlikely to rationalize all basicity tendency based on the PA values alone.¹⁷⁸

In summary, the intrinsic basicity of MOFs can originate from either metal sites or ligands. In comparison with metal sites that were normally limited to alkaline earth metal ones, organic ligands seem to provide more possibilities due to their

Table 2. Proton Affinities (PAs) of M_2DHTP for the Phenolate Oxygen Atom (PA1) and Carboxylate Oxygen Atom (PA2) as Well as the Calculated Adsorption Energies of Acetonitrile (ΔE_{ads})^a

M	PA1 (kJ·mol ⁻¹)	PA2 (kJ·mol ⁻¹)	ΔE_{ads} (kJ·mol ⁻¹)
Mg	930	913	-91
Co	947	918	-83
Ni	946	757	-91
Cu	923	905	-47
Zn	944	917	-79

^aAdapted with permission from ref 178. Copyright 2014 Elsevier.

diversity. The ligand NH_2 -BDC is extensively used for the construction of various MOFs with basicity. In these MOFs, N-containing moieties function as basic sites. It should be noted that the basicity of this kind of material is relatively weak, because of the electron-withdrawing carboxylic groups on the same aromatic ring. Aiming to enhance the base strength, ligands with stronger basicity are expected for the fabrication of MOFs. Of course, the successful fabrication of stronger basic MOFs depends on the development of synthetic techniques. In the meanwhile, decontamination of the basic sites should also be considered in the synthetic process. In contrast to the use of N-containing ligands as the source of basicity, much less attention has been paid to the intrinsic basicity of MOFs arising from the presence of phenolate oxygen atoms coordinated to metal ions. Such intrinsic basicity is believed to exist in MOFs other than the M_2DHTP series, which deserves further design and discovery. For MOFs with intrinsic basicity, more characterization on basic properties and their applications in base-catalyzed reactions are expected.

2.2. MOFs with Modified Basicity

Rather than preparing functional MOFs via direct solvothermal synthesis, functionalities can be introduced through modification in a heterogeneous manner after the formation of MOFs.^{180–182} The type and number of basic functional groups can be incorporated into MOFs with great controllability. As a result, much attention has been paid to the generation of basic sites on MOFs through postsynthetic modification. The judicious combination of basic guests with MOFs allows the fabrication of new types of materials with a range of interesting properties. Moreover, a given MOF structure can be modified with different reagents, thereby generating a large number of topologically identical but functionally diverse MOFs. By use of postsynthetic modification, both the metals and the organic linkers can be functionalized without affecting the overall structure of MOFs. In other words, modification of MOFs with basicity can be accomplished by either grafting of organic molecules on the metal sites that created after solvent removal or introducing covalent attachment to the organic ligands.

2.2.1. Functionalization of Metal Sites. Through proper treatment, solvents and/or water coordinated on metal sites can be removed, resulting in the exposure of CUSs in MOFs (Figure 13). These CUSs are suitable for introducing chemical bonding with electron-rich amine molecules, which leads to the production of basic sites in MOFs.^{183–186} To date, a series of amines (ranging from aliphatic^{187–189} to aromatic¹⁹⁰ and even to chiral amines^{191,192}) has been grafted onto the CUSs in various MOFs such as IRMOF-1,¹⁹⁰ IRMOF-10,¹⁹⁰ MIL-101(Cr),^{87,193} and Mg_2DHTP ,¹⁹⁴ and a variety of basic MOFs

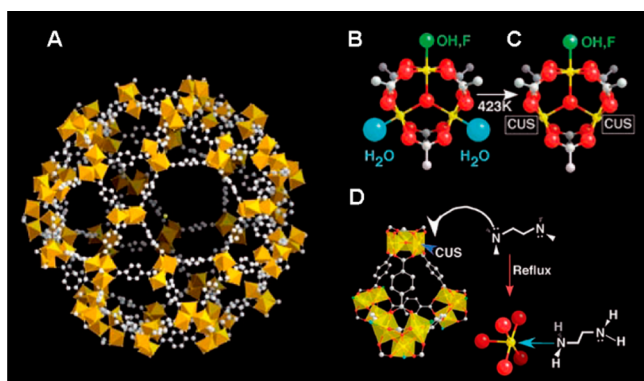


Figure 13. Grafting amines onto the metal sites of MIL-101(Cr). (A) Perspective view of the mesoporous cage of MIL-101(Cr) with hexagonal windows; (B and C) evolution of CUSs from chromium trimers in mesoporous cages of MIL-101(Cr) after thermal treatment in vacuum; (D) modification of MIL-101(Cr) via selective grafting of typical amine molecules, namely, EA onto CUSs. Color scheme: for Cr/octahedra atoms, yellow; for C atoms, gray; for O atoms, red. Adapted with permission from ref 87. Copyright 2008 Wiley-VCH.

with interesting properties have been fabricated as summarized in Table 3.

Diamines are commonly employed for the functionalization of metal sites. If one amino group of diamine is grafted onto a CUS in MOFs, the other amino group is capable of acting as immobilized basic site. Among various diamines, ED is the most frequently used one. Due to the robust frameworks and very accessible unsaturated Cr sites with high concentration (up to $3.0 \text{ mmol}\cdot\text{g}^{-1}$), MIL-101(Cr) becomes one of the most frequently studied MOFs for amine functionalization.¹⁹⁷ The trimeric Cr octahedral clusters possess terminal water molecules, which can be eliminated from MIL-101(Cr) subjected to thermal treatment at $150 \text{ }^\circ\text{C}$ in vacuum (Figure 13). This leads to the formation of CUSs in the framework that is suitable for modification. As a result, electron-rich ED molecules can be successfully immobilized on the CUSs.⁸⁷ Typically, the modification of CUSs by amines was conducted in refluxing toluene.^{87,193} It should be stated that this idea is not applicable to the surface modification of mesoporous silica materials because of the absence of unsaturated silica sites.^{198–201}

Various techniques, including XRD, IR, N_2 adsorption, XPS, and TG, were employed to characterize the MOFs modified with ED.^{87,193,194} MIL-101(Cr)-ED exhibited quite similar XRD patterns to MIL-101(Cr) while with minor changes in the Bragg intensity, indicating that the crystallinity was well preserved.¹⁸⁹ The introduction of amine molecules was observable from N_2 adsorption results. The BET surface area decreased from $4230 \text{ m}^2\cdot\text{g}^{-1}$ for the parent MOF MIL-101(Cr) to $3555 \text{ m}^2\cdot\text{g}^{-1}$ for MIL-101(Cr)-ED; also, the decline of pore size was visible after modification.⁸⁷ The IR spectrum of MIL-101(Cr)-ED showed the bands ascribed to C–H and N–H stretching vibrations, which suggests the existence of ED. Moreover, the C–H stretching bands shifted to high wavenumbers due to the coordination of ED with metal sites, and thus, the grafting of ED molecules onto CUSs was evidenced.⁸⁷ The selective grafting of ED onto CUSs can also be demonstrated by the decline of CUSs concentration with the increase of ED loading from CO adsorption results.⁸⁷

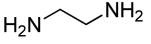
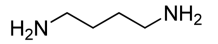
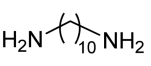
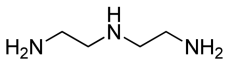
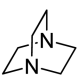
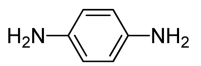
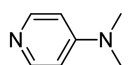
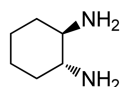
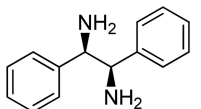
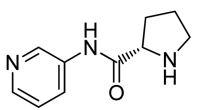
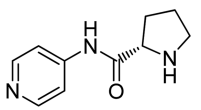
In addition to IR, the XPS technique was used to characterize the coordination of introduced ED molecules with the CUSs in

MOFs as well. As reported by Chen et al. in ED-modified IRMOF-10, introduction of ED was confirmed by the N 1s signal.¹⁹⁰ Furthermore, the N 1s signal of IRMOF-10-ED can be deconvoluted into two peaks at 399.9 and 401.2 eV, which is caused by the free amino group and the coordinated amino group, respectively.²⁰² The comparison of Zn 2p XPS spectra for the materials before and after amine modification also gives interesting results. In the case of parent IRMOF-10, the Zn 2p XPS spectrum showed doublet peaks at 1019.3 eV derived from Zn $2p_{3/2}$ and 1042.2 eV stemming from Zn $2p_{1/2}$ (Figure 14), implying the existence of the coordination of Zn with the ligand 4,4'-biphenyldicarboxylic acid (BPDC). For IRMOF-10-ED, the Zn 2p spectra were deconvoluted into two main doublet peaks. In addition to the typical peaks at 1019.3 and 1042.2 eV originated from the Zn carboxylate of framework, new doublet peaks at 1020.8 and 1043.2 eV ascribed to amine-coordinated Zn appeared.²⁰³ These results verify the coordination of ED molecules with the CUSs.

Several methods including nuclear magnetic resonance (NMR),¹⁹⁰ TG,¹⁹⁴ and element analysis⁸⁷ have been used to quantify the loading amount of amines in MOFs. For NMR analysis, the samples are digested in deuterated solvents, and the areas of ^1H NMR peaks give precise amine loading levels.¹⁹⁰ As a result, the empirical formula of amine-modified MOFs can be obtained as listed in Table 4. In the case of IRMOF-10, the grafting amount of 4-dimethylaminopyridine (DMAP) was about 95% based on Zn sites. However, the grafting amount for IRMOF-1 was only about 48% under the same conditions. This is probably because IRMOF-1 has smaller pore sizes as compared with IRMOF-10, and a relatively limited amount of amine molecules can be incorporated. It should be stated that TG data also provide information on the stability of amines in MOFs besides the quantitative analysis of amines loading. As shown in Table 4, the amine-modified MOFs are stable at temperatures higher than the boiling points of corresponding amines.¹⁹⁰ This confirms that the amines are grafted onto CUSs in MOFs.

Basic MOFs with different properties can be obtained by introduction of the same diamine to different MOFs; in the meanwhile, the type of diamine also has an effect. A systematic study on the effect of diamine was conducted by Kasinathan et al.¹⁸⁹ Four diamines, namely, ED, butane-1,4-diamine (BD), decane-1,10-diamine (DD), and benzene-1,4-diamine (PD), with different pK_a (see Table 3) were grafted onto the same MOF MIL-101(Cr). The XRD patterns showed that the crystalline frameworks of MIL-101(Cr) were retained, while the intensity of the diffraction lines decreased to some extent owing to the introduction of diamines. Upon modification, the pore sizes of MOFs decreased in general, and the decrease for the material from small molecules was not that obvious. The quantitative results from elemental analysis displayed that the nitrogen contents were 2.1, 1.9, 1.4, and 1.3 $\text{mmol}\cdot\text{g}^{-1}$ for MIL-101(Cr)-ED, MIL-101(Cr)-BD, MIL-101(Cr)-PD, and MIL-101(Cr)-DD, respectively.¹⁸⁹ The decrease in nitrogen content with the increase of amine size reveals the steric hindrance effect during modification. In the case of MIL-101(Cr)-PD, the low nitrogen content may also be caused by the weak electronegativity of the phenyl amine group, which functions as an obstacle to amine grafting onto the CUSs. The Knoevenagel condensation of benzaldehyde with ethyl cyanoacetate was performed to evaluate the basic properties of MIL-101(Cr) modified with different diamines.¹⁸⁹ The activity of materials in terms of turnover frequency (TOF)

Table 3. Summary of the Modification of Metal Sites with Amines

No	amine	structure	pK_a^a	MOF	ref
1	ethylenediamine (ED)		9.92	IRMOF-1, IRMOF-10, MIL-101(Cr), Mg ₂ DHTP, H ₃ [(Cu ₄ Cl) ₃ (BTTri) ₈] ^b	87,18 7,188, 190,1 94
2	butane-1,4-diamine (BD)		10.80	MIL-101(Cr)	189
3	decane-1,10-diamine (DD)		10.97	MIL-101(Cr)	189
4	diethylenetriamine (DETA)		9.97	MIL-101(Cr)	87,19 3
5	1,4-diazabicyclo[2,2,2]octane (DABCO)		3.00	[Zn(TPDC)]·DMF·2H ₂ O ^c	195,1 96
6	benzene-1,4-diamine (PD)		6.31	MIL-101(Cr)	189
7	4-dimethylaminopyridine (DMAP)		9.52	IRMOF-1 IRMOF-10	190
8	(1 <i>R</i> ,2 <i>R</i>)-1,2-cyclohexanediamine		9.93	MIL-101(Cr)	191
9	(1 <i>R</i> ,2 <i>R</i>)-1,2-diphenylethylenediamine		9.78	MIL-101(Cr)	191
10	(<i>S</i>)- <i>N</i> -(pyridin-3-yl)-pyrrolidine-2-carboxamide		13.34	MIL-101(Cr)	192
11	(<i>S</i>)- <i>N</i> -(pyridin-4-yl)-pyrrolidine-2-carboxamide		13.05	MIL-101(Cr)	192

^aData from the *CRC Handbook of Chemistry and Physics*; CRC Press: London, 2005 and SCIFinder. ^bH₃BTTri = 1,3,5-tris(1*H*-1,2,3-triazol-5-yl)benzene); TPDC = terphenyl-3,3'-dicarboxylate.

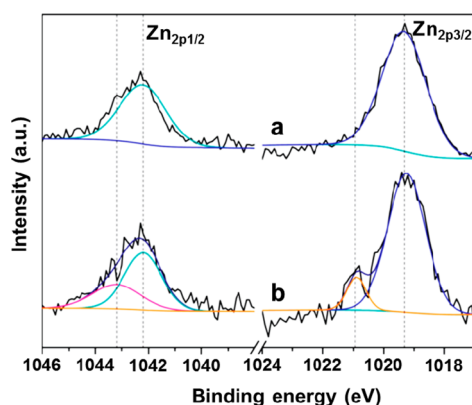


Figure 14. Zn 2p_{1/2} and Zn 2p_{3/2} XPS spectra of (a) IRMOF-10 and (b) IRMOF-10-ED. Adapted with permission from ref 190. Copyright 2014 Royal Society of Chemistry.

decreased in the order of MIL-101(Cr)-BD > MIL-101(Cr)-DD > MIL-101(Cr)-ED > MIL-101(Cr)-PD, which is generally consistent with the pK_a value of the corresponding diamine except MIL-101(Cr)-DD. Among the four diamines, DD exhibits the highest pK_a value. The relatively low activity of MIL-101(Cr)-DD originates from the long carbon chain that obstructs the diffusion of substrates. In addition, the diamine possessing a long chain may form a hydrogen bond with adjacent amino groups or the pending amino groups further coordinate with the neighboring CUSs.

In summary, functionalization of metal sites with amines provides a fascinating method to create basicity in MOFs. Amines with various basicity can be immobilized on the CUSs due to the intrinsic chelating property. Upon immobilization, one amino group is grafted onto one CUS by coordination, whereas the other amino group serves as the immobilized basic site. This method is convenient for MOFs but unlikely for some conventional supports such as mesoporous silica because there is no CUSs on the surface. It should be stated that diamines are frequently used for grafting, and basicity derives from free amino groups. This means that the molar amount of basic sites is only one-half of the molar amount of diamines. To enhance the amount of basic sites, triamines such as DETA can be utilized for functionalization. Among various MOFs, MIL-101(Cr) is the most frequently investigated one; this should be related to the high chemical stability of MIL-101(Cr). To this end, chemically stable MOFs should be considered for amines functionalization. Despite the fact that the reusability of these basic MOFs in catalysis has been proven by some researchers, leaching of basic sites could be a concern in some cases owing to the coordination bonds. In this regard, the amines functionalization of ligands via covalent bonds presents high stability against leaching as shown in the next section.

2.2.2. Functionalization of Ligands. Basic functional groups can be attached covalently to ligands via direct synthesis

or modification after the formation of MOF lattices. In the case of direct synthesis, prefunctionalized ligands are utilized to assemble with metals in the fabrication of MOFs (as discussed in section 2.1.3). For postsynthetic functionalization, MOFs are synthesized first and then basic functional groups are immobilized on ligands via covalent bonding. The attachment of basic functionality permits the modification of features while maintaining the crystalline structure of parent MOFs. Thus far, three predominant approaches have been adopted to attach basic functionality to ligands, namely, (i) direct amination of aromatic rings, (ii) amination of the aromatic amine/aldehyde tags, and (iii) exchange of pending hydroxyl protons to alkaline/alkali earth metal cations.

A typical example of direct amination of aromatic rings in ligands was reported by Stock's group.¹⁶⁸ Although some amine-containing MOFs can be synthesized directly by replacing the unfunctionalized ligands by corresponding amine-functionalized ligands (e.g., H₂BDC by NH₂-BDC), this is not always easily accomplished. There are two possible difficulties, namely, the coordination of amino groups with metal sites as well as the stability of amine-functionalized ligands. A case in point is the synthesis of NH₂-MIL-101(Cr); the method of direct synthesis is challenging. Traditionally, MIL-101(Cr) is prepared under hydrothermal conditions above 200 °C. Under such conditions the decomposition of NH₂-BDC takes place simultaneously in the synthetic process of NH₂-MIL-101(Cr).¹⁶⁸ Hence, Stock's group developed a postsynthetic approach to attach amino groups on the ligands of MIL-101(Cr).¹⁶⁸ As illustrated in Figure 15, two steps were

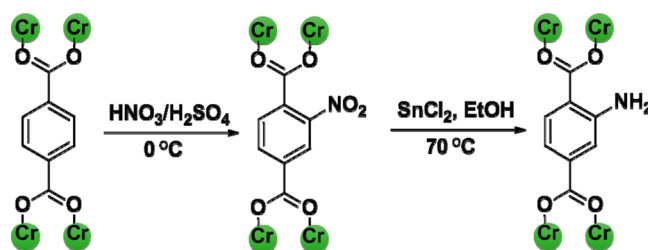


Figure 15. Schematic illustration of direct amination of ligand aromatic rings in MIL-101(Cr). Process includes nitration of MIL-101(Cr) to NO₂-MIL-101(Cr) followed by reduction of NO₂-MIL-101(Cr) to NH₂-MIL-101(Cr).

designed including the nitration of MIL-101(Cr) to NO₂-MIL-101(Cr) and subsequent reduction to NH₂-MIL-101(Cr).¹⁶⁸ Nitration of MIL-101(Cr) was performed in the nitrating acid containing HNO₃ and H₂SO₄ for 5 h at 0 °C. The reduction step was conducted in the presence of SnCl₂ and ethanol for 6 h at 70 °C. EDX analysis showed the existence of Sn composition, which can be removed via dissolution using concentrated HCl followed by treatment with H₂O and ethanol. The result of XRD indicated that the crystalline

Table 4. Physical and Chemical Properties of Some Amine-Grafted MOFs via Metal Sites^a

sample	molecular formula ^b	density of basic sites (mmol·g ⁻¹)	thermal stability ^c (°C)	boiling point of amine (°C)
IRMOF-1-ED	Zn ₄ O(BDC) ₃ ·(ED) _{1,2}	0.76	200	117–119
IRMOF-10-ED	Zn ₄ O(BPDC) ₃ ·(ED) _{4,2}	0.81	200	117–119
IRMOF-1-DMAP	Zn ₄ O(BDC) ₃ ·(DMF) _{1,2} ·(DMAP) _{1,9}	0.53	275	162 (50 mmHg)
IRMOF-10-DMAP	Zn ₄ O(BPDC) ₃ ·(DMAP) _{3,8}	0.59	315	162 (50 mmHg)

^aData from ref 190. ^bDerived from the ¹H NMR data of digested MOFs. ^cOn the basis of TG data.

structure of the obtained material NH₂-MIL-101(Cr) was well maintained. The permanent porosity was evidenced by N₂ adsorption measurement. The successful ligand modification can be proven by IR spectra.¹⁶⁸ In NO₂-MIL-101(Cr) the distinct stretching vibration of nitro groups was observed clearly but disappeared due to the succedent reduction of the nitro to amino groups. Instead, the asymmetric and symmetric N–H stretching vibrations of the amino groups in NH₂-MIL-101(Cr) were observed. The ¹H NMR measurement of digested materials gave further evidence of the attachment of amino groups.¹⁶⁸ If the nitration reaction was performed for 5 h, only nitroterephthalic acid was detected after the digestion of NO₂-MIL-101(Cr). In addition, only NH₂-BDC was observed for NH₂-MIL-101(Cr). This indicates the successful amination of aromatic rings in ligands through the postsynthetic method. The reactivity of the amino groups in NH₂-MIL-101(Cr) was investigated by the reaction with ethyl isocyanate.¹⁶⁸ The NMR results confirmed the generation of the desirable urea derivative. No additional signals in NMR spectra indicated the conversion of amino groups was nearly complete. The results suggest the accessibility and reactivity of the amines covalently attached to ligands.

The amination of aromatic rings in ligands affords basic sites to MOFs. In the meanwhile, aromatic amine as well as aldehyde tags present opportunities for the introduction of new basic functionalities to MOFs.^{204–208} The base strength of aromatic amine-containing MOFs is relatively low because of the low pK_a values and low electron densities caused by the adjacent carboxylate groups. The amination of aromatic amine/aldehyde tags can introduce aliphatic amines which are more basic than aromatic amines. A recent study on the amination of aromatic amine tags was conducted by Chen et al.¹⁹⁰ The alkylation of NH₂-MIL-53(Al) with 2-chloro-*N,N*-dimethylethanamine was realized, and new pendant aliphatic tertiary amines were covalently bonded to the original aromatic amines (Figure 16A). The functionalization process was performed in a water solution in which 2-chloro-*N,N*-dimethylethanamine was added to the suspension of NH₂-MIL-53(Al) in the presence of K₂CO₃. After the reaction at 80 °C for 2 days under a nitrogen atmosphere, the functionalized material NMe₂-NH-MIL-53(Al)

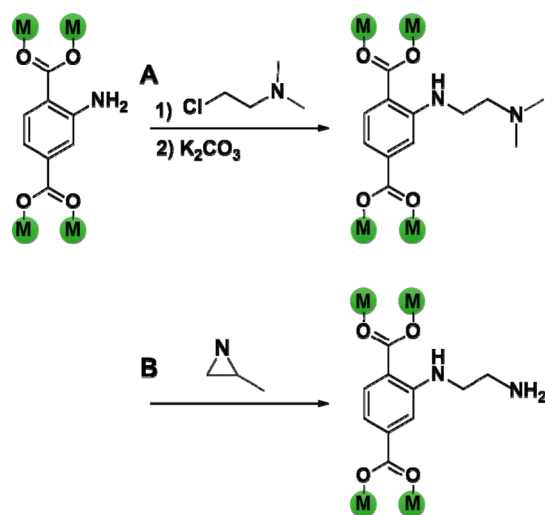


Figure 16. Covalent postsynthetic functionalization of aromatic amine-tagged MOFs with (A) 2-chloro-*N,N*-dimethylethanamine and (B) 2-methylalridine.

can be obtained. The XRD results indicated that there was no obvious loss in crystallinity after covalent grafting.¹⁹⁰ The grafting percentage was about 45% (based on the organic ligand NH₂-BDC) according to the ¹H NMR spectrum of digested NMe₂-NH-MIL-53(Al). TG results indicated that NMe₂-NH-MIL-53(Al) was thermally stable up to 450 °C, which is similar to the parent material NH₂-MIL-53(Al). The result of acid–base titration showed that the amount of basic sites was 0.65 mmol·g⁻¹. Through suspending NMe₂-NH-MIL-53(Al) in a water solution, the apparent pH of 8.49 was measured. The characterization of basic properties implies that NMe₂-NH-MIL-53(Al) could serve as an immobilized base catalyst.¹⁹⁰ In the liquid-phase transesterification of triglycerides with methanol, the conversion over NMe₂-NH-MIL-53(Al) exceeded 99%, which is much higher than that over the parent material NH₂-MIL-53(Al) (3.9%) under the same reaction conditions. In other words, the aliphatic tertiary amines are more basic than aromatic amines.

To further enhance the base strength, aliphatic primary amines were immobilized on MOFs through tagged amine sites. Recently, Wang's group employed 2-methylalridine as the precursor for functionalization (Figure 16B).²⁰⁹ Amine-tagged MOFs were suspended in chloroform followed by the addition of the precursor 2-methylalridine. The modification process was conducted at 45 °C for 6 h. A collection of amine-tagged MOFs was used for modification including IRMOF-3, NH₂-UiO-66, NH₂-MIL-53(Al), and NH₂-MIL-101(Cr). The powder XRD results showed that after 2-methylalridine modification, all MOFs except IRMOF-3 can preserve their crystalline structure. This means that IRMOF-3 is not proper for modification with strongly basic species. On the basis of the results of ¹H NMR and elemental analysis, the modification rate was calculated.²⁰⁹ The modification rate for NH₂-MIL-101(Cr) was 36%, which is higher than that for NH₂-UiO-66 (28%) and NH₂-MIL-53(Al) (15%). The high modification rate of NH₂-MIL-101(Cr) should be related to its larger pores, which is beneficial to the diffusion of the precursor 2-methylalridine. The MOFs containing aliphatic primary amines were used as solid base catalysts. Their activity in the Knoevenagel condensation of benzaldehyde with malononitrile is apparently higher than that of their parent materials.²⁰⁹ In the case of primary amine-modified NH₂-UiO-66, the conversion of benzaldehyde reached 97% at 2 h; under identical reaction conditions, however, the parent material NH₂-UiO-66 exhibited a conversion of around 5%.

In addition to aromatic amine tags, the aldehyde tags in ligands can also be used for amination, which leads to the introduction of extra basic sites. An interesting study was carried out by Yaghi's group using ZIF-90.²⁰⁸ ZIF-90 was assembled from Zn(NO₃)₂ with imidazolate-2-carboxyaldehyde (ICA); it showed the structure related to the sodalite topology through substituting the O and Si for ICA ligands and Zn, respectively (Figure 17). The pendant aldehyde groups make it possible to modify ZIF-90 with basic species. Ethanolamine was employed to react with ZIF-90 in the methanol solution at 60 °C, and the obtained material possessing amino groups was named as ZIF-92.²⁰⁸ In the solid-state NMR spectrum of sample after reaction for 3 h, no resonance of aldehyde groups (ZIF-90) was detected, suggesting the quantitative formation of imine (ZIF-92). In the IR spectrum, there was no C=O stretching vibration ascribed to aldehyde groups in ZIF-92, while the band originating from C=N bonds became visible. The IR results thus confirmed the NMR data, demonstrating

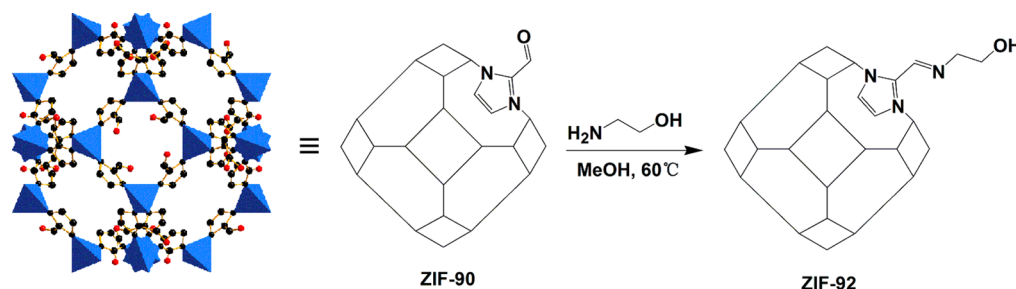


Figure 17. Crystal structure of ZIF-90 and the covalent postsynthetic functionalization of aldehyde groups with ethanolamine to give ZIF-92. Color scheme: for C atoms, black; for N atoms, green; for O atoms, red.

the complete conversion of aldehyde to imine. Due to the high stability of ZIF-90, introduction of basic groups did not cause any damage to the crystalline structure.²⁰⁸

Although organic amines are frequently used for the functionalization of ligands, inorganic alkaline/alkali earth metals have been attempted to decorate ligands as well. The idea is based on the exchange of pending hydroxyl protons to alkaline/alkali earth metal cations. A representative study was reported by Hupp and co-workers.²¹⁰ As depicted in Figure 18,

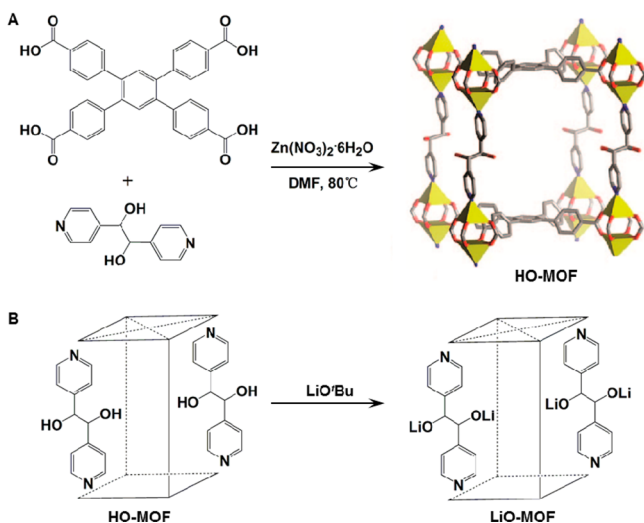


Figure 18. (A) Synthesis and crystal structure of the diol-containing MOF (HO-MOF), and (B) exchange of pending hydroxyl protons to Li ions. Color scheme: for C atoms, gray; for N atoms, blue; for O atoms, red; for Zn/tetrahedra, yellow.

the hydroxyl-containing MOF (denoted as HO-MOF) was utilized for modification and synthesized from Zn(II) centers and two ligands. The single-crystal XRD characterization indicated that HO-MOF had a single framework possessing large cavities, which makes the hydroxyl groups highly accessible for modification. Taking account of the stability of

HO-MOF in the presence of some harsh reagents (such as methylolithium), a mild reagent lithium *tert*-butoxide (LiO^tBu) was used.²¹¹ To realize the exchange of hydroxyl protons, the solvent DMF was replaced by tetrahydrofuran (THF) and HO-MOF was stirred in the THF/CH₃CN solution of LiO^tBu, leading to the formation of LiO-MOF. The degree of exchange could be controlled by tuning the stirring time and rate. The results of nitrogen adsorption suggested that the microporous structure of LiO-MOF was maintained after Li exchange.²¹⁰ In the extreme of low Li content, LiO-MOF preserved a surface area comparable to HO-MOF. For the material with high Li content, nevertheless, the surface area decreased significantly and the crystalline structure was destroyed. This may be caused by the fractional displacement of Zn by Li. Similarly, the reaction of HO-MOF with Mg(OMe)₂ could replace hydroxyl protons with Mg cations. By adjusting the exchange conditions, the samples possessing about one or two Mg cations per glycol strut can be prepared.²¹⁰ The purpose of the introduction of Li (or Mg) to MOFs is to enhance the heat of adsorption for hydrogen in Hupp's work, and the basic properties of materials are not explored.²¹⁰ However, these materials should be strongly basic according to our previous study on mesoporous silica.²¹² The exchange of silanol protons to Li cations in SBA-15 using LiO^tBu yielded solid strong bases. The optimal Li-containing SBA-15 sample was quite active in the transesterification reaction between methanol and ethylene carbonate. The results of reactions showed that the yield of target product reached 41.3%. This catalytic activity was higher than a series of solid bases including MgO (7.6%), CsX (6.1%), CaO/ZrO₂ (15.1), and Na₂O/Al₂O₃ (28.2%).²¹²

It is worth mentioning that both metal sites and organic ligands are modifiable, which makes it possible to introduce different and even antagonistic functionalities to MOFs simultaneously. In addition to basic functionality, the introduction of incompatible acidic functionality through spatial isolation is realized in MOFs.^{140,213,214} The acid–base bifunctional MOFs are able to catalyze multistep or cascade reactions in one pot, being cost efficient and time saving (details on cascade reactions are shown in section 4.7).^{140,215–218} An

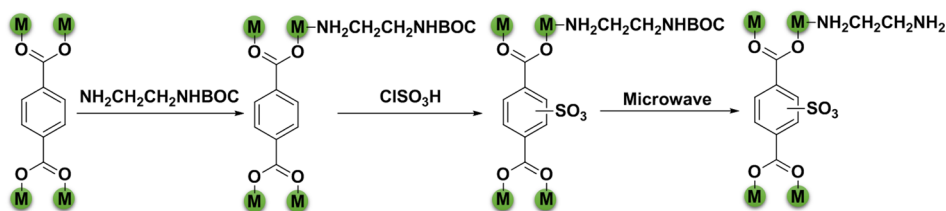


Figure 19. Formation of acid–base bifunctional active sites on MOFs.

interesting example of functionalization of both metal sites and ligands was shown by Li et al. on MIL-101(Cr).²¹³ A process containing three steps was designed as illustrated in Figure 19. In the first step, mono-BOC-ethylenediamine was grafted onto CUSs via a primary amino group and amine-protected MIL-101(Cr)-NHBOC was produced. In the second step, the obtained MIL-101(Cr)-NHBOC was sulfonated at the skeleton phenylene units using chlorosulfonic acid, which led to the formation of SO₃H-MIL-101(Cr)-NHBOC. In the third step, deprotection of the amino groups by thermal treatment gave the bifunctional catalyst SO₃H-MIL-101(Cr)-NH₂. The results of elemental analysis showed that about 1.08 SO₃²⁻ and 0.85 ED per formula unit were immobilized on the ligands and CUSs.²¹³ The structure of the materials was not altered after the functionalization process based on the XRD patterns. The N–H and C–H vibrational bands which displayed on the IR spectra demonstrated that basic sites were retained after the following modification process. The N₂ adsorption–desorption isotherms revealed the characteristic type I shape of materials. Due to the presence of functionalized groups, a downward trend on the BET surface area and pore volume appeared after grafting, but the open pores and high surface areas were still maintained, which is essential for the diffusion of substrates and products in catalysis.

In conclusion, postsynthetic modification is a useful approach to introduce basic functionality to MOFs. It is noticeable that aliphatic amines are successfully attached on organic ligands via postsynthetic modification. Due to the comparatively high pK_a values of aliphatic amines, the basicity of these MOFs are relatively strong. This is obviously different from their counterparts from direct synthesis, through which only aromatic amines with relatively low basicity are involved. Meanwhile, direct synthesis of MOFs using amine-containing ligands generally presents a relatively low basicity because of the competitive coordination of basic nitrogen sites with metal centers. It should be mentioned that in the postsynthetic modification, attention should be paid to the chemical stability of MOFs in the presence of aliphatic amines. The degradation of some MOFs is observed during modification owing to the strong basicity of aliphatic amines. An obvious advantage of the basic sites introduced by ligand functionalization is the resistance to leaching. In comparison with functionalization of metal sites through coordination, the functionalization of ligands is realized by covalent bonding. As a result, the leaching of active sites during catalysis can be well avoided. Thus far, several pathways have been designed for the postsynthetic functionalization of organic ligands, and amino groups can be directly attached to aromatic rings. Also, the aromatic amines and aldehyde tags are suitable for further modification reactions to form new basic sites. Actually, a variety of approaches including click reactions for postsynthetic modification of MOFs have been developed (as summarized by Cohen et al.).^{219–221} Inspired by such approaches, a series of new basic MOFs, which are extremely desirable for organic transformations, is expected to be synthesized via postsynthetic modification.

3. CHARACTERIZATION OF BASIC SITES

Various techniques have been used to characterize the basic sites on MOFs. Results from different techniques present different information regarding the basic characteristics. Each technique is able to reveal part of the characteristics rather than all of them. The combination of data from different techniques

enables one to clarify the characteristics systematically including the strength, amount, and activity of basic sites in MOFs. To date, both experimental methods and theoretical calculations have been employed to evaluate the basicity of MOFs. This section will deal with the experimental techniques first and subsequently the computational ones.

3.1. Experimental Techniques

3.1.1. CO₂-TPD. Temperature-programmed desorption of CO₂ (CO₂-TPD) is a frequently used technique for the evaluation of basic properties. In general, in a TPD plot the desorption temperature of CO₂ can reflect the strength of basic sites, while the desorption amount represents the number of basic sites. A larger peak area means a higher amount of basic sites, and a higher desorption temperature of CO₂ reflects stronger basicity. It should be stated that this technique is hard to express the base strength and the amount of basic sites in an accurate way. Provided that a series of solid catalysts is measured under similar conditions, their relative strength and amount of basic sites can be compared from the CO₂-TPD results.

The CO₂-TPD experiments for MOFs are generally identical to that for conventional solid bases.^{222–224} A certain amount of sample (typically ~0.1 g) is pretreated at a prescribed temperature (e.g., 100 °C) in an inert atmosphere (e.g., N₂ or He) to remove impurities adsorbed on the surface (e.g., water). After the pretreated sample is exposed to CO₂ until saturation, the physically adsorbed CO₂ is purged by an inert gas flow. At last the sample is heated to a certain temperature, and the CO₂ liberated is detected by a thermal conductivity detector (TCD) or MS. A case in point is the work from Ahn's group;⁷⁷ they reported the solvothermal synthesis of a series of typical MOFs with high purity, including IRMOF-1, IRMOF-3, HKUST-1, UiO-66, NH₂-UiO-66, Mg₂DHTP, MIL-101(Cr), and ZIF-8. The TPD plots of CO₂ desorbed from these MOF samples were obtained (Figure 20). No CO₂ signal peaks appeared for IRMOF-1 and HKUST-1, showing that no basic sites existed in these samples. Only one weak peak was observed at about 300 °C in MIL-101(Cr), which could be attributed to medium to strong basicity. The desorption peaks

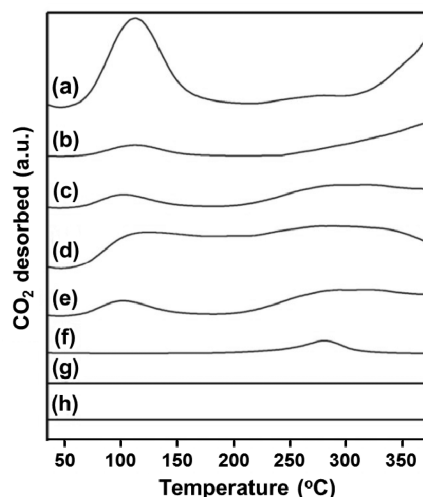


Figure 20. CO₂-TPD profiles of different MOFs (a) NH₂-UiO-66, (b) UiO-66, (c) Mg₂DHTP, (d) IRMOF-3, (e) ZIF-8, (f) MIL-101(Cr), (g) HKUST-1, and (h) IRMOF-1. Adapted with permission from ref 77. Copyright 2012 Elsevier.

of IRMOF-3 and ZIF-8 with similar characteristics were located around 120 and 320 °C, which implies the presence of feeble medium to strong basicity. Mg₂DHTP and UiO-66 exhibited two desorption peaks as well, which were caused by some weak and strong basic sites. Obviously, there were three TPD peaks in the pattern of NH₂-UiO-66 at approximately 120, 300, and 370 °C, corresponding to the significant strong basicity with a distinctively high population of weak basic sites. The amine-functionalized organic ligands (for NH₂-UiO-66 and IRMOF-3) and basic N atoms in the imidazolium ring (for ZIF-8) could contribute to the basicity of MOFs.⁷⁷ Meanwhile, the O atoms in the organic ligands [for UiO-66, Mg₂DHTP, and MIL-101(Cr)] connected to metal clusters via covalent bonding were also likely responsible for the basicity.⁷⁷ On the basis of the CO₂-TPD results, it is apparent that MOFs constructed from N-containing ligands possess stronger basicity than their counterparts without N-containing ligands.

To summarize, CO₂-TPD is an effective technique for the estimation of basicity on MOFs. However, the thermal stability of MOFs should be taken into full account during examination. Due to the existence of organic ligands, the degradation of MOFs can also yield CO₂ in most cases. It is unlikely to distinguish the CO₂ desorbed from basic sites and the CO₂ from MOFs degradation. In other words, CO₂-TPD is not suitable for characterization of basic sites in MOFs with very high strength. In any case, CO₂-TPD can be viewed as a convenient approach for the evaluation of weak and medium basicity with regard to both strength and amount.

3.1.2. IR of Adsorbed CO₂. Apart from CO₂-TPD, IR spectroscopy of adsorbed CO₂ is also a useful technique for characterization of basic MOFs. Carbon dioxide is an electron acceptor and able to function as a Lewis acid to interact with functional groups on MOFs that act as electron donors.²²⁵ IR spectra of adsorbed CO₂ on MOFs can reflect whether the MOFs have basic sites available for the interaction. Because an acidic molecule may interact strongly with basic sites, this technique gives information about the adsorption state of the acidic molecule and subsequently the surface properties of basic MOFs.

For the convenience of comparison, IR spectra of MOFs are often used as background and subtracted from that of CO₂-adsorbed samples. IR spectra of CO₂ adsorbed on two amine-containing MOFs, namely, IRMOF-3 and NH₂-MIL-53(Al), were recorded by Gascon et al. (Figure 21).⁸⁶

The spectrum on IRMOF-3 gave two IR bands (a double band) at 653 and 669 cm⁻¹ as well as a shoulder at 667 cm⁻¹ derived from gaseous CO₂. The double band is caused by the stretching vibration of CO₂, implying the decrease of symmetry after adsorption.²²⁶ The low and high bands could be ascribed, respectively, to in-plane and out-of-plane bending vibrations. The two bands exhibit quite similar intensity in the spectrum, which indicates the presence of only one kind of adsorbed species on IRMOF-3. In comparison with that on IRMOF-3, the IR spectrum of CO₂ adsorbed on NH₂-MIL-53(Al) showed more bands, indicating more complicated interaction between CO₂ molecules and the MOF framework.⁸⁶ Four IR bands at 649, 655, 661, and 669 cm⁻¹ appeared (Figure 21B). Among them, the bands at 669 and 655 cm⁻¹ are in accord with that detected on IRMOF-3, while the two new IR bands are consistent with that observed on unfunctionalized MIL-53(Cr).²²⁶ These results indicate that CO₂ adsorbed on NH₂-MIL-53(Al) via two approaches, creating electron donor-acceptor complexes by interacting with amine and hydroxyl

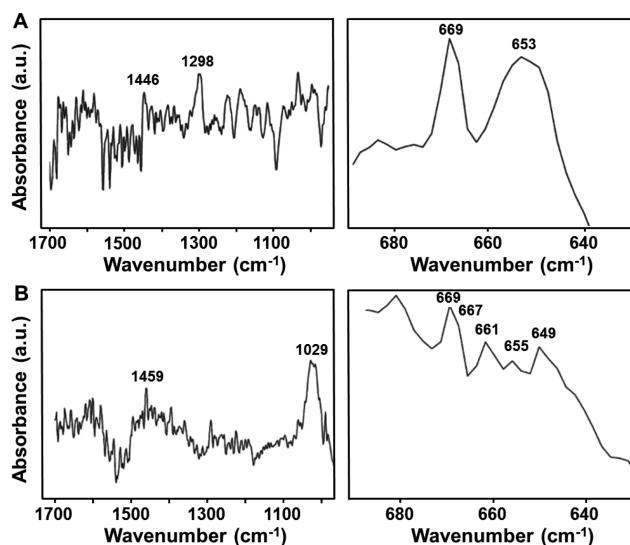


Figure 21. IR spectra of CO₂ adsorbed on (A) IRMOF-3 and (B) NH₂-MIL-53(Al). Adapted with permission from ref 86. Copyright 2009 Elsevier.

groups in the framework. Additionally, a number of IR bands were visible in 1000–1700 cm⁻¹. The band at 1450 cm⁻¹ suggests the formation of carbamic acid due to the interaction of CO₂ with amines. Subsequently, carbonates (bicarbonates or formates) may be produced from the reaction of carbamate species with adsorbed hydroxyl groups or adsorbed water. Besides, hydrogen carbonates were also created as evidenced by the band at 1029 cm⁻¹ in NH₂-MIL-53(Al). These IR data of adsorbed CO₂ thus show the distinct feature of basicity in different MOFs.

In summary, CO₂ is able to interact with the functional groups, and the adsorption state of CO₂ reflects the surface structure of MOFs including basic sites. In contrast to CO₂-TPD that treats MOFs at elevated temperatures, IR spectra of adsorbed CO₂ can be recorded at room temperature. This is of great importance for MOFs, especially those with lower thermal stability, although thermal treatment of inorganic materials (such as silica) at high temperatures is quite common. On the other hand, the IR spectra of adsorbed CO₂ are sort of complex sometimes. The combination of theoretical and experiential methods is beneficial to give rational explanations.

3.1.3. IR of Adsorbed Pyrrole. Besides CO₂, pyrrole is also an acidic molecule which can be used to probe the basicity of materials. Due to the interaction of the hydrogen atoms in pyrroles with basic sites, the IR band of the N–H stretching vibration shifts to a low wavenumber.^{227,228} Moreover, such a shift of frequency is related to the strength of basic sites.

IR of adsorbed pyrrole was used to characterize the basicity of Ni₂DHTP.²²⁹ In a typical measurement, the sample is treated under vacuum at certain temperatures to remove the contaminants on the surface, and then the vapor of pyrrole is introduced for adsorption at room temperature.¹⁷⁸ After the physical adsorbed pyrrole is evacuated, the spectrum of chemisorbed pyrrole can be collected. In the IR spectrum of pyrrole adsorbed on Ni₂DHTP, two distinct signals were observed (Figure 22).¹⁷⁸ The absorption band at 3405 cm⁻¹ could be assigned to the stretching vibration of the NH group interacting via an NH– π complex with the ring of another pyrrole molecule. Another absorption band with a high intensity was monitored at 3253 cm⁻¹, distinguishing from

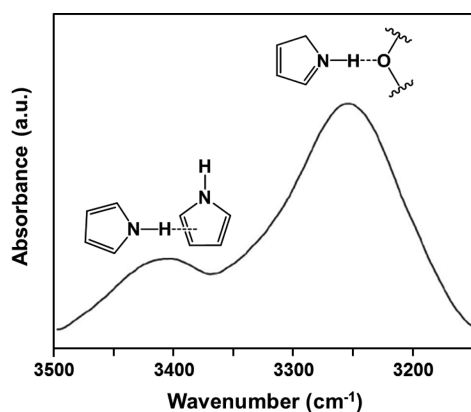


Figure 22. IR spectrum of pyrrole adsorbed on Ni₂DHTP. Adapted with permission from ref 178. Copyright 2014 Elsevier.

the exact position of free pyrrole (3500 cm⁻¹). The strong bathochromic shift of this band was generally attributed to pyrrole species interacting with an H-bond acceptor (e.g., a basic site on the surface) stronger than pyrrole. The shift of the N–H stretching vibration frequency could be viewed as a measure for the base strength of the adsorption site. A shift of 250 cm⁻¹ is analogous to that detected for the interaction of pyrrole with alumina.²³⁰ In addition to Ni₂DHTP, the IR spectra of pyrrole adsorbed on Mg₂DHTP, Co₂DHTP, and Zn₂DHTP were studied (Table 5).¹⁷⁸ A shift of 202–270 cm⁻¹

Table 5. N–H Vibration Frequency [$\nu(\text{N–H})$] of Free Pyrrole as Well as Pyrrole Adsorbed on Different M₂DHTP Materials¹⁷⁸

sample	$\nu(\text{N–H})$ (cm ⁻¹)
free pyrrole	3500
pyrrole on Mg ₂ DHTP	3230
pyrrole on Co ₂ DHTP	3281
pyrrole on Ni ₂ DHTP	3253
pyrrole on Zn ₂ DHTP	3298

was observed for the N–H vibration of pyrrole, indicating the presence of strong H-bond acceptors in all MOFs. In the meanwhile, different shifts of the N–H vibration band imply that the environment of basic sites is associated with the type of metal ions in M₂DHTP.

To summarize, the adsorption of pyrrole and subsequent characterization with IR spectroscopy provide a good alternative for the investigation of basic MOFs. To interact with a basic site, pyrrole is via the H atom while CO₂ is via the carbon atom as an electron acceptor. As a result, information about the basic properties of MOFs can be obtained. It should be stated that the molecular size of pyrrole is larger than that of CO₂, and some basic sites in small micropores may be inaccessible. In this case, CO₂ can be used as the probe molecule thanks to its small molecular size.

3.1.4. Propyne Adsorption. Propyne is an interesting probe molecule and can explore both the acidity and the basicity of MOFs. This is different from CO₂ and pyrrole, which are only able to probe the basicity. Propyne presents double active centers, a basic center and an acid center, that is, propyne acting as a probe molecule can interact simultaneously with acidic and basic sites.²³¹ As a basic center, the C≡C bond of propyne acts as a proton acceptor and can perturb the IR

$\nu(\text{O–H})$ band of the hydroxyl groups on the surface. As an acidic center, the ≡C–H band as the acid site functions as a proton donor and can undergo a perturbation of its IR $\nu(\text{C–H})$ band in the spectral range. As a result, the basic properties as well as the acidic ones of a MOF can be determined through propyne adsorption.

The experimental process of propyne is similar to that of CO₂ and pyrrole. The sample is pretreated thermally under vacuum followed by introduction of propyne. Adsorption is carried out at different pressures of propyne, and a collection of IR spectra can be obtained. A typical example is the adsorption of propyne on CH₃-MIL-53(Fe), which was synthesized via a solvothermal method from iron(III) perchlorate hydrate and 2-methylterephthalic acid (CH₃-BDC).²³³ In the IR spectrum of CH₃-MIL-53(Fe) after activation, the characteristic bands of $\delta(\text{OH})$ at 843 cm⁻¹ and $\nu(\text{OH})$ at 3646 cm⁻¹ were observed (Figure 23), reflecting the existence of free hydroxyl groups

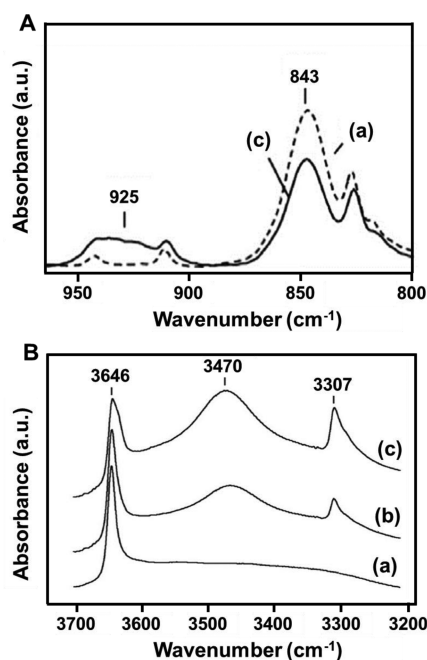


Figure 23. IR spectra in the (A) low and (B) high wavenumber range of (a) CH₃-MIL-53(Fe) pretreated at 150 °C in vacuum followed by introduction of a different amount of propyne at the equilibrium pressure of (b) 2 and (c) 6 mbar at room temperature. Adapted with permission from ref 232. Copyright 2014 Elsevier.

lack of any intraframework interaction.²³² After the adsorption of propyne on CH₃-MIL-53(Fe), the $\nu(\text{OH})$ band of free hydroxyl groups was perturbed and shifted from 3646 to 3470 cm⁻¹. Similarly, the perturbation led to the shift of the $\delta(\text{OH})$ band from 843 to 925 cm⁻¹. Such variations in IR bands demonstrate the creation of hydrogen-bonded species via modes 1 and 3, where the C≡C bond plays the role of proton acceptor (Figure 24). In addition, an intense band was visible at 3307 cm⁻¹ in the range of $\nu(\equiv\text{CH})$ and was somewhat dissymmetric toward lower wavenumbers.²³² The peak shape of $\nu(\equiv\text{CH})$ did not vary after introduction of more propyne. The band at 3307 cm⁻¹ means the formation of the special species adsorbed on CH₃-MIL-53(Fe), where the ≡CH group acts as proton-donor center and forms a hydrogen bond via mode 2 as shown in Figure 24. The IR spectra of adsorbed propyne indicate that the OH groups free of intramolecular interactions

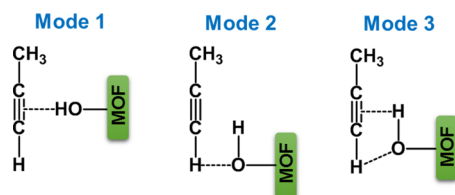


Figure 24. Proposed adsorbed modes of propyne on acidic sites (mode 1), basic sites (mode 2), and acid–base pair sites (mode 3).

in $\text{CH}_3\text{-MIL-53(Fe)}$ have a predominant effect on the interaction with the probe molecule propyne as proton donors and via the oxygen atom. Besides $\text{CH}_3\text{-MIL-53(Fe)}$, Cl-MIL-53(Fe) and Br-MIL-53(Fe) were also examined through IR spectra of adsorbed propyne.²³² A supplementary interaction was proved at high propyne dosages, involving the halogen atoms, which act as basic sites toward propyne.

In summary, various experimental techniques have been attempted to evaluate the basicity of MOFs. These techniques provide information on different aspects of basic properties. Information on both the strength and the amount of basic sites can be offered by $\text{CO}_2\text{-TPD}$. However, the application of $\text{CO}_2\text{-TPD}$ is limited due to the relatively poor thermal stability of some MOFs. Actually, the desorption of CO_2 on some superbasic sites occurs at temperatures even higher than 700°C .^{224,234} At such harsh conditions no MOFs reported until now can survive. On the contrary, the adsorption of probe molecules (e.g., CO_2 , pyrrole, and propyne) and subsequent characterization with IR spectroscopy can be operated under mild conditions. Most MOFs are capable of preserving their structure during characterization. This characterization technique can afford qualitative results and to some extent quantitative analysis, while the accuracy is dependent on operation conditions. It should be stated that some well-known methods used for characterization of inorganic solid bases have not been employed for basic MOFs to date. A typical one is the measurement of base strength using Hammett indicators.^{17,235,236} During measurement an acidic indicator is adsorbed on the surface of solids whose color can be changed to that of the corresponding conjugate base if the solid base shows sufficient strength to donate electrons to the acidic indicator. For the application of this technique in MOFs, white samples are preferred for the convenience of the observation of color change. In addition, XPS characterization of oxygen and nitrogen can reflect the base strength. A good correlation between the binding energy of the N_{1s} band and the basicity has been established for a wide variety of organic compounds. To discover the basic properties of MOFs systematically, more characterization techniques are expected. Last but not the least, some base-catalyzed reactions such as Knoevenagel condensation can be used as model reactions to characterize solid bases. The capacity of converting different substrates catalytically and the yield of target products over different solid bases reflect their basicity evidently (see section 4).

3.2. Theoretical Calculations

Theoretical calculations play an important role in exploring the basic properties of materials. With the development of calculation methods, theoretical calculations can provide more and more reliable information at a molecular/atomic level. The calculation approach has been used for the investigation of reactions to build an understanding of some catalytic processes. In the meanwhile, this approach is also able to characterize the

structure and properties of the working catalysts.^{237–239} Furthermore, the basicity of newly generated active sites can be verified by theoretical analysis. To examine the basicity of MOFs, DFT-based simulations are frequently employed. The basicity of MOFs can be estimated via two ways, namely, the PA values of MOFs and the electron transfer from MOFs to probe molecules.

The PA of a MOF is closely related to its basicity, and a higher PA suggests a MOF with a high strength of basic sites. After thermal treatment, nitrate can be removed from $\text{Ba}_2(\text{BTC})(\text{NO}_3)$, which leads to the formation of $\text{Ba}^{2+}\text{-O}^{2-}\text{-Ba}^{2+}$ motifs with basicity.⁴ DFT calculations were used to estimate the PAs of newly formed sites and compared with the original nitrate-rich MOF before thermal treatment.¹⁷⁸ The computed PAs of the optimized MOF clusters are shown in Figure 25.⁴ The PA value of the MOF cluster increases

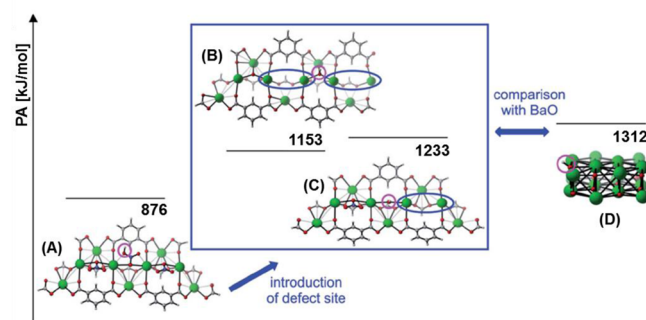


Figure 25. Calculated PAs of the $\text{Ba}_2(\text{BTC})(\text{NO}_3)$ and BaO clusters with optimized structure. (A) Original NO_3 -containing cluster before activation. (B) Cluster containing defect sites after activation. (C) Cluster containing defect sites and NO_3 units after activation. (D) Theoretical PA of the $(\text{BaO})_{16}$ cluster. Protonated structure is illustrated; position of the proton is marked using a purple circle, while position of the defect site is marked using a blue circle. Adapted with permission from ref 4. Copyright 2014 Royal Society of Chemistry.

obviously during decomposition of nitrate. The calculated PA value is enhanced from 876 to 1153 $\text{kJ}\cdot\text{mol}^{-1}$ when a defect site -Ba-[*]-Ba-O- is generated. Moreover, the PA value increases to 1233 $\text{kJ}\cdot\text{mol}^{-1}$ in the case of a defect site combined with a residual nitrate unit. These results indicate the enhancement of basicity after thermal treatment, which is inconsistent with experimental data and confirms the enhanced basicity caused by the formation of defect sites.⁴ To further study the feature of basic sites on the MOF, the typical solid base, cubic BaO , was employed as a comparison. The PA of the BaO cluster is calculated to be 1312 $\text{kJ}\cdot\text{mol}^{-1}$, which is comparable to that of the activated $\text{Ba}_2(\text{BTC})(\text{NO}_3)$. These calculations suggest that the basicity of the newly formed O^{2-} defect sites is similar to that of the edge sites in BaO .

The basic properties of MOFs can be evaluated through calculating the electron transfer from MOFs to probe molecules.⁷⁶ Among probe molecules, CO is a frequently used one and quite sensitive to the electronic environment of adsorption sites. By incorporating W into Cu-BTC , a basic material W-Cu-BTC can be produced and the surface properties are monitored based on DFT calculations using the probe molecule CO .¹²⁶ The calculation was first conducted on Cu-BTC before hybridization. The results showed that Cu centers in Cu-BTC were Lewis acid sites upon CO adsorption. This is in line with the results of CO adsorption over Cu-BTC

reported previously.²⁴⁰ It is known that the CO molecule can bind linearly on the exposed Cu sites of Cu-BTC in an end-on fashion via the carbon atom.²⁴¹ In a similar approach, a linear structure is also observed for the adsorption of CO on the W centers of W-Cu-BTC. This presents a binding energy of 2.15 eV, which is apparently stronger than that of the interaction between CO and MOFs. The natural bond orbital charge analysis implies that 0.04 electrons are transferred from the W site to the CO molecule. Actually, CO is a π -acceptor because of the empty π^* orbitals. It is found that the d orbital of W interacts with the empty LUMO of CO, leading to the formation of π -back-donation. Unlike losing electrons upon adsorption on the parent Cu-BTC, CO draws a small amount of electrons from the exposed W site and makes the W ion function as a Lewis base.¹²⁶ Similarly, by DTF calculations of CO adsorbed on the surface, the existence of basic sites (hydroxyl groups and N^- moieties) on ZIF-8 is evidenced.⁷⁶

In conclusion, theoretical calculations provide useful alternatives to examine the basic properties of MOFs. Through DFT calculations, the PAs and the electron transfer from MOFs to probe molecules can be obtained. On the basis of these data, the basicity of different MOFs can be easily compared. By combining theoretical calculations and experimental techniques, one is likely to gain further insight into the features of basic MOFs. Of course, theoretical calculations can be used to verify the experimental results. More importantly, theoretical calculations are able to predict some properties of materials, which are difficult or inefficient to achieve through experimental approaches. Under the guidance of theoretical calculations, it is possible to develop new basic MOFs via a time-saving and cost-efficient way.

4. CATALYTIC APPLICATIONS

From an environmentally friendly point of view, heterogeneous reactions catalyzed by solid bases are attracting more and more attention.^{242–244} There is a parallel relation between the catalytic performance of a catalyst and its basic properties (e.g., structure, strength, and amount of basic sites).^{245–247} Rational design of basic active centers allows one to substantially improve the catalytic performance, in particular, to enhance the activity and selectivity. In theory, MOFs-derived solid bases have potential to catalyze the well-known “base-catalyzed reactions” like Knoevenagel condensation and Michael addition. Meanwhile, in contrast to conventional solid bases, MOFs may show some different catalytic features due to their particular structural and surface properties. In this section, selected examples of heterogeneous reactions catalyzed by basic MOFs are described (Figure 26). The one-pot cascade reactions catalyzed by basic sites and acidic sites via a cooperative way are included as well.

4.1. Knoevenagel Condensation

Knoevenagel condensation is defined as the reaction between an aldehyde (or ketone) and a compound with an active methylene group. It is an extensively employed approach for C–C bond formation with applications in the synthesis of diverse chemicals such as intermediates of antihypertensive drugs and calcium antagonists.^{248–250} Figure 27 shows the representative Knoevenagel condensation of benzaldehyde with various active methylene compounds (e.g., malononitrile, ethyl cyanoacetate, and ethyl acetoacetate). Different reaction mechanisms have been proposed according to the nature of the solid base catalysts.^{251–253} For catalysts with high base

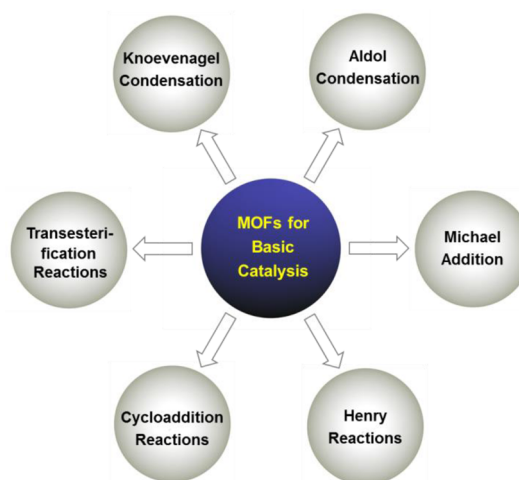


Figure 26. Some of the typical heterogeneous reactions catalyzed by basic MOFs.

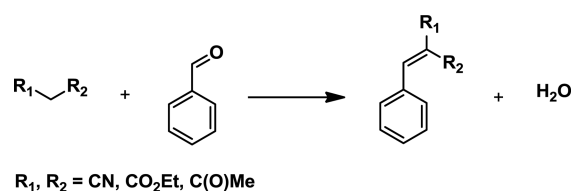


Figure 27. Schematic representation of Knoevenagel condensation of benzaldehyde with methylene compounds.

strength, direct abstraction of proton from active methylene compounds by basic sites takes place. This leads to the formation of carbanion, which attacks the carbonyl carbon atom of benzaldehyde. For weaker bases such as amine-containing MOFs, it is generally accepted that the reaction initiates on the interaction of amine sites with benzaldehyde and an imine intermediate is formed along with one molecule of water.^{138,141} The addition of methylene compound causes a molecular arrangement, leading to the yield of condensation product. This mechanism is not only for amine-containing MOFs but also for other catalysts with similar base strength. It is noticeable that Knoevenagel condensation is not only an approach that generates a C–C bond but also a model reaction to evaluate the basicity of MOFs.

A large number of MOFs with different types of basic sites have been applied to catalyze Knoevenagel condensation. Among various reactants, benzaldehyde and malononitrile/ethyl cyanoacetate are most frequently used, and the activity of different MOFs in these two reactions is summarized in Table 6. Various kinds of basic sites (CUSs-immobilized diamines, pendant amino groups on ligands, alkaline earth metal centers, structural phenolate-derived basic sites, etc.) are active in the reactions. In the case of unfunctionalized MOFs like UiO-66, however, the catalytic activity was negligible, and the yield was <1% for the reaction of benzaldehyde with malononitrile in toluene at 23 °C for 2 h.²⁰⁹ Under the same reaction conditions, the yield over NH_2 -UiO-66 was increased to 5%, indicating that the aromatic amines are active in the Knoevenagel reaction. Interestingly, the sample RNH_2-NH -UiO-66 subjected to further primary aliphatic amines functionalization exhibited much higher activity with a high yield of 97%.²⁰⁹ Similar activity (98% at RT for 2 h) was also observed on MIL-101(Cr)-DETA whose CUSs were grafted

Table 6. Knoevenagel Condensation Reactions of Benzaldehyde (BA) with Malononitrile (MN) or Ethyl Cyanoacetate (EC) Catalyzed by Different Solid Bases

catalyst	synthetic method	reactants, solvent, and ratio (reactant1:reactant2: solvent:catalyst/mmol: mmol:mL:mg)	reaction temperature, time	yield (%)	ref	
MIL-101(Cr)-ED	grafting of ED onto the CUSs of MIL-101(Cr)	BA, MN, cyclohexane, 1:1: 25:20	80 °C, 0.5 h	90	87	
			80 °C, 2 h	96		
			80 °C, 19 h	97	87	
MIL-101(Cr)-BD	grafting of BD onto the CUSs of MIL-101(Cr)	BA, EC, toluene, 1:1:30:20	60 °C, 15 h	89	189	
			60 °C, 15 h	98	189	
			60 °C, 15 h	82	189	
MIL-101(Cr)-DD	grafting of DD onto the CUSs of MIL-101(Cr)	BA, EC, toluene, 1:1:30:20	60 °C, 15 h	82	189	
MIL-101(Cr)-PD	grafting of PD onto the CUSs of MIL-101(Cr)	BA, EC, toluene, 1:1:30:20	60 °C, 15 h	45	189	
MIL-101(Cr)-DETA	grafting of DETA onto the CUSs of MIL-101(Cr)	BA, MN, toluene, 1:2:2.6:10.5	RT, 0.5 h	48	193	
			RT, 2 h	98		
			80 °C, 19 h	97	87	
NH ₂ -MIL-101(Al)	solvothermal synthesis from AlCl ₃ and NH ₂ -BDC	BA, MN, toluene, 1:1:2.5:17.5	80 °C, 0.5 h	61	141	
			80 °C, 3 h	90		
			40 °C, 1 h	10	255	
			40 °C, 3 h	30		
NH ₂ -MIL-101(Fe)	solvothermal synthesis from FeCl ₃ and NH ₂ -BDC	BA, EC, toluene, 1:0.88:0.63:5.7	40 °C, 1 h	52	255	
			40 °C, 3 h	78		
			80 °C, 0.5 h	78	141	
UiO-66	solvothermal synthesis from ZrCl ₄ and BDC	BA, MN, toluene, 1:1.5:2:2.9	80 °C, 3 h	92		
			23 °C, 2 h	<1	209	
			23 °C, 2 h	5	209	
NH ₂ -UiO-66	solvothermal synthesis from ZrCl ₄ and NH ₂ -BDC	BA, MN, toluene, 1:1.5:2:2.9	40 °C, 0.5 h	25	138	
			40 °C, 2 h	79		
			80 °C, 2 h	94		
			40 °C, 0.5 h	27		
			40 °C, 2 h	92		
			60 °C, 0.5 h	58		
			80 °C, 0.5 h	91		
			40 °C, 0.5 h	31		
			40 °C, 2 h	95		
			40 °C, 2 h	5		
			40 °C, 2 h	3		
RNH ₂ -NH-UiO-66	modification of NH ₂ -UiO-66 with 2-methylimidazole	BA, EC, THF, 1:2:1:28.8	40 °C, 2 h	2		
			40 °C, 2 h	<1		
			40 °C, 2 h	97	209	
			23 °C, 2 h	97		
			BA, MN, toluene, 1:2:1:28.8	40 °C, 2 h	<1	
			BA, MN, toluene, 1:1.5:2:10.6	23 °C, 2 h	97	209
			23 °C, 2 h	97		
[Cd(4-BTAPA) ₂ (NO ₃) ₂].6H ₂ O.2DMF	solvothermal synthesis from Cd(NO ₃) ₂ .4H ₂ O and 4-BTAPA	BA, MN, benzene, 1:1:5:50	RT, 12 h	98	153	
IRMOF-3	solvothermal synthesis from Zn(NO ₃) ₂ and NH ₂ -BDC	BA, EC, DMF, 1:0.88:0.63:6.1	40 °C, 0.5 h	58	86	
			40 °C, 2 h	74		
ZIF-8	solvothermal synthesis from Zn(NO ₃) ₂ and H-MeIM	BA, MN, toluene, 1:2:2.6:10.5	RT, 1 h	20	150	
			RT, 2 h	51		
Ba ₂ (BTC)(NO ₃)	activation at 320 °C for 16 h to decompose nitrate	BA, MN, toluene, 1:1:2:50	RT, 6 h	97		
			110 °C, 24 h	97	4	
Co ₂ DHTP	solvothermal synthesis from Co(NO ₃) ₂ and DHTP	BA, EC, toluene, 1:1:2:50	110 °C, 24 h	85		
			70 °C, 2 h	4	178	
			70 °C, 24 h	32		
			70 °C, 2 h	0	178	
		BA, EC, toluene, 1:1: 2:50	70 °C, 24 h	9		

Table 6. continued

catalyst	synthetic method	reactants, solvent, and ratio (reactant1:reactant2: solvent:catalyst/mmol: mmol:mL:mg)	reaction temperature, time	yield (%)	ref
Cu ₂ DHTP	solvothermal synthesis from Cu (NO ₃) ₂ and DHTP	BA, MN, toluene, 1:1:2:50	70 °C, 2 h	39	178
			70 °C, 24 h	69	
			70 °C, 2 h	0	178
Mg ₂ DHTP	solvothermal synthesis from Mg (CH ₃ COO) ₂ and DHTP	BA, MN, toluene, 1:1:2:37	70 °C, 24 h	9	
			70 °C, 2 h	17	178
			70 °C, 24 h	73	
Ni ₂ DHTP	solvothermal synthesis from Ni (CH ₃ COO) ₂ and DHTP	BA, MN, toluene, 1:1:2:50	70 °C, 2 h	3	178
			70 °C, 24 h	69	178
			70 °C, 24 h	99	
Zn ₂ DHTP	solvothermal synthesis from Zn (NO ₃) ₂ and DHTP	BA, MN, toluene, 1:1:2:50	70 °C, 2 h	9	178
			70 °C, 24 h	13	178
			70 °C, 24 h	77	
MgO		BA, MN, toluene, 1:1:2.5:50	80 °C, 0.5 h	72	141
NaY-850N	nitridation of NaY zeolite with ammonia at 850 °C	BA, MN, toluene, 1:1:2.5:50	80 °C, 0.5 h	40	256
NH ₂ -SBA-15	grafting of 3- aminopropyltrialkoxysilane onto SBA-15	BA, EC, cyclohexane, 1:1:25:20	80 °C, 16 h	70	87

with primary aliphatic amines.¹⁹³ In the case of ZIF-8, the yield for the reaction of benzaldehyde with malononitrile was 51% under similar conditions. With the increase of reaction temperature, the yield of target product raises. Under the catalysis of NH₂-MIL-101(Fe) at 80 °C for 3 h, the yield was 92%,²⁵⁴ while the yield was 69% over Ni₂DHTP after reaction at 70 °C for 2 h.¹⁷⁸ These results clearly show that among various active sites, primary aliphatic amines exhibit the best performance in the Knoevenagel condensation.

Attention has been paid to the comparison of basic MOFs with conventional solid bases. The ED-grafted MIL-101(Cr) presented a yield of 97% in the Knoevenagel condensation of benzaldehyde with ethyl cyanoacetate in cyclohexane (80 °C, 19 h).⁸⁷ As a comparison, typical mesoporous silica SBA-15 was functionalized with 3-aminopropyltrialkoxysilane and NH₂-SBA-15 was obtained. The solid base NH₂-SBA-15 was employed to catalyze the same reaction under similar conditions. It is worthy of note that the yield was only 70%. Further calculation displayed that MIL-101(Cr)-ED had a TOF of 328 h⁻¹, which is over 10 times higher than that of NH₂-SBA-15 (32 h⁻¹).⁸⁷ The higher catalytic activity of MIL-101(Cr)-ED could be ascribed to the large surface area as well as the high accessibility of amino groups. However, the poorer activity of NH₂-SBA-15 should be caused by the creation of hydrogen bonds between active amines. The comparison was also conducted between NH₂-MIL-100(Fe) and conventional solid bases. For NH₂-MIL-100(Fe) with pendant aromatic amino groups, the yield reached 78% in the Knoevenagel condensation of benzaldehyde and malononitrile (80 °C, 0.5 h).¹⁴¹ Under the same reaction conditions, the yield over the classic solid base MgO was 72%.¹⁴¹ The nitridized NaY zeolite, NaY-850N, gave a yield of 40%.²⁵⁶ On the basis of these results, it is clear that amine-containing MIL-100(Fe) shows superior

activity in Knoevenagel condensation as compared with conventional solid bases MgO and nitridized NaY zeolite.

The type of diamines grafted onto CUSs has an effect on the catalytic activity in Knoevenagel condensation. As listed in Table 6, the same conditions (the reaction of benzaldehyde with ethyl cyanoacetate in toluene at 60 °C for 15 h) were employed to compare the catalytic activity of MIL-101(Cr) functionalized with different diamines including ED, BD, DD, and PD.¹⁸⁹ The activity of different materials was associated with the pK_a of diamines (Table 3). MIL-101(Cr)-BD showed a high yield of 98% due to the high pK_a value of the diamine BD (10.80). In the case of MIL-101(Cr)-ED and MIL-101(Cr)-PD, the yield was 89% and 45%, respectively, which is lower than that over MIL-101(Cr)-BD owing to the low pK_a value of ED (9.92) and PD (6.31). The low pK_a value of PD (6.31) is caused by the delocalization of a lone pair of electrons on the nitrogen atom. It is interesting to note that under the catalysis of MIL-101(Cr)-DD, the yield was only 82%, despite the high pK_a value of DD (10.97). The lower activity of MIL-101(Cr)-DD is caused by the longest chain length of DD that obstructs the diffusion of substrate/product molecules. In addition, the formation of hydrogen bonds from the neighboring amino groups in the long carbon chain is possible or the pendant amines coordinate with the CUSs.²⁵⁷

Different substrates (both aldehydes and active methylene compounds) show quite different reactivity toward the Knoevenagel condensation over basic MOFs. From the viewpoint of the aldehyde reactant, an interesting size selectivity has been observed.²⁰⁹ Benzaldehyde with a size of 5.0 × 5.6 Å is able to enter all of the three MOFs functionalized with aliphatic amines, namely, RNH₂-NH-Uio-66, RNH₂-NH-MIL-53(Al), and RNH₂-NH-MIL-101(Cr) (Figure 28 and Table 7). All of the three MOFs exhibited high activity (87–99%) in the Knoevenagel reaction of benzaldehyde with

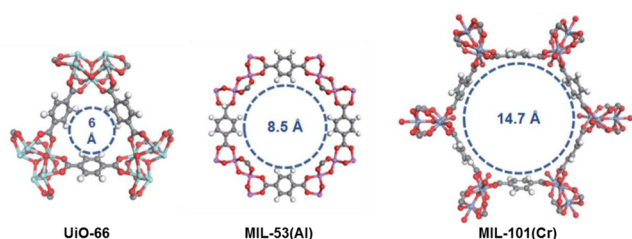


Figure 28. Schematic representation of the window sizes of different MOFs. Adapted with permission from ref 209. Copyright 2015 Royal Society of Chemistry.

malononitrile. When 1-naphthaldehyde, the aldehyde with a larger size, was used for the reaction, RNH₂-NH-UiO-66 and RNH₂-NH-MIL-53(Al) presented obviously declined activity with a yield of 11–27%. The molecular dimension of 1-naphthaldehyde is 5.6 Å × 7.5 Å, which is comparable to the pore windows of RNH₂-NH-UiO-66 and RNH₂-NH-MIL-53(Al). Due to the large pore size of RNH₂-NH-MIL-101(Cr), the conversion of 1-naphthaldehyde was less influenced. An even larger reactant 9-anthracenecarboxaldehyde (9.6 Å × 6.4 Å) was finally employed, and a negligible amount of products was obtained over RNH₂-NH-UiO-66 and RNH₂-NH-MIL-53(Al). Under the catalysis of RNH₂-NH-MIL-101(Cr), the yield of Knoevenagel product was still as high as 35%. From the viewpoint of the active methylene compound, the acidity determines the reactivity, since it acts as a donor molecule in base-catalyzed Knoevenagel condensation. The effect of active

methylene compounds was examined over activated Ba₂(BTC)-(NO₃).⁴ Three typical active methylene compounds malononitrile (pK_a = 11.1, in dimethyl sulfoxide, DMSO), ethyl cyanoacetate (pK_a = 13.1, in DMSO), and ethyl acetoacetate (pK_a = 14.3, in DMSO) were employed to react with benzaldehyde. For the three reactions, the yield of Knoevenagel product was 97%, 85%, and 6%, respectively (see Table 7 for the reaction conditions). This means that the reactivity decreases with the increase of pK_a values of donor molecules. In short, both substrates including aldehydes and active methylene compounds strongly affect the Knoevenagel condensation over basic MOFs.

The polarity of solvent shows a great effect on MOFs-catalyzed Knoevenagel reactions. To examine the effect of solvent polarity, a series of reactions between benzaldehyde and ethyl cyanoacetate was carried out over NH₂-UiO-66 under the same conditions except solvent (Figure 29).¹³⁸ For the reactions in solvents DMF (dielectric constant, ε = 36.7) and DMSO (ε = 48.9) with high polarity, the yield reached 92% and 95%, respectively, at 40 °C for 2 h (Table 6). Protic solvent ethanol (EtOH) with the ε value of 36.7 was a nice medium for the Knoevenagel condensation as well, and the yield was 79%. Nevertheless, in less polar solvents such as toluene (ε = 2.4), ethyl acetate (EtOAc, ε = 6.02), THF (ε = 7.5), and dichloromethane (DCM, ε = 9.1), the yield was less than 5%. Apparently, polar solvents are beneficial to the Knoevenagel condensation. This can be explained by the fact that solvents with high polarity help to stabilize the charged transition-state

Table 7. Effect of Substrate Size on the Knoevenagel Condensation of Different Aldehydes with Malononitrile^a

No.	aldehyde ^b	yield over different catalysts (%)		
		RNH ₂ -NH-UiO-66	RNH ₂ -NH-MIL-53(Al)	RNH ₂ -NH-MIL-101(Cr)
1	 benzaldehyde	97	87	99
2	 1-naphthaldehyde	11	27	93
3	 9-anthracenecarboxaldehyde	0	1	35

^aAdapted with permission from ref 209. Copyright 2015 Royal Society of Chemistry. Reaction conditions: 1 mmol of aldehyde, 1.5 mmol of malononitrile, 2 mL of toluene, 1 mol % of catalyst, RT, 2 h. ^bSimulated by use of Wave function Spartan 08.

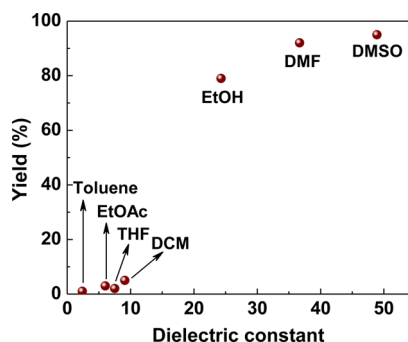


Figure 29. Effect of dielectric constant (ϵ) on the Knoevenagel condensation of benzaldehyde with ethyl cyanoacetate. Reaction conditions: 5 mmol of benzaldehyde, 10 mmol of ethyl cyanoacetate, 5 mL of solvent, 144 mg of catalyst ($\text{NH}_2\text{-UiO-66}$), 40 °C, 2 h. Data used with permission from ref 138. Copyright 2014 Elsevier.

intermediate of the condensation reaction.²⁵⁸ Moreover, the polar solvents DMF and DMSO exhibit a strong hydrogen-bonding acceptor capacity which is able to favor proton transfer.⁸⁶

In summary, MOFs-derived solid bases are widely applied in heterogeneous Knoevenagel reactions of various aldehydes and active methylene compounds. Although reaction conditions may vary in the literature, it is possible to compare the activity of different catalysts under similar reaction conditions. MOFs with different basic sites show quite different activity. For instance, MOFs functionalized with aliphatic amines are obviously superior to that with aromatic amines. Some factors such as the molecular size of aldehydes, the acidity of active methylene compounds, and the polarity of solvents affect the reactions significantly. Because Knoevenagel condensation has been carried out on a large number of MOFs, it can be used as a probe reaction to characterize the basicity of catalysts as well. For MIL-101(Cr)-ED obtained by grafting the diamine ED onto CUSs, the activity in Knoevenagel condensation is higher than the well-known solid base $\text{NH}_2\text{-SBA-15}$. Also, the catalytic activity of $\text{NH}_2\text{-MIL-100(Fe)}$ containing pendant amines is comparable to, if not higher than, the conventional solid bases MgO and nitrified NaY zeolite. This information is valuable for a comparison of the basicity of different basic MOFs as well as the basicity between MOFs and conventional solid bases.

4.2. Aldol Condensation

Aldol condensation is another important group of organic reactions available for C–C bond formation.^{259,260} The aldol condensation includes reactions producing β -hydroxy aldehydes (β -aldols) or β -hydroxy ketones (β -ketols) by self-condensations or mixed condensations of aldehydes and ketones as well as reactions yielding α,β -unsaturated aldehydes or α,β -unsaturated ketones.²⁶¹ The α,β -unsaturated ketones are formed by the dehydration of intermediates β -aldols or β -ketols. By and large, the aldol condensation is catalyzed by either acids or bases, but the latter is more frequently employed.^{262,263} Basic MOFs are catalytically active in a variety of aldol condensation reactions between ketones (e.g., acetone, cyclohexanone, acetophenone, and cyclopentanone) and aldehydes (e.g., aromatic aldehydes with different substituting groups including NO_2 , Cl, Br, Me, and OMe).^{106,115,261,264} Representative examples of the reactions between aldehydes and a typical ketone (cyclopentanone) are shown in Figure 30.

The Mg-based MOF, $\text{Mg}_3(\text{PDC})(\text{OH})_3(\text{H}_2\text{O})_2$, was employed to catalyze aldol condensation due to its basic feature as

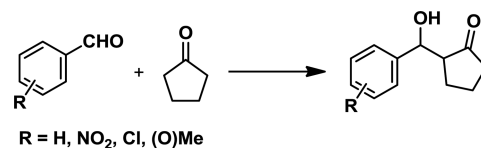


Figure 30. Schematic representation of the Aldol reaction of aldehydes with a typical ketone cyclopentanone.

shown above.¹⁰⁶ To avoid the self-condensation of aldehydes, the aldol reactions were carried out in the presence of an excess amount of ketones.²⁶⁴ A mixture of THF/ H_2O was used as the medium for reactions by Koner's group.¹¹⁵ They found that the ratio of THF to H_2O strongly affected the reactions. The highest yield of β -aldol product could be obtained in the medium with 3:1 THF/ H_2O for the reaction of acetone and *p*-nitrobenzaldehyde (82%, Table 8).²⁶¹ Such a yield was much higher than that obtained in the single solvent THF (62%) or water (29%). The optimum solvent was then employed for the aldol reactions of various substrates as listed in Table 8. In the reactions investigated, all aldehydes were converted to their corresponding β -aldols as the individual product. The catalytic activity of the Mg-based MOF was compared with the conventional solid base MgO. In contrast to the yield of 82% over $\text{Mg}_3(\text{PDC})(\text{OH})_3(\text{H}_2\text{O})_2$ for the aldol reaction of acetone and *p*-nitrobenzaldehyde in 6 h, the yield of 75% was obtained over MgO in 24 h.^{261,265} This indicates that the Mg-based MOF is superior to the traditional solid base MgO with regard to aldol reaction. It is known that unsaturated ketones can be further produced from the dehydration of aldols. However, all of the reactions listed in Table 8 were conducted at a temperature of 5–10 °C. Under such conditions, aldols were formed as the sole product. With the increase of reaction temperature, the aldols can be further converted to corresponding unsaturated ketones.²⁶⁴

The structure of aldehydes and ketones greatly influences the aldol reaction on basic MOFs. From the viewpoint of aldehydes, both the type of substituting group and its position in the benzene ring matter. For benzaldehyde without additional substituting groups, the yield of aldol product is 58% (Table 8).²⁶¹ The presence of nitro, an electron-accepting group, in the ring facilitates the reaction, and the yield from the aldol condensation of acetone and *p*-nitrobenzaldehyde increased to 82%. Similarly, the yield of β -aldol product increased to 69% by replacing benzaldehyde with *p*-chlorobenzaldehyde. In contrast, introduction of an electron-donating group like methyl in the ring hampers the aldol reactions evidently. The yield declined to 46% for the reaction of acetone with *p*-methylbenzaldehyde. The effect of the position of substituting groups can be reflected from the reactions involving *p*-nitrobenzaldehyde, *o*-nitrobenzaldehyde, and *m*-nitrobenzaldehyde. Upon reaction with acetone, the yield of β -aldol product was 82%, 77%, and 70%, respectively (Table 8).²⁶¹ The presence of a nitro group at the ortho and para positions offers a negative mesomeric and inductive effect, which enhances the electrophilicity of the aldehyde group. However, the nitro substituent at the meta position provides merely the negative inductive effect. For *o*-nitrobenzaldehyde and *p*-nitrobenzaldehyde, the steric hindrance at the ortho position may obstruct the reaction. From the viewpoint of the other substrates, namely, ketones, the yield of β -aldol product overall declined in the order of acetone > acetophenone > cyclopentanone.²⁶¹ In the case of cyclopentanone and

Table 8. Aldol Reactions of Different Aldehydes with Ketones Catalyzed by $Mg_3(PDC)(OH)_3(H_2O)_2^a$

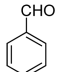
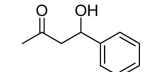
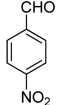
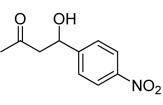
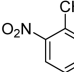
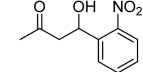
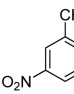
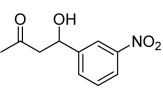
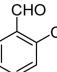
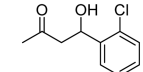
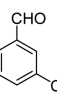
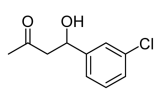
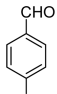
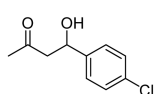
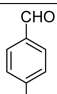
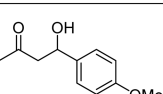
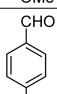
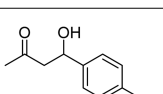
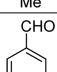
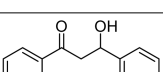
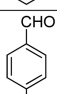
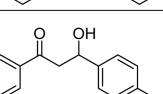
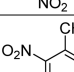
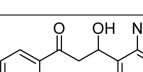
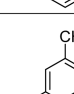
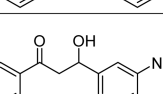
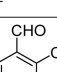
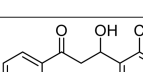
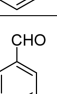
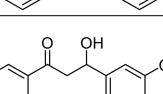
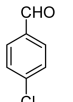
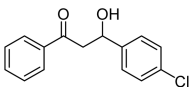
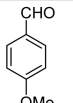
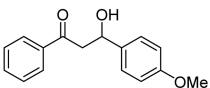
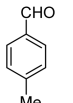
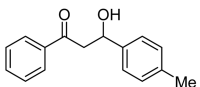
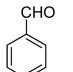
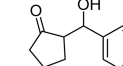
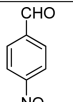
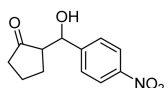
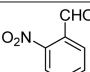
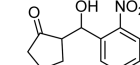
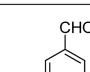
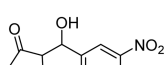
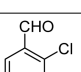
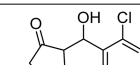
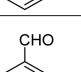
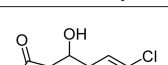
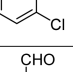
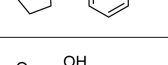
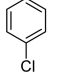
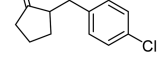
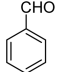
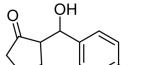
No.	ketone	aldehyde	product	isolated yield (wt%)	TON
1	acetone			58	84
2	acetone			82	120
3	acetone			77	112
4	acetone			70	100
5	acetone			80	109
6	acetone			74	102
7	acetone			69	92
8	acetone			52	79
9	acetone			46	65
10	acetophenone			50	79
11	acetophenone			78	116
12	acetophenone			71	110
13	acetophenone			65	97
14	acetophenone			75	106
15	acetophenone			70	96

Table 8. continued

No.	ketone	aldehyde	product	isolated yield (wt%)	TON
16	acetophenone			66	87
17	acetophenone			44	72
18	acetophenone			37	61
19	cyclopentanone			51	74
20	cyclopentanone			75	112
21	cyclopentanone			70	107
22	cyclopentanone			64	96
23	cyclopentanone			74	102
24	cyclopentanone			70	94
25	cyclopentanone			65	84
26	cyclopentanone			45	69
27	cyclopentanone			36	59

^aData used with permission from ref 261. Copyright 2013 Royal Society of Chemistry. Reaction conditions: 2 mmol of aldehyde, 4 mmol of ketone, 3 mL of THF, 1 mL of H₂O, 5 mg of catalyst, 5–10 °C, 6 h.

acetophenone, a similar tendency to acetone in the aldol reactions was observed.

Besides the Mg-based MOF, another alkaline earth metal Ba-based MOF, Ba(PDC)H₂O, was also catalytically active in the aldol reactions.¹¹⁵ For the reaction of acetone with benzaldehyde, the yield of β -aldol product was 67%. The reaction conditions were identical to that for Mg₃(PDC)(OH)₃(H₂O)₂ as shown in Table 8 except temperature (5–10 °C for Ba-MOF and 0–5 °C for Mg-MOF) and time (8 h for Ba-MOF and 6 h for Mg-MOF). It is reasonable to consider that the reaction conditions for the Ba-MOF are equivalent to,

if not stricter than, that for Mg-MOF. As a result, Ba-MOF with a yield of 67% should be more active than Mg-MOF with a yield of 58% from the reaction of acetone with benzaldehyde under their respective conditions. Similarly, for the reaction between acetone and *p*-nitrobenzaldehyde, the yield was 96% over Ba-MOF and apparently higher than that over Mg-MOF (82%).^{115,261} These results indicate that Ba(PDC)H₂O is more active upon aldol reactions than Mg₃(PDC)(OH)₃(H₂O)₂, which is consistent with the order of base strength of the corresponding alkaline earth metal oxides.

For MOFs-based catalysts, attention should be paid to their stability in catalytic processes. After the catalytic reactions are finished, basic MOF catalysts can be recovered through filtration or centrifugation followed by additional treatments such as washing and drying. The structure of recovered MOFs is usually characterized by XRD. For instance, $\text{Mg}_3(\text{PDC})(\text{OH})_3(\text{H}_2\text{O})_2$ and $\text{Ba}(\text{PDC})\text{H}_2\text{O}$ were analyzed by XRD after aldol reactions.^{115,261} Quite similar XRD patterns of the recovered MOFs to the fresh ones were observed. This suggested that the structure of basic MOFs was well maintained after the aldol reactions. The recyclability of MOFs in aldol condensation was also examined. Under the catalysis of $\text{Mg}_3(\text{PDC})(\text{OH})_3(\text{H}_2\text{O})_2$, the yield at the fifth cycle was 80% for the reaction of acetone with *p*-nitrobenzaldehyde, which was analogous to the fresh one (82%).²⁶¹ $\text{Ba}(\text{PDC})\text{H}_2\text{O}$ also exhibited high stability upon recycling, and the conversion could be well kept after several runs.¹¹⁵

To summarize, both Knoevenagel and aldol reactions are elegant approaches for C–C bond formation, while the application of basic MOFs in aldol reactions is much less. Besides alkaline earth metals-based MOFs, amine-containing MOFs are also good catalysts for aldol condensation, and attention should be given to the catalysis of this kind of solid base. In the aldol condensation of a series of aldehydes and ketones, the Ba-based MOF is superior to its Mg-based counterpart, which is in line with the order of basicity of the corresponding metal oxides. It is interesting to note that the Mg-based MOF, $\text{Mg}_3(\text{PDC})(\text{OH})_3(\text{H}_2\text{O})_2$, shows better catalytic activity in comparison with the traditional solid base MgO. The alkaline earth metals-based MOFs exhibit good stability and recyclability in aldol reactions and can be used several times without loss of activity.

4.3. Michael Addition

The Michael reaction typically refers to the base-catalyzed addition of a nucleophile (Michael donor) to an activated α,β -unsaturated carbonyl-containing compound (Michael acceptor).^{266,267} The Michael addition is also normally termed conjugate addition and attracts increasing attention in the synthesis of fine chemicals as well as functional polymers for various applications.^{268,269} Basic MOFs are catalytically active in a range of Michael addition reactions.^{4,178,191} Characteristic examples of the Michael addition reactions between different donors and a typical acceptor (methyl vinyl ketone) are illustrated in Figure 31. In this subsection, the catalytic activity

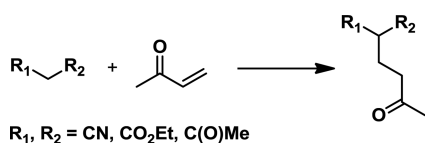


Figure 31. Schematic representation of Michael addition of different donors with a typical acceptor methyl vinyl ketone.

of different MOFs in Michael addition will be compared, and the effect of the donor on the reaction will be then discussed over the optimized catalysts.

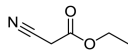
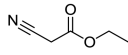
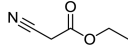
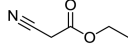
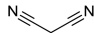
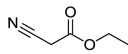
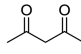
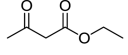
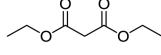
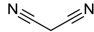
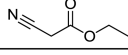
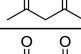
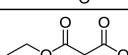
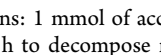
The activity of M_2DHTP ($\text{M}^{2+} = \text{Mg}^{2+}, \text{Co}^{2+}, \text{Ni}^{2+}, \text{Cu}^{2+}$, and Zn^{2+}) in the Michael addition of methyl vinyl ketone with ethyl cyanoacetate is summarized in Table 9. As described above, the basicity derives from phenolate oxygen atoms in the frameworks, which is supposed to be active in Michael addition. The type of metal center influences the reaction obviously. For the

reaction of methyl vinyl ketone with ethyl cyanoacetate at 70 °C, the catalyst Ni_2DHTP gave a yield of 26% in 2 h and 66% in 24 h.¹⁷⁸ Other catalysts showed lower yields under the same reaction conditions, for instance, the yield was 6% in 2 h and 35% in 24 h over Mg_2DHTP . The catalytic activity of M_2DHTP is in accordance with their basicity (see section 2.1.4), indicating that the Michael addition is catalyzed by basic sites in this case. After proper activation to decompose the nitrite, $\text{Ba}_2(\text{BTC})(\text{NO}_3)$ was also active in Michael addition.⁴ Because some reactions were conducted at the exactly same conditions for $\text{Ba}_2(\text{BTC})(\text{NO}_3)$ and Ni_2DHTP , it is easy to compare their catalytic activity (Table 9). By comparing the yields from the reactions of a series of substrates, it is safe to say that Ni_2DHTP is somewhat superior to $\text{Ba}_2(\text{BTC})(\text{NO}_3)$.

The effect of donor on Michael addition has been studied by use of both Ni_2DHTP ¹⁷⁸ and $\text{Ba}_2(\text{BTC})(\text{NO}_3)$.⁴ The same acceptor methyl vinyl ketone was employed for all reactions, while various donors with $\text{p}K_a$ values ranging from 11.1 to 16.4 were used (Table 9). Prior to Michael addition, the effect of donor on Knoevenagel condensation was investigated using Ni_2DHTP .¹⁷⁸ The yield of Knoevenagel product is closely related to the $\text{p}K_a$ value of the donor, and the highest yield was obtained for the most acidic compound malononitrile with the lowest $\text{p}K_a$ value of 11.1. In the Michael addition over Ni_2DHTP , however, the reactivity of different donors is complicated. On the face of it, the yield was reverse from what was expected. The lowest yield was detected for malononitrile (18% in 2 h) with the lowest $\text{p}K_a$ value of 11.1, while the highest yield was obtained for not so acidic donor, ethyl acetoacetate (93% in 2 h), with a $\text{p}K_a$ value of 14.3. By use of diethyl malonate with a $\text{p}K_a$ value of 16.4, the yield was 66% at 2 h, which was lower than that using ethyl acetoacetate.¹⁷⁸ A similar trend was also found in the Michael addition reactions catalyzed by $\text{Ba}_2(\text{BTC})(\text{NO}_3)$.⁴ To clarify such a tendency in reactivity, Valvenkens et al. proposed a different mechanism for Michael addition, in which both donor and acceptor could be activated.¹⁷⁸ During the reaction, a proton is abstracted from the donor by a basic site in MOFs, while the α,β -unsaturated carbonyl compound is able to be activated through coordination on a CUS. Nonetheless, if the anion is more readily created from the donor, as for the more acidic donor molecules, or if there is an excessive amount of coordinated nitrile groups (such as in malononitrile), the CUSs might be entirely occupied by either carbanions stemmed from the donor or the nitrile groups. The coordination could limit the activation of acceptor molecule and subsequently hinder the overall reaction. As a result, malononitrile possessing two nitrile functional groups exhibits the poorest activity, which is closely followed by the donor ethyl cyanoacetate. The site-blocking phenomenon is less anticipated for other donors without nitrile groups including ethyl acetoacetate, 2,4-pentanedione, and diethyl malonate.

In conclusion, MOFs with certain basicity are capable of catalyzing Michael addition reactions between various nucleophiles and α,β -unsaturated ketones under prescribed conditions. The results from the reactions of various substrates demonstrate that Ni_2DHTP (with basic sites derived from phenolate oxygen atoms) is somewhat more active than $\text{Ba}_2(\text{BTC})(\text{NO}_3)$ (with basic sites similar to corresponding alkaline earth metal oxide). Interestingly, the reactivity of donor molecules in the Knoevenagel condensation over MOFs is dominated by their $\text{p}K_a$ values, but total different donor reactivity order is observed in the Michael addition reactions.

Table 9. Michael Addition Reactions of Methyl Vinyl Ketone with Different Donors under the Catalysis of Different Basic MOFs^a

catalyst	donor	p <i>K</i> _a of donor (DMSO)	reaction temperature, time	yield (%)
Mg ₂ DHTP		13.1	70 °C, 2 h	6
			70 °C, 24 h	35
Co ₂ DHTP		13.1	70 °C, 2 h	9
			70 °C, 24 h	42
Cu ₂ DHTP		13.1	70 °C, 2 h	13
			70 °C, 24 h	38
Zn ₂ DHTP		13.1	70 °C, 2 h	19
			70 °C, 24 h	44
Ni ₂ DHTP		11.1	110 °C, 2 h	18
			110 °C, 24 h	55
		13.1	70 °C, 2 h	26
			70 °C, 24 h	66
			110 °C, 2 h	32
			110 °C, 24 h	75
		13.3	110 °C, 2 h	58
			110 °C, 24 h	99
		14.3	110 °C, 2 h	93
			110 °C, 24 h	99
	16.4	110 °C, 2 h	66	
		110 °C, 24 h	86	
Ba ₂ (BTC)(NO ₃) ^b		11.1	110 °C, 24 h	33
		13.1	110 °C, 24 h	77
		13.3	110 °C, 24 h	99
		14.3	110 °C, 24 h	99
		16.4	110 °C, 24 h	1

^aData from refs 4 and .178 Reaction conditions: 1 mmol of acceptor (methyl vinyl ketone), 1 mmol of donor, 2 mL of toluene, 50 mg of catalyst.

^bThe sample was activated at 320 °C for 16 h to decompose nitrate.

This is due to the different mechanism for the activation of substrate molecules. Moreover, Michael addition commonly requires stronger bases than Knoevenagel condensation, whereas competition between the two reactions is observed owing to different reaction mechanism.¹⁷⁸

4.4. Henry Reaction

Henry (or nitroaldol) reaction is a valuable alternative for C–C bond formation between a nitroalkane and a carbonyl compound bearing α hydrogens. Representative examples of Henry reactions between different nitroalkanes and a typical carbonyl compound, *p*-nitrobenzaldehyde, are depicted in Figure 32. As a coupling reaction in essential, the overall transformation in Henry reaction enables the formation of a C–C bond with the concomitant generation of a new

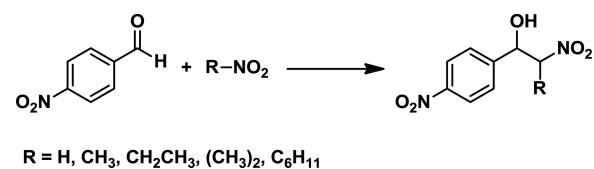


Figure 32. Schematic representation of Henry reactions of different nitroalkanes with a typical carbonyl compound *p*-nitrobenzaldehyde.

functional group, namely, the β -nitroalcohol function. Henry reactions are widely employed in organic synthesis. The product nitroalcohols are useful intermediates in the preparation of nitroalkenes, α -nitroketones, and β -aminoalcohols derivatives (e.g., ephedrine and norephedrine).^{270,271} Previous

reports show that Henry reaction could be catalyzed by the Lewis acidic Cu(II) centers in the MOF framework.²⁷² In this section, Henry reaction catalyzed by the basic sites of MOFs will be described.

The MOF, [Zn(TPDC)]·DMF·2H₂O, with the potential structural linker DABCO, was utilized to catalyze Henry reactions.¹⁹⁵ Because only one nitrogen atom in DABCO is coordinated on the Zn center, the other free nitrogen atom can act as a basic site. Such a MOF has 1D channels containing cage-like open spaces interconnected with windows possessing a smaller size of about 6.48 Å × 5.32 Å.¹⁹⁶ The accessibility of the free nitrogen atoms in MOF channels has been evidenced by the high adsorption enthalpy of CO₂.¹⁹⁶ Henry reactions between *p*-nitrobenzaldehyde and nitroalkanes with various molecular dimension were carried out over [Zn(TPDC)]·DMF·2H₂O (Figure 33).¹⁹⁵ If the Henry reaction takes place

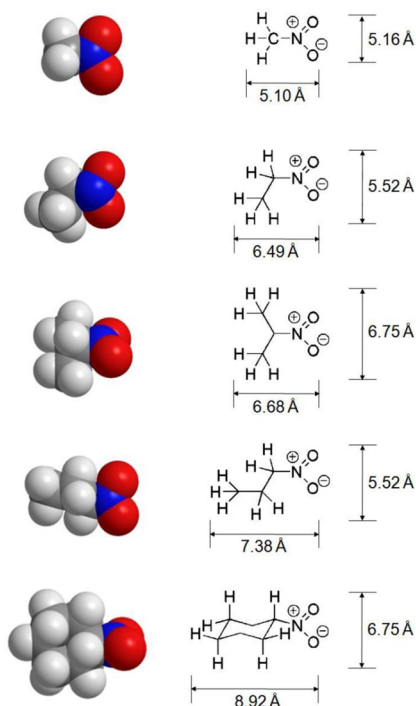


Figure 33. Molecular dimensions of various nitroalkanes. To estimate the dimensions of the molecules, two suitable atoms were selected to calculate their center-to-center distance by Chem3D followed by adding their van der Waals radii. Color scheme: for N atoms, blue; for O atoms, red; for C atoms, gray; for H atoms, white. Adapted with permission from ref 195. Copyright 2011 Royal Society of Chemistry.

on the basic sites in the 1D channels, the conversion would be inversely proportional to the molecular dimension of nitroalkanes. This is caused by the reactant size selection effect of the microporous channels as reported in the catalytic processes involving zeolites.^{273,274}

On the basis of the assumption above, a series of Henry reactions between *p*-nitrobenzaldehyde and nitroalkanes was conducted over [Zn(TPDC)]·DMF·2H₂O (Figure 34).¹⁹⁵ When nitromethane with the smallest molecular dimension (5.10 Å × 5.16 Å) was used as the reactant, the conversion reached 80%. Under the same reaction conditions, the conversion decreased sharply to 34% for the reactant nitroethane with a larger molecular dimension (6.49 Å × 5.20 Å). Further increasing the molecular dimension of reactant

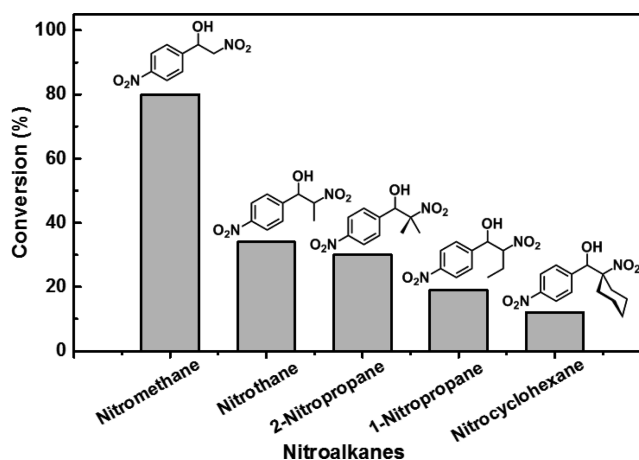


Figure 34. Henry reactions of *p*-nitrobenzaldehyde with nitroalkanes possessing different molecular dimensions over [Zn(TPDC)]·DMF·2H₂O. Reaction conditions: 1 mmol of *p*-nitrobenzaldehyde, 10 mL of nitroalkanes, 10 mg of catalyst, 60 °C, 120 h. Adapted with permission from ref 195. Copyright 2011 Royal Society of Chemistry.

molecules from 2-nitropropane (6.68 Å × 6.75 Å) to 1-nitropropane (7.38 Å × 5.52 Å) and nitrocyclohexane (8.92 Å × 6.75 Å), the conversion decreased accordingly from 2-nitropropane (30%) to 1-nitropropane (19%) and nitrocyclohexane (12%). Hence, the conversion of reactants is strongly dependent on the molecular dimension of nitroalkanes. The electronic effect of nitroalkanes was examined as well.¹⁹⁵ Nitromethane has a p*K*_a value of 10.24, which is obviously higher than 2-nitropropane (p*K*_a = 7.7–7.8), nitroethane (p*K*_a = 8.60), and 1-nitropropane (p*K*_a = 8.98). In other words, nitromethane is less acidic than other nitroalkanes investigated but the most active in the Henry reaction. It is thus clear that the higher reactivity of nitromethane is ascribed to the size-selectivity effect rather than the electronic effect.¹⁹⁵

The stability of MOFs after Henry reactions has attracted attention as well due to the importance of catalyst stability in practical applications. In order to assess the stability, the powder XRD pattern of retrieved [Zn(TPDC)]·DMF·2H₂O after the fourth run between *p*-nitrobenzaldehyde and nitromethane was recorded (Figure 35).¹⁹⁵ The recovered MOF presented an almost identical XRD pattern to the as-synthesized one after desolvation, revealing the MOF is robust for the Henry reaction. It is interesting to witness a weak diffraction line at 2θ of about 5.6°, which was also detected at a comparable position for the MOF subjected to desolvation and CHCl₃ exchange.^{195,196} Hence, in the process of catalytic reactions, the solvate molecules in the as-synthesized MOF were exchanged with the reactant molecules nitroalkanes. In this regard, the as-synthesized MOF could be used for catalysis without any pretreatment. During the Henry reactions involving nitroalkanes, the solvate molecules (i.e., water and DMF) were exchanged with the substrates readily.¹⁹⁵

To summarize, the free nitrogen atoms in MOFs are able to serve as active basic sites for Henry reactions. In the case of MOFs with pore sizes comparable to the dimensions of reactant molecules, the strong dependence of reactant dimension is observed while the electronic effect (reflected by the p*K*_a values of reactant) is negligible. Although the activity of the nitrogen atoms in DABCO has been demonstrated, the base strength is weaker than that of a variety of basic centers

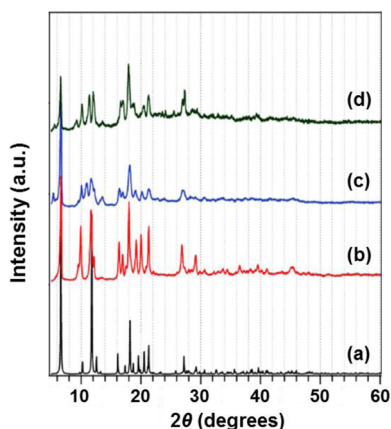


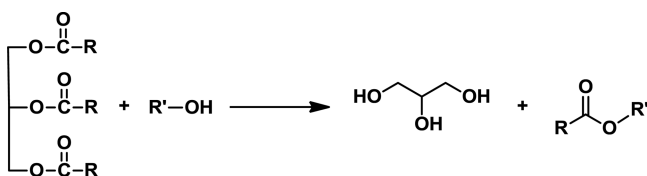
Figure 35. Powder XRD patterns of (a) the simulation from X-ray crystallography, (b) as-synthesized $[\text{Zn}(\text{TPDC})]\cdot\text{DMF}\cdot 2\text{H}_2\text{O}$, (c) CHCl_3 -exchanged and desolvated MOF, and (d) the recovered sample after 4 times of Henry reaction in nitromethane. Adapted with permission from ref 195. Copyright 2011 Royal Society of Chemistry.

such as primary amines. The applications of other basic MOFs in Henry reactions are thus expected. In short, Henry reaction is a useful alternative for the synthesis of intermediates. Further transformations involving the newly formed β -nitroalkanol functionality (e.g., oxidation, reduction, and dehydration) will follow, thereby depending on the requirements and the overall goals of multistep synthetic plans.

4.5. Transesterification Reaction

Transesterification is one of the classic organic reactions with numerous laboratorial and industrial applications. It is a process where an ester is transformed to another one through interchange of the alkoxy moiety.^{275–278} Organic chemists take advantage of this reaction quite often as a convenient means to prepare esters. Besides producing the esters of oils and fats, transesterification processes also play a central role in the paint industry such as curing of alkyd resins. Since transesterification is an equilibrium process, the transformation occurs essentially by simply mixing the two components. In other words, excess alcohol can be used to shift the equilibrium to the products side due to the reversibility of the reaction. It has long been known that the presence of a base catalyst can accelerate the conversion, which is similar to aldol condensation.²⁷⁹

The transesterifications of triglycerides (e.g., glyceryl triacetate and glyceryl tributyrate) with alcohols (e.g., methanol) are important model reactions for biodiesel production (Figure 36). A series of basic MOFs was employed to catalyze the transesterification of glyceryl triacetate with methanol.¹⁹⁰ Due to the Lewis acidity resulted from CUSs, the



$\text{R}' = \text{Me, Et, } n\text{-Pr, } n\text{-Bu, } i\text{-Pr, } t\text{-Bu}$

Figure 36. Schematic representation of transesterification reactions of triglycerides with different alcohols.

unfunctionalized MOFs showed weak catalytic performance, for example, 10.4% of conversion over IRMOF-10 (Table 10).¹⁹⁰

Table 10. Transesterification Reactions of Triglycerides with Methanol under the Catalysis of Different Basic MOFs^a

entry	catalyst	triglyceride	reaction temperature, time	conversion (%)
1	IRMOF-1	glyceryl triacetate	50 °C, 4 h	9.2
2	IRMOF-10	glyceryl triacetate	50 °C, 4 h	10.4
3	$\text{NH}_2\text{-MIL-53(Al)}$	glyceryl triacetate	50 °C, 3 h	3.9
4	IRMOF-1-ED	glyceryl triacetate	50 °C, 3 h	>99.9
5	IRMOF-10-ED	glyceryl triacetate	50 °C, 4 h	>99.9
6	$\text{NMe}_2\text{-NH}_2\text{-MIL-53(Al)}$	glyceryl triacetate	50 °C, 4 h	>99.9
7	IRMOF-1-DMAP	glyceryl triacetate	50 °C, 4 h	92.0
8	IRMOF-10-DMAP	glyceryl triacetate	50 °C, 4 h	93.3
9	IRMOF-1-ED	glyceryl tributyrate	60 °C, 6 h	>99.9
10	IRMOF-10-ED	glyceryl tributyrate	60 °C, 6 h	>99.9
11	$\text{NMe}_2\text{-NH}_2\text{-MIL-53(Al)}$	glyceryl tributyrate	60 °C, 6 h	94.7
12	IRMOF-1-DMAP	glyceryl tributyrate	60 °C, 6 h	78.1
13	IRMOF-10-DMAP	glyceryl tributyrate	60 °C, 6 h	83.9

^aData used with permission from ref 190. Copyright 2014 Royal Society of Chemistry. Reaction conditions for the reaction of glyceryl triacetate with methanol: 181 mg of glyceryl triacetate, 1 mL of methanol, 30 mg of catalyst. For the reaction of glyceryl tributyrate with methanol: 302 mg of glyceryl triacetate, 1.2 mL of methanol, 30 mg of catalyst.

By contrast, the amine-containing MOFs exhibited much better activity, and almost 100% of conversion was observed over IRMOF-10-ED. Similar conversion of >99.9% was also detected on IRMOF-1-ED and $\text{NMe}_2\text{-NH}_2\text{-MIL-53(Al)}$. Slightly lower conversion was obtained under the catalysis of the other two MOFs modified with DMAP, namely, IRMOF-1-DMAP (92.0%) and IRMOF-10-DMAP (93.3%). These results evidently show that basic sites in MOFs are responsible for the activity in transesterification. However, different basic MOFs exhibit quite different catalytic activity. It is known that the catalytic activity is related to a collection of factors including catalyst structure, morphology, pore architecture, basic feature, etc. Hence, it is not easy to correlate the activity with one special characteristic of a catalyst. Nevertheless, for IRMOF-1 and IRMOF-10, they possess parallel structure and the identical postsynthetic modification is used for introduction of basic species ED and DMAP.¹⁹⁰ This makes it possible to clarify the relationship between basic feature and catalytic activity quantitatively. Interestingly, a linear correlation between the density of basic sites and the TOF of four MOFs in the transesterification of glyceryl triacetate with methanol is observed (Figure 37).¹⁹⁰ These results demonstrate that the density of basic sites plays an important role in the transesterification reactions.

Both reactants have an essential effect on the transesterification reactions over basic MOFs. In addition to glyceryl

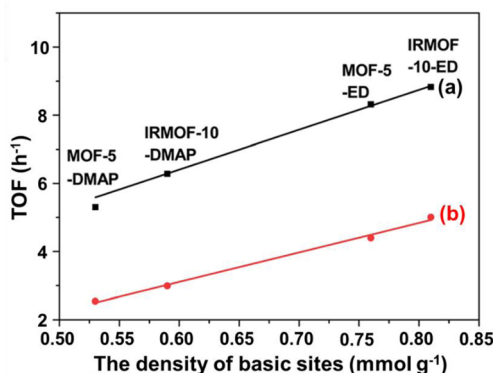


Figure 37. Catalytic activity of basic MOFs versus the density of basic sites in the transesterification reactions of methanol with (a) glyceryl triacetate and (b) glyceryl tributyrate. Adapted with permission from ref 190. Copyright 2011 Royal Society of Chemistry.

triacetate, the transesterification of glyceryl tributyrate with methanol can also proceed smoothly over basic MOFs. When amine-functionalized MOFs were used as catalysts, the conversion was higher than 78.1% (Table 10).¹⁹⁰ Taking IRMOF-10-ED as an example, almost 100% conversion can be obtained. By comparing the catalytic activity between glyceryl triacetate and glyceryl tributyrate, it is easy to find that the reactivity of short-chain glyceryl triacetate is higher than the long-chain counterpart. Further evidence is displayed in Figure 37; the TOF of glyceryl triacetate was about twice as high as that of glyceryl tributyrate methanolysis.¹⁹⁰ This can be explained by the molecular sieving effect of MOFs, namely, the higher accessibility of relatively smaller glyceryl triacetate to the basic sites inside the pores of MOFs than that of glyceryl tributyrate.^{276,280} The effect of alcohols on the transesterification reactions was examined as well.⁷⁶ For the transesterification of vegetable oil with alcohols, a series of linear alcohols including methanol, ethanol, 1-propanol, and 1-butanol as well as branched ones including isopropanol and *tert*-butanol was employed (Figure 38). Obviously, the reactivity of alcohols relies on their feature greatly. The

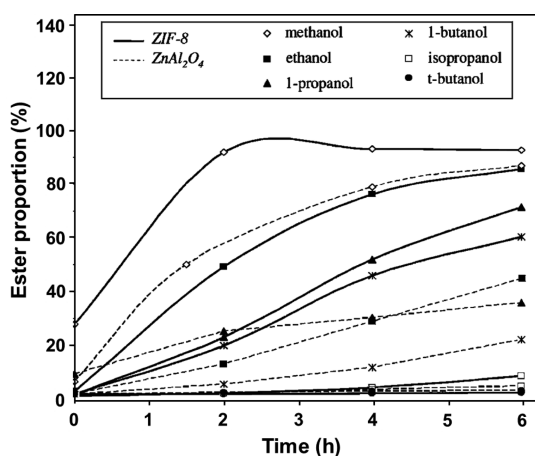


Figure 38. Transesterification of vegetable oil with different alcohols into monoglyceride under the catalysis of ZIF-8 as well as the conventional catalyst ZnAl_2O_4 . Reaction conditions: 50 g of methanol and rapeseed oil (molar ratio 27.5), 0.5 g of catalyst, 200 °C. Adapted with permission from ref 76. Copyright 2010 American Chemical Society.

conversion declined with the acidity of linear alcohols, while quite low conversion was detected for branched alcohols. The traditional catalyst ZnAl_2O_4 was also applied to catalyze the same reactions.⁷⁶ For the reaction of vegetable oil with methanol, ZIF-8 was able to convert oil to monoglycerides completely within 2 h. Under the same conditions, however, the conversion over ZnAl_2O_4 was only about 55%. A similar trend was also observed when other alcohols were used for the reactions, indicating the better performance of ZIF-8 in comparison with the traditional ZnAl_2O_4 catalyst in transesterification.

The recyclability of basic MOFs in heterogeneous catalysis attracts much attention. The recyclability of a typical catalyst, IRMOF-10-ED, in the transesterification between methanol and glyceryl triacetate was evaluated.¹⁹⁰ In order to gain deep insight into the reusability, the recycling experiments were carried out at a low conversion level. For the fresh catalyst, the conversion of glyceryl triacetate was 57.6%. The conversion declined progressively, and after four cycles, only 36.6% of glyceryl triacetate was converted. These results suggest that the catalyst IRMOF-10-ED was partially deactivated. To inspect the reasons, XRD and IR techniques were employed to characterize the catalysts before and after catalysis.¹⁹⁰ The recovered sample exhibited an identical XRD pattern to the fresh IRMOF-10-ED, implying that the crystalline structure was well preserved. From IR spectra it is easy to find that the relative intensity of ED in IRMOF-10-ED declined apparently after reaction. By combining the XRD and IR results it is clear that the loss of activity is caused by the leaching of ED in the IRMOF-10-ED catalyst. Taking into consideration that the active species ED are grafted onto CUSs via coordination, the leaching in the polar medium methanol after several recycles is conceivable.

In conclusion, in comparison with some other solid base-catalyzed reactions like Knoevenagel condensation, transesterification requires catalysts with stronger basicity. To improve the catalytic efficiency, a series of amine-functionalized MOFs have been introduced. These functionalized MOFs display admirable activity in transesterification. By comparing the activity for MOFs with similar structure and identical functionalization method, a linear correspondence between the density of basic sites and the activity in terms of TOF is proposed. It should be stated that for the diamines grafted onto CUSs, the leaching of diamines from MOFs is observed in the process of transesterification involving polar solvents like methanol. In this regard, the covalently attached basic species should be more stable upon recycling. ZIF-8 exhibits considerable activity in transesterification at high temperatures, and such activity is higher than the traditional ZnAl_2O_4 catalyst.

4.6. Cycloaddition Reaction

In recent years, cycloaddition reactions involving CO_2 have received increasing attention since the excessive emission of CO_2 is considered a predominant anthropogenic contributor to climate change and greenhouse effect.^{281–284} Actually, CO_2 is an alternative C_1 source and can be transformed into useful chemicals. One of the few commercial routes using CO_2 as a raw material in this area is the insertion of CO_2 into epoxides to produce cyclic carbonates by chemical fixation,^{285–291} that is, one carbon atom and two oxygen atoms from CO_2 can be incorporated in one step with high atom efficiency. In general, the addition reaction of CO_2 to epoxides can produce cyclic carbonates, which have wide applications such as alkylating agents, electrolytes in secondary batteries, monomers for

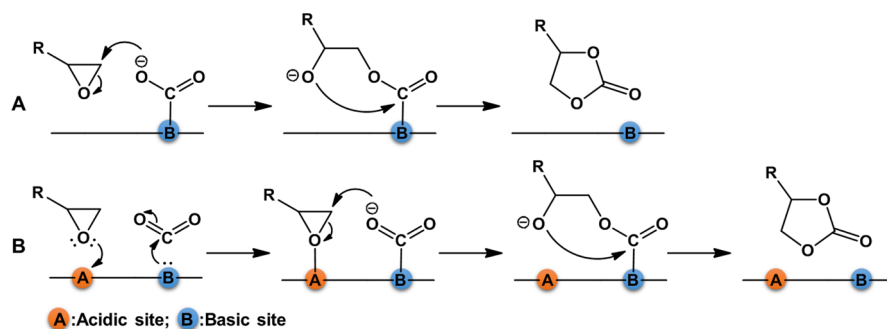


Figure 39. Reaction pathway for the cycloaddition between an epoxide and CO_2 catalyzed by (A) basic sites as well as (B) acidic and basic sites. Adapted with permission from ref 77. Copyright 2012 Elsevier.

synthesizing polycarbonate, and polar aprotic solvents. Interestingly, such reactions can be catalyzed by basic sites, acidic sites, or acidic/basic sites.^{77,133,292–297} The reaction mechanism involving basic sites is presented in Figure 39. In the presence of a basic site, CO_2 is adsorbed and activated followed by insertion into the C–O bond of the epoxide through nucleophilic attack.²⁹⁸ The high ring strain in the ethylene oxide portion of styrene oxide can easily lead to ring opening once it is attacked by a δ^- charge in CO_2 . Such nucleophilic attack will be enhanced once the δ^- charge in CO_2 becomes stronger after the adsorption of CO_2 on a basic site. Figure 39 also depicts the mechanism of the cycloaddition reaction catalyzed by the collaboration of acidic and basic sites.⁷⁷ CO_2 adsorbed on a basic site and an epoxide adsorbed on an adjacent acidic site lead to the reaction of intermediates and subsequently the production of cyclic carbonates.

A variety of basic MOFs have been utilized to catalyze the cycloaddition reactions as summarized in Table 11. In the reaction of CO_2 with styrene oxide, 4-phenyl-1,3-dioxolan-2-one was detected as a single product in most cases.^{77,296} The high conversion (>94%) was obtained by using $\text{NH}_2\text{-UiO-66}$ and Mg_2DHTP as the catalysts after the reaction for 4 h. Moreover, the conversion over $\text{NH}_2\text{-UiO-66}$ reached 70% in 1 h, suggesting the best activity among the MOFs investigated.⁶⁵ Under the catalysis of HKUST-1 and $\text{MIL-101}(\text{Cr})$ possessing open metal centers, a moderate conversion of styrene oxide was observed (48% and 68% in 4 h, respectively). Despite their good catalytic performance in Knoevenagel condensation, IRMOF-3 and ZIF-8 exhibited relatively poor activity in cycloaddition and the conversion was only 33% and 11%, respectively. In the case of IRMOF-1 , the conversion was as low as 1%, indicating the negligible activity in cycloaddition. To clarify the catalytic performance, the acidity/basicity of these MOF catalysts was determined by use of TPD.⁷⁷ The basicity of MOFs decreased in the order of $\text{IRMOF-3} > \text{NH}_2\text{-UiO-66} > \text{ZIF-8} > \text{Mg}_2\text{DHTP} \gg \text{MIL-101}(\text{Cr}) > \text{HKUST-1}$, IRMOF-1 , while the sequence of acidity is Mg_2DHTP , $\text{MIL-101}(\text{Cr}) > \text{NH}_2\text{-UiO-66} > \text{HKUST-1} \gg \text{ZIF-8}$, IRMOF-1 , IRMOF-3 . Inspection of acidity/basicity implied that the high catalytic activity in cycloaddition appeared in MOFs containing both basic and acidic sites (e.g., $\text{NH}_2\text{-UiO-66}$ and Mg_2DHTP).⁷⁷ Similar results were also reported in conventional solid bases such as $\text{Cs}/\text{Al}_2\text{O}_3$, pointing out that the collaboration of basic and acidic sites favors the cycloaddition reactions.²⁹⁹

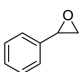
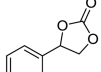
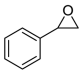
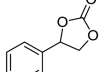
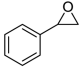
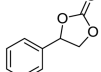
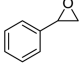
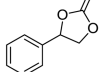
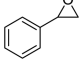
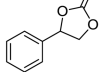
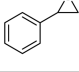
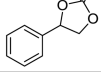
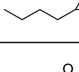
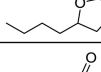
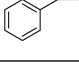
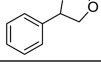
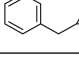
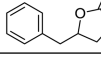
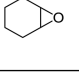
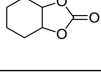
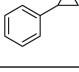
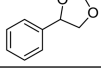
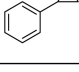
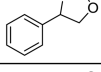
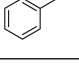
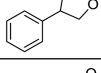
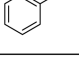
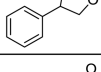
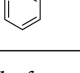
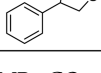
In order to understand the catalytic behavior of MOFs deeply, the cycloaddition reactions were conducted under the catalysis of the synthetic precursors of MOFs as a comparison.^{133,292} In the case of $\text{NH}_2\text{-UiO-66}$, the precursors

including Zr compounds and $\text{NH}_2\text{-BDC}$ were employed as catalysts.⁶⁵ The catalyst $\text{NH}_2\text{-UiO-66}$ gave a high conversion of 95% as shown in Table 11. Under identical conditions, no styrene oxide was converted at all by using ZrO_2 or ZrCl_4 as catalysts, while the ligand $\text{NH}_2\text{-BDC}$ showed a conversion of 45%. When both Zr compounds and $\text{NH}_2\text{-BDC}$ were used for catalysis, the conversion was raised obviously. The combination of $\text{NH}_2\text{-BDC}$ with ZrCl_4 was more active (with the conversion of 73%) than that of $\text{NH}_2\text{-BDC}$ combined with ZrO_2 (with the conversion of 65%), which can be ascribed to the much higher solubility of ZrCl_4 in the solvent chlorobenzene (ZrO_2 was insoluble at all). In short, the catalytic activity of precursors is obviously lower than that of the corresponding MOF.⁶⁵ This reveals the heterogeneous catalysis of MOFs in cycloaddition, in which basic and acidic active sites are located closely in frameworks with high porosity and accessibility.

The structure of the reactant epoxide has an apparent effect on the cycloaddition of CO_2 . Usually three kinds of epoxides are employed, namely, aliphatic epoxides, styrene oxide, and cyclohexene oxide (disubstituted epoxide).^{294,296} Cycloaddition reactions of typical epoxides with CO_2 over $\text{NH}_2\text{-UiO-66}$ are shown in Table 11.⁷⁷ Despite the use of different epoxides, $\text{NH}_2\text{-UiO-66}$ was able to convert them into corresponding cycloaddition products. The conversion of hexene oxide was 97% after the reaction for 3 h, which was analogous to that of styrene oxide after the reaction for a longer time (4 h). In the case of cyclohexene oxide, the conversion was 83% in 4 h and increased to 95% with prolonged time to 6 h. The low reactivity of the disubstituted epoxide, cyclohexene oxide, should be attributed to the high steric hindrance during cycloaddition. The general reactivity over $\text{NH}_2\text{-UiO-66}$ declines in the order of aliphatic epoxides > styrene oxide > cyclohexene oxide,⁷⁷ which is also observed in other MOF catalysts such as $\text{NH}_2\text{-UMCM-1}$ ²⁹⁶ and MOF-205 .²⁹²

To summarize, the cycloaddition reactions are rather different with some typical base-catalyzed reactions such as Knoevenagel condensation and transesterification reactions. Not only basic sites but also acidic sites are active in cycloaddition, and the existence of additional acidic sites increases the catalytic activity of basic sites. It has been reported that a nucleophilic cocatalyst (tetraalkylammonium halides) is favorable to the cycloaddition reactions.^{133,292,296} In some cases almost full conversion of epoxides can be obtained at room temperature in the presence of the cocatalyst, whereas in the absence of the cocatalyst, around 100 °C is normally required to realize the same conversion. This indicates that different concepts should be adopted for design of efficient catalyst systems for cycloaddition. Thanks to the use of CO_2 , which is a

Table 11. Cycloaddition of CO₂ with Different Epoxides under the Catalysis of Various Materials^a

catalyst	epoxide	cycloaddition product	reaction time (h)	conversion (%)
IRMOF-1			4	1
ZIF-8			4	11
IRMOF-3			4	33
HKUST-1			4	48
MIL-101(Cr)			4	63
Mg ₂ DHTP			1	59
			4	94
NH ₂ -UiO-66			3	97
			1	70
			4	95
			4	96
		4	83	
		6	95	
ZrO ₂			4	0
ZrCl ₄			4	0
NH ₂ -BDC			4	45
NH ₂ -BDC+ZrO ₂			4	65
NH ₂ -BDC+ZrCl ₄			4	73

^aData from ref 77. Reaction conditions: 5 mmol of epoxide, 2 MPa CO₂ pressure, 30 mL of chlorobenzene, 20 mg of catalyst, 100 °C.

gaseous reactant at reaction temperatures, the cycloaddition reactions are often carried out at certain pressures. As a result, a

high-pressure stainless-steel autoclave is frequently employed in the reactions.

4.7. One-Pot Cascade Reaction

Nature offers enzyme catalysts which can catalyze complex reactions via a sophisticated way. The high catalytic performance of enzymes is due to the cooperation of isolated active sites with different functionalities. Inspired by enzymes, fabrication of artificial cooperative catalysts attracts much attention.^{300–302} MOFs are of great interest for the synthesis of cooperative catalysts because both metal sites and ligands are available for functionalization.^{303–306} In addition to basic sites, the antagonistic acidic sites can coexist in MOFs due to site isolation.^{307,308} The obtained bifunctional MOF catalysts can catalyze some interesting cascade reactions in one pot (e.g., deacetalization–Henry reaction²¹³ and Meinwald rearrangement–Knoevenagel reaction¹⁴⁰), which is unlikely to realize in homogeneous catalytic systems.

The bifunctional catalyst $\text{SO}_3\text{H-MIL-101}(\text{Cr})\text{-NH}_2$ with $-\text{NH}_2$ and $-\text{SO}_3\text{H}$ immobilized, respectively, on the metal center and ligand was used to catalyze one-pot deacetalization–Henry reaction (Figure 40).²¹³ The deacetalization of

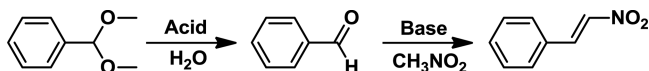


Figure 40. One-pot cascade reaction including deacetalization of benzaldehyde dimethyl acetal over acidic sites and subsequent Henry reaction of benzaldehyde with nitromethane over basic sites.

benzaldehyde dimethyl acetal to benzaldehydes takes place over acidic sites, and subsequently, the Henry reaction of benzaldehyde with nitromethane occurs over basic sites, leading to the formation of 2-nitrovinylbenzene as the ultimate product. As shown in Table 12, the initial substrate

Table 12. One-Pot Cascade Reaction Including Deacetalization of Benzaldehyde Dimethyl Acetal (BDA) to Benzaldehyde (BA) and Henry Reaction of BA to 2-Nitrovinyl Benzene (NVB)^a

entry	catalyst	conversion of BDA (%)	yield of BA (%)	yield of NVB (%)
1	$\text{SO}_3\text{H-MIL-101}(\text{Cr})\text{-NH}_2$	100	3.0	97.0
2	$\text{SO}_3\text{H-MIL-101}(\text{Cr})\text{-NHBOC}$	100	100	trace
3	$\text{MIL-101}(\text{Cr})\text{-NH}_2$	trace	trace	trace
4	$\text{SO}_3\text{H-MIL-101}(\text{Cr})$	100	100	0
5	$\text{SO}_3\text{H-MIL-101}(\text{Cr})\text{-NH}_2$ + <i>p</i> -toluene sulfonic acid	100	95.5	4.5
6	$\text{SO}_3\text{H-MIL-101}(\text{Cr})\text{-NH}_2$ + ethylamine	trace	trace	trace
7	<i>p</i> -toluene sulfonic acid + ethylamine	trace	trace	trace

^aData used with permission from ref 213. Copyright 2012 Royal Society of Chemistry. Reaction conditions: 1 mmol of benzaldehyde dimethyl acetal (BDA), 5 mL of CH_3NO_2 , 90 °C, 24 h.

benzaldehyde dimethyl acetal was converted to the ultimate product 2-nitrovinylbenzene with a high yield of 97% over the bifunctional catalyst $\text{SO}_3\text{H-MIL-101}(\text{Cr})\text{-NH}_2$.²¹³ Under the catalysis of $\text{SO}_3\text{H-MIL-101}(\text{Cr})$ and $\text{SO}_3\text{H-MIL-101}(\text{Cr})\text{-NHBOC}$, benzaldehyde was detected as the main product, and the yield of 2-nitrovinylbenzene was very tiny since there was no basic active sites. When $\text{MIL-101}(\text{Cr})\text{-NH}_2$ was employed as the catalyst, only a trace amount of 2-nitrovinylbenzene was yielded due to the absence of acidic

sites; meanwhile, the yield of benzaldehyde was negligible. After introduction of the corresponding amount of free base (ethylamine) or acid (*p*-toluene sulfonic acid) to $\text{SO}_3\text{H-MIL-101}(\text{Cr})\text{-NH}_2$, the yield of 2-nitrovinylbenzene decreased sharply because of the contamination of acidic or basic active sites. In addition, no catalytic activity was observed upon use of the homogeneous mixture of free base (ethylamine) and acid (*p*-toluene sulfonic acid). These results thus demonstrate the cooperative catalytic behavior of the acid–base bifunctional $\text{SO}_3\text{H-MIL-101}(\text{Cr})\text{-NH}_2$ in the deacetalization–Henry cascade reaction.

It is known that some metal centers in MOFs may act as Lewis acids, which can thus cooperate with basic sites to catalyze cascade reactions in one pot. A case in point is $\text{NH}_2\text{-MIL-101}(\text{Al})$ assembled from trimeric Al^{3+} clusters and $\text{NH}_2\text{-BDC}$.¹⁴⁰ The free amino groups function as basic sites, while Al^{3+} centers function as acidic sites. Through the cooperation of acidic/basic sites, $\text{NH}_2\text{-MIL-101}(\text{Al})$ can thus catalyze the Meinwald rearrangement–Knoevenagel condensation cascade reaction.¹⁴⁰ As depicted in Figure 41, Meinwald rearrangement

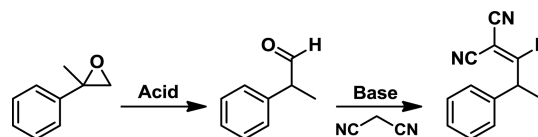


Figure 41. Typical one-pot cascade reaction including the Meinwald rearrangement of epoxide over acidic sites and subsequent Knoevenagel condensation of aldehyde with malononitrile over basic sites.

of the epoxide first takes place over acidic sites followed by the Knoevenagel condensation of intermediate aldehyde with malononitrile over basic sites. Control experiments were also conducted by using acid or base as a sole catalyst.¹⁴⁰ In the presence of AlCl_3 , a typical Lewis acid, the Meinwald rearrangement reaction proceeded, whereas the Knoevenagel condensation did not occur. When dimethyl 2-aminoterephthalate, an ester analogue of the organic ligand in $\text{NH}_2\text{-MIL-101}(\text{Al})$, was employed as the catalyst, the Meinwald rearrangement cannot take place at all. This indicates that the cascade Meinwald rearrangement–Knoevenagel condensation reaction only proceeds in the presence isolated acidic and basic sites which work in a cooperative way.

To summarize, the bifunctional MOFs with basicity and acidity are highly efficient in catalyzing one-pot cascade reactions including deacetalization–Henry reaction and Meinwald rearrangement–Knoevenagel reaction, which are unlikely to realize by monofunctional catalysts with only basic or acidic sites. In consideration of possessing two antagonistic functions, acid–base bifunctional MOFs exhibit activity that is not achievable by homogeneous catalysts. By spatial isolation in frameworks, two incompatible active sites coexist and work cooperatively. Regardless of the increasing interest, the possibility of combining bifunctional catalytic sites in MOFs remains largely unexplored. These acid–base bifunctional MOFs possess potential in catalyzing various cascade reactions. In addition to acidic sites, other functionalities (e.g., metal nanoparticles) are also possible to be introduced to MOFs, leading to fabrication of novel catalysts with two or even more functionalities.

5. CHARACTERISTIC FEATURES OF MOFS-DERIVED SOLID BASES

In general, basic MOFs are one important branch on the great tree of solid bases. They have some common features of solid bases, for instance, the obvious merits regarding postreaction separation and reuse over their homogeneous analogues. However, the special composition (constructed coordinately from metal ions and organic ligands) makes basic MOFs different with conventional solid bases derived from alumina, zeolites, mesoporous materials, etc. In this section, characteristic features of MOFs-derived solid bases will be described (from the aspects of preparation, activation, and basic properties) and compared with those of conventional basic materials.

5.1. Preparation

For the preparation of MOFs-derived solid bases, the stability (including hydrostability and thermal stability) of MOFs should be taken into consideration. Some classic methods for the preparation of solid bases may not be applicable to MOFs directly. Taking the conventional solid base K_2O/Al_2O_3 as an example, it is prepared via impregnation of the support Al_2O_3 in the aqueous solution of precursor KNO_3 followed by thermal treatment to decompose KNO_3 to basic species K_2O . For the use of MOFs as supports, organic solvents (e.g., methanol) are recommended more than water. Water molecules can attack coordination bonds in frameworks, and degradation of the structure may occur for some MOFs with low hydrostability.^{309–311} MOFs are less thermally stable when compared to the conventional inorganic supports such as Al_2O_3 . Therefore, the stability of MOFs is crucial during thermal treatment to decompose the base precursor. As a result, thermal treatment of MOFs is often conducted under vacuum, which decreases the temperature for treatment. For instance, the nitrate in $Ba_2(BTC)(NO_3)$ can be decomposed at about 300 °C under a pressure of <1 mbar.⁴ Recently, our work reveals that KNO_3 can be converted to basic species on some MOFs at 300 °C under atmospheric pressure, which is achieved by using the redox interaction between the base precursor (possessing oxidizing ability) and some metal ions like Cr^{3+} in MIL-101(Cr) (possessing reducing ability). Therefore, it is necessary to design proper methods to generate basic sites on MOFs in terms of the nature of given MOFs. It is worth mentioning that rapid progress has been made on the synthesis of MOFs with enhanced stability; some MOFs (e.g., PCN-224,³¹² PCN-777,³¹³ and BUT-12³¹⁴) are reported to be stable in harsh conditions including boiling water, concentrated HCl, and/or NaOH solution. These robust MOFs provide interesting alternatives for construction of solid bases.

In fact, the occurrence of MOFs brings new opportunities for the preparation of solid bases. The special structure of MOFs (constructed from metal ions and organic ligands) presents some marked advantages for generation of basicity. First, the diversity of origins and types of basicity is noticeable for MOFs-derived solid bases. The structure of basic MOFs is tailorable through the judicious choice of metal centers and organic ligands, which gives almost infinite variations in theory and is impossible for traditional solid bases. On one hand, by using proper metal ions and/or functional ligands it is possible to fabricate MOFs with intrinsic basicity. These MOFs are inherently active in heterogeneous basic catalysis. On the other hand, basicity can be incorporated into the frameworks through postsynthetic modification. This is particularly useful

for MOFs without inherent basicity. Second, the methods for introduction of basic sites to MOFs are noteworthy. Both metal centers and organic ligands in MOFs are easy to modify with basic species. These connections are abundant, site isolated, and periodically organized, which is not possible to realize for any conventional supports. For example, an interesting strategy for functionalization of metal sites is coordination using diamines. One of the amino groups in diamine is immobilized on a metal site by coordination, and the other pendant amino group acts as the basic site. This convenient method is widely used for functionalization of MOFs but improbable in the case of conventional supports such as mesoporous silica due to the absence of CUSs.^{315–317} In addition, various methods have been developed for covalent attachment of functionalities on the ligands of MOFs, as shown in Cohen's reviews and references therein.^{73,219} In short, the discovery of MOFs opens up a great deal of opportunities for the fabrication of new solid bases with characteristic features. Different types of basic sites can be introduced to both metal nodes and organic ligands, resulting in the fabrication of a range of base catalysts which are unattainable by conventional porous materials.

5.2. Activation

Prior to catalytic reactions, activation of solid bases to remove contaminants (such as CO_2) from active sites is frequently required. For conventional inorganic solid bases, high-temperature calcination is quite popular, while for MOFs the activation conditions are dependent on the nature of basic sites. If the basicity is originated from metal centers, MOFs are usually subjected to solvent exchange (e.g., from DMF to methanol and CH_2Cl_2). The new solvent molecules are weakly bonded with metal centers and thus can be removed under mild conditions. In the case of other basic sites such as amines, thermal treatment at relatively low temperatures is usually enough to remove the contaminants. Of course, evacuation can be utilized to facilitate activation if need be.

5.3. Basic Properties

To discuss the characteristic basic properties of MOFs, the origins of basicity in MOFs are grouped into three classes. For the first class, the origin of basicity in MOFs is identical to that in conventional solid bases. For example, immobilized primary amines are the basic source for ED-grafted MOF, MIL-101(Cr)-ED, as well as 3-aminopropyltrialkoxysilane-grafted mesoporous silica, NH_2 -SBA-15.⁸⁷ The base strength of these materials should be the same. For the second class, the basicity in MOFs stems from alkaline earth metals. Despite the fact that alkaline earth metal oxides are well-known solid bases, the basic properties of alkaline earth metals cannot be predicted and strongly depend on the structure of MOFs. A case in point is $Ba_2(BTC)(NO_3)$, the $Ba^{2+}-O^{2-}-Ba^{2+}$ species formed after activation of the basic source, which is reminiscent of the low-coordination sites in BaO .⁴ Such low-coordination sites locate at the corner and edge as well as on the surface of BaO ; nevertheless, almost all $Ba^{2+}-O^{2-}-Ba^{2+}$ species are uniformly dispersed in the framework of $Ba_2(BTC)(NO_3)$ and available as active sites. For the third class, the origins of basicity are only observable in MOFs and have never happened in conventional solid bases. These include the basicity from hybrid metal nodes (see section 2.1.2) as well as from the interplay between metal ions and organic ligands (see basic sites from structural phenolates in section 2.1.4). Such interesting intrinsic basicity may also exist in a range of MOFs and deserves much attention, although more characterization on the basicity is demanded. In

contrast to traditional solid bases, MOFs are crystalline materials with highly periodical order. When a given MOF is used as a solid base (for those with intrinsic basicity) or as a support (for those not basic in nature) for introduction of basic species, the position and amount of basic sites are already recognized. As a result, the basic properties of MOFs are somewhat predictable, which is impossible for traditional solid bases.

It is possible to compare the catalytic performance of basic MOFs with conventional solid bases when the same reactions are carried out under identical conditions. Although pendant primary amines act as active sites for both MIL-101(Cr)-ED and NH₂-SBA-15 as discussed above, MIL-101(Cr)-ED exhibits higher activity than NH₂-SBA-15 in Knoevenagel condensation.⁸⁷ This means that the structure of solid bases has a significant effect on the catalytic activity. Pendant aromatic amino groups are common basic sites in MOFs as well. In the case of NH₂-MIL-100(Fe) with pendant aromatic amino groups, the yield of Knoevenagel product is higher than that on classic solid base MgO and the nitrified NaY zeolite.¹⁴¹ These investigations indicate MOFs-derived solid bases are more active in some reactions as compared with a collection of conventional solid bases. From the viewpoint of pore sizes, MOFs bridge two conventional materials with ordered pore structure, namely, zeolites and mesoporous silicas. The suitable pore sizes, in combination with the tunable basic functionalities, make basic MOFs promising in size-selectivity catalysis despite the fact that the use of basic MOFs in this field is still in its infancy.^{155,209}

6. SUMMARY AND PERSPECTIVES

Increasing attention is given to MOFs-derived solid bases because of their attractive structural features and catalytic performance in various organic reactions. Remarkable progress has been made regarding their preparation, characterization, and catalytic applications especially in the past decade, which becomes an exciting research area. It is worthy of note that MOFs-derived solid bases are much more than straightforward immobilization of corresponding homogeneous basic species on the frameworks. Some reactions proceed solely over heterogeneous base catalysts. The extraordinary skeleton structure offers numerous possibilities for the incorporation of diverse basic functions. Two antagonistic functions are able to harmonize in the frameworks and work in a cooperative way, which is incredible for their homogeneous counterparts. Unlike most conventional solid bases, basic MOFs are crystalline materials with high periodicity and regularity, and all of the basic sites are supposed to possess exactly the same structure. This makes it easy to predict/characterize the basic properties and, more importantly, design MOFs-derived solid bases precisely to promote a given reaction.

There are a large variety of organic ligands available, and MOFs with nearly all of the transition metals have been reported. This suggests the extraordinary diversity in the design and synthesis of MOFs-derived solid bases. The basic sites of MOFs can be generated by either direct synthesis or postsynthetic modification. In the case of direct synthesis, the basicity may originate from metal centers, organic ligands, and the interplay between the two. For postsynthetic modification, both metal sites and ligands are available for introduction of basic species. Each method has its advantages and disadvantages. Some basic sites such as aromatic amines in MOFs can be obtained via either direct synthesis or postsynthetic mod-

ification, while the former is evidently simpler. For other basic sites like aliphatic amines, nevertheless, it is easy to introduce through postsynthetic modification but quite difficult through direct synthesis. Therefore, the preparation method should be selected according to the type of basic species required for a prescribed reaction. In comparison with inorganic porous materials, one of the predominant issues for MOFs is stability. This limitation, however, can be overcome if suitable preparation conditions are used, for instance, utilization of organic solvents instead of water and treatment at relatively low temperatures under vacuum. Moreover, there are existing examples of MOFs in this field exhibiting enhanced thermal and chemical stability, which are robust enough to survive under various preparation conditions. An increasing number of MOFs can be anticipated to add to the list, part of them possessing high potential in the preparation of solid bases. Although a great deal of organic basic species have been incorporated into MOFs, introduction of inorganic ones is scarce. More attention should be paid to the functionalization of MOFs with inorganic basic species, since they represent an important type of active component with interesting catalytic performance and are already widely employed for the fabrication of conventional solid bases.

Systematical characterization of basic sites in MOFs is important for understanding the catalytic mechanism. A number of MOFs do show high activity in base-catalyzed reactions, but the origination of activity is not always well clarified. Some experimental techniques (mainly CO₂-TPD and adsorption with probe molecules) have been employed to characterize the basicity of MOFs. Such techniques can give various information on the basic sites in MOFs. Also, some base-catalyzed reactions like Knoevenagel condensation are useful probe reactions to characterize basic MOFs. The ability in converting substrates with different reactivity mirrors the basicity of catalysts. Actually, some renowned techniques for characterization of conventional solid bases have not been utilized for basic MOFs. A case in point is the detection of base strength using Hammett indicators, which is operated under mild conditions, and the structure can be well preserved even for MOFs with poor stability. Of course, the color of MOFs should be fully considered because the mechanism for Hammett indicators is based on color change. To systematically reveal the basic properties of MOFs, more characterization techniques are expected. Actually, each technique can only disclose part of basic properties rather than all. The combination of different characterization results enables one to disclose the basic properties comprehensively including the strength, amount, and activity of basic sites in MOFs. It should be stated that such techniques principally offer overall information about basic MOFs. Detailed information at the molecular level (such as the spatial position and distance of different active sites) is more vital, particularly for MOFs with more than one functionality. For conventional inorganic solid bases, the surface basic properties are complicated, and usually basic sites with different amounts and strengths coexist. On the contrary, thanks to the crystal lattice of the ideal structure, high periodicity and regularity of basic sites can be presented on MOFs-derived solid bases. This ensures that all of the basic sites should possess an identical environment in MOFs. In this regard, theoretical calculations are very suitable for clarifying the nature of basic sites in MOFs. The combination of theoretical calculations with experimental techniques delivers a powerful way to elucidate the relationship between structure

and activity, which is of significant importance for the fabrication of efficient basic catalysts.

MOFs-derived solid bases have been demonstrated to be active in various organic reactions. Some MOFs with basic functionalities show higher activity than their conventional counterparts with the same functionalities. Also, the highly ordered pore architecture makes basic MOFs promising in catalyzing reactions with size selectivity, especially the reactions hitherto inaccessible for conventional catalysts based on zeolites and mesoporous silicas due to the special needs on pore sizes and functionalities. It is noticeable that industrial applications are much behind the preparation of MOFs-derived solid bases. Actually, stability should not be considered an issue, since there are already examples of MOFs with sufficient robustness and more are anticipated to add to the list. As for industrial applications of basic MOFs, two factors should be taken into account. The first factor is the scale up of basic MOFs. Although industrial production of several MOFs has been reported, some special issues concerning the preparation of basic MOFs should be considered (e.g., the of raw materials and synthetic routes). Another issue worthy of note for basic MOFs is that basic sites are sensitive to CO₂, and loss of activity may take place if the materials are handled in air. Hence, special attention should be paid to the preparation and storage of basic MOFs. The second factor is that restricted attention is given to the organic reactions from the standpoint of industrial applications, in spite of the high potential of basic MOFs in some industrially significant organic reactions. Some organic reactions are merely used to probe the basicity, and some literature only report proof-of-concept investigations. Aiming at industrial applications, further investigations concerning the scale up of basic MOFs and the applications beyond proof-of-concept inspections are expected. Perhaps there is still a long way to go, but we are really heartened by the recent commercial successes of MOFs in gas storage.^{318,319}

AUTHOR INFORMATION

Corresponding Author

*E-mail: lbsun@njtech.edu.cn.

ORCID

Hai-Long Jiang: 0000-0002-2975-7977

Lin-Bing Sun: 0000-0002-6395-312X

Notes

The authors declare no competing financial interest.

Biographies

Li Zhu received her B.Sc. degree from Southeast University Chengxian College in 2013 and M.Ch.E. degree from Nanjing Tech University in 2016 under the guidance of Prof. Lin-Bing Sun. After that she joined Oriental Energy Company Limited as a technical support. Her current research interests are mainly focused on the fabrication of solid base catalysts and their applications in heterogeneous catalysis.

Xiao-Qin Liu is a full professor in the State Key Laboratory of Materials-Oriented Chemical Engineering and Nanjing Tech University. She received her Ph.D. degree in 1999 from Nanjing Tech University under the guidance of Prof. Jun Shi and Prof. Hu-Qing Yao. Her current research interests are mainly focused on the controlled preparation and applications of various porous functional materials with emphasis on metal-organic frameworks and zeolites.

Hai-Long Jiang is a professor of chemistry at University of Science and Technology of China (USTC) and PI of Hefei National Laboratory

for Physical Sciences at the Microscale. He received his Ph.D. degree (2008) from the Fujian Institute of Research on the Structure of Matter, Chinese Academy of Sciences (CAS) and then worked with Prof. Qiang Xu at AIST (Japan) as a postdoctoral and JSPS fellow in 2008–2011. After a postdoctoral stint at Texas A&M University (USA) with Prof. Hong-Cai JOE Zhou, he joined the faculty of USTC in 2013. He has published more than 90 papers with over 7000 citations (H index 40). His main research interest is in the development of MOF-based materials for energy- and environment-related catalysis.

Lin-Bing Sun is a full professor in the State Key Laboratory of Materials-Oriented Chemical Engineering and Nanjing Tech University. He received his Ph.D. degree from Nanjing University in 2008 under the guidance of Prof. Jian Hua Zhu and Prof. Yuan Chun. After that he joined the faculty of Nanjing Tech University. From 2011 to 2012, he worked with Prof. Hong-Cai JOE Zhou as a postdoctoral fellow at Texas A&M University. His current research interests are mainly focused on the synthesis of porous functional materials (typically metal-organic frameworks) as well as their applications in heterogeneous basic catalysis and adsorption.

ACKNOWLEDGMENTS

We acknowledge financial support of this work by the National Natural Science Foundation of China (21576137 and 21676138), the Distinguished Youth Foundation of Jiangsu Province (BK20130045), the Fok Ying-Tong Education Foundation (141069), the National Basic Research Program of China (973 Program, 2013CB733504), and the Project of Priority Academic Program Development of Jiangsu Higher Education Institutions.

ABBREVIATIONS

Chemicals Including Ligands

ATZ 3-amino-1,2,4-triazole
 BD butane-1,4-diamine
 BPDB 1,4-bis(3-phenol)-2,3-diaza-1,3-butadiene
 BPDC 4,4'-biphenyldicarboxylic acid
 4-BTAPA 1,3,5-benzene tricarboxylic acid tris[*N*-(4-pyridyl)-amide]
 CH₃-BDC 2-methylterephthalic acid
 DABCO 1,4-diazabicyclo[2,2,2]octane
 DD decane-1,10-diamine
 DETA diethylenetriamine
 DHTP 2,5-dihydroxyterephthalate
 DMAP 4-dimethylaminopyridine
 DMF *N,N'*-dimethylformamide
 DMSO dimethyl sulfoxide
 4-MT 4-methylthiazole
 ED ethylenediamine
 H₂BDC benzene-1,4-dicarboxylate
 H₂OA oxalic acid
 H₃BTATB 4,4',4''-(benzene-1,3,5-triyltris(azanediyl))-tribenzoate
 H₃BTC 1,3,5-benzenetricarboxylic acid
 H₃BTri 1,3,5-tris(1*H*-1,2,3-triazol-5-yl)benzene
 H₃PDC 3,5-pyrazoledicarboxylic acid
 H₃TATAB 4,4',4''-s-triazine-1,3,5-triyltri-*p*-aminobenzoate
 H₃TCA 4,4',4''-tricarboxytriphenylamine
 H₄PDAI 5,5'-((pyridine-3,5-dicarbonyl)bis(azanediyl))-diisophthalate
 H-MeIM 2-methylimidazole

ICA imidazolate-2-carboxyaldehyde
 LiO^tBu lithium *tert*-butoxide
 NH₂-BDC 2-aminoterephthalic acid
 PD benzene-1,4-diamine
 THF tetrahydrofuran
 TPDC terphenyl-3,3'-dicarboxylate

Common Terminology

BET Brunauer–Emmett–Teller
 CUS coordinatively unsaturated metal site
 DFT density functional theory
 1D one-dimensional
 3D three-dimensional
 EDD electron density difference
 EPR electron paramagnetic resonance
 FM fluorescence microscopy
 HOMO highest occupied molecular orbital
 ICP inductively coupled plasma
 IR infrared
 LUMO lowest unoccupied molecular orbital
 MS mass spectrometer
 MOF metal–organic framework
 MOF-R MOF functionalized with R groups via metal sites, e.g., MIL-101(Cr)-NH₂
 R-MOF MOF functionalized with R groups via organic ligands, e.g., NH₂-MIL-101(Cr)
 NMR nuclear magnetic resonance
 PCN porous coordination network
 PCP porous coordination polymer
 PA proton affinity
 SEM scanning electron microscopy
 SBU secondary building unit
 TCD thermal conductivity detector
 TG thermal gravimetric
 TOF turnover frequency
 TON turnover number
 TPD temperature-programmed desorption
 XRD X-ray diffraction
 XPS X-ray photoelectron spectroscopy
 ZIF zeolite imidazolate framework

REFERENCES

- (1) Zhao, M.; Yuan, K.; Wang, Y.; Li, G.; Guo, J.; Gu, L.; Hu, W.; Zhao, H.; Tang, Z. Metal–Organic Frameworks as Selectivity Regulators for Hydrogenation Reactions. *Nature* **2016**, *539*, 76–80.
- (2) Sun, J.; Baylon, R. A. L.; Liu, C.; Mei, D.; Martin, K. J.; Venkatasubramanian, P.; Wang, Y. Key Roles of Lewis Acid-Base Pairs on Zn_xZr_yO_z in Direct Ethanol/Acetone to Isobutene Conversion. *J. Am. Chem. Soc.* **2016**, *138*, 507–517.
- (3) Kou, J.; Lu, C.; Wang, J.; Chen, Y.; Xu, Z.; Varma, R. S. Selectivity Enhancement in Heterogeneous Photocatalytic Transformations. *Chem. Rev.* **2017**, *117*, 1445–1514.
- (4) Valvickens, P.; Jonckheere, D.; De Baerdemaeker, T.; Kubarev, A.; Vandichel, M.; Hemelsoet, K.; Waroquier, M.; Van Speybroeck, V.; Smolders, E.; Depla, D. Base Catalytic Activity of Alkaline Earth MOFs: A (Micro) Spectroscopic Study of Active Site Formation by the Controlled Transformation of Structural Anions. *Chem. Sci.* **2014**, *5*, 4517–4524.
- (5) Buß, F.; Mehlmann, P.; Muck-Lichtenfeld, C.; Bergander, K.; Dielmann, F. Reversible Carbon Dioxide Binding by Simple Lewis Base Adducts with Electron-Rich Phosphines. *J. Am. Chem. Soc.* **2016**, *138*, 1840–1843.
- (6) Peng, P.; Schmidt, R. R. An Alternative Reaction Course in O-Glycosidation with O-Glycosyl Trichloroacetimidates as Glycosyl Donors and Lewis Acidic Metal Salts as Catalyst: Acid-Base Catalysis with Gold Chloride-Glycosyl Acceptor Adducts. *J. Am. Chem. Soc.* **2015**, *137*, 12653–12659.
- (7) Hattori, H. Heterogeneous Basic Catalysis. *Chem. Rev.* **1995**, *95*, 537–558.
- (8) Jin, X.; Balasubramanian, V. V.; Selvan, S. T.; Sawant, D. P.; Chari, M. A.; Lu, G. e. Q.; Vinu, A. Highly Ordered Mesoporous Carbon Nitride Nanoparticles with High Nitrogen Content: A Metal-Free Basic Catalyst. *Angew. Chem., Int. Ed.* **2009**, *48*, 7884–7887.
- (9) Mondal, B.; Acharyya, K.; Howlader, P.; Mukherjee, P. S. Molecular Cage Impregnated Palladium Nanoparticles: Efficient, Additive-Free Heterogeneous Catalysts for Cyanation of Aryl Halides. *J. Am. Chem. Soc.* **2016**, *138*, 1709–1716.
- (10) Cargnello, M.; Doan-Nguyen, V. V.; Gordon, T. R.; Diaz, R. E.; Stach, E. A.; Gorte, R. J.; Fornasiero, P.; Murray, C. B. Control of Metal Nanocrystal Size Reveals Metal-Support Interface Role for Ceria Catalysts. *Science* **2013**, *341*, 771–773.
- (11) Burrows, A.; Lamberti, C.; Pidko, E.; Minguez, I. L.; de Vos, D.; Hupp, J. T.; Juan-Alcaniz, J.; García, H.; Palkovits, R.; Kapteijn, F. *Metal Organic Frameworks as Heterogeneous Catalysts*; Royal Society of Chemistry, 2013.
- (12) Wu, C.-D.; Lin, W. Heterogeneous Asymmetric Catalysis with Homochiral Metal–Organic Frameworks: Network-Structure-Dependent Catalytic Activity. *Angew. Chem.* **2007**, *119*, 1093–1096.
- (13) Verma, S.; Baig, R. B. N.; Nadagouda, M. N.; Varma, R. S. Titanium-Based Zeolitic Imidazolate Framework for Chemical Fixation of Carbon Dioxide. *Green Chem.* **2016**, *18*, 4855–4858.
- (14) Davis, M. E. New Vistas in Zeolite and Molecular Sieve Catalysis. *Acc. Chem. Res.* **1993**, *26*, 111–115.
- (15) Pines, H.; Haag, W. Communications-Stereoselectivity in the Carbanion-Catalyzed Isomerization of 1-Butene. *J. Org. Chem.* **1958**, *23*, 328–329.
- (16) Sun, L.-B.; Liu, X.-Y.; Li, A.-G.; Liu, X.-D.; Liu, X.-Q. Template-Derived Carbon: An Unexpected Promoter for the Creation of Strong Basicity on Mesoporous Silica. *Chem. Commun.* **2014**, *50*, 11192–11195.
- (17) Sun, L. B.; Yang, J.; Kou, J. H.; Gu, F. N.; Chun, Y.; Wang, Y.; Zhu, J. H.; Zou, Z. G. One-Pot Synthesis of Potassium-Functionalized Mesoporous Gamma-Alumina: A Solid Superbase. *Angew. Chem., Int. Ed.* **2008**, *47*, 3418–3421.
- (18) Puertolas, B.; Keller, T. C.; Mitchell, S.; Perez-Ramirez, J. Deoxygenation of Bio-Oil over Solid Base Catalysts: From Model to Realistic Feeds. *Appl. Catal., B* **2016**, *184*, 77–86.
- (19) Zhou, Y.; Jin, Y. H.; Wang, M.; Zhang, W.; Xie, J. Y.; Gu, J.; Wen, H. M.; Wang, J.; Peng, L. M. One-Pot Synthesis of Zeolitic Strong Solid Bases: A Family of Alkaline-Earth Metal-Containing Silicalite-1. *Chem. - Eur. J.* **2015**, *21*, 15412–15420.
- (20) Wach, A.; Drozdek, M.; Dudek, B.; Biazik, M.; Latka, P.; Michalik, M.; Kustrowski, P. Differences in Catalytic Activity of Poly(vinylamine) Introduced on Surface of Mesoporous SBA-15 by Grafting from and Grafting onto Methods in Knoevenagel Condensation. *J. Phys. Chem. C* **2015**, *119*, 19954–19966.
- (21) Bohre, A.; Saha, B.; Abu-Omar, M. M. Catalytic Upgrading of 5-Hydroxymethylfurfural to Drop-in Biofuels by Solid Base and Bifunctional Metal-Acid Catalysts. *ChemSusChem* **2015**, *8*, 4022–4029.
- (22) Roeser, J.; Kailasam, K.; Thomas, A. Covalent Triazine Frameworks as Heterogeneous Catalysts for the Synthesis of Cyclic and Linear Carbonates from Carbon Dioxide and Epoxides. *ChemSusChem* **2012**, *5*, 1793–1799.
- (23) Sun, L.-B.; Kang, Y.-H.; Shi, Y.-Q.; Jiang, Y.; Liu, X.-Q. Highly Selective Capture of the Greenhouse Gas CO₂ in Polymers. *ACS Sustainable Chem. Eng.* **2015**, *3*, 3077–3085.
- (24) Sun, L.-B.; Shen, J.; Lu, F.; Liu, X.-D.; Zhu, L.; Liu, X.-Q. Fabrication of Solid Strong Bases with a Molecular-Level Dispersion of Lithium Sites and High Basic Catalytic Activity. *Chem. Commun.* **2014**, *50*, 11299–11302.
- (25) Zhu, L. F.; Dai, J. H.; Liu, M. Y.; Tang, D. Y.; Liu, S. Q.; Hu, C. W. Formyl-Modified Polyaniline for the Catalytic Dehydration of Fructose to 5-Hydroxymethylfurfural. *ChemSusChem* **2016**, *9*, 2174–2181.

- (26) Liu, F. J.; Li, W.; Sun, Q.; Zhu, L. F.; Meng, X. J.; Guo, Y. H.; Xiao, F. S. Transesterification to Biodiesel with Superhydrophobic Porous Solid Base Catalysts. *ChemSusChem* **2011**, *4*, 1059–1062.
- (27) Sun, L.-B.; Li, A.-G.; Liu, X.-D.; Liu, X.-Q.; Feng, D.; Lu, W.; Yuan, D.; Zhou, H.-C. Facile Fabrication of Cost-Effective Porous Polymer Networks for Highly Selective CO₂ Capture. *J. Mater. Chem. A* **2015**, *3*, 3252–3256.
- (28) Shi, Y.-Q.; Zhu, J.; Liu, X.-Q.; Geng, J.-C.; Sun, L.-B. Molecular Template-Directed Synthesis of Microporous Polymer Networks for Highly Selective CO₂ Capture. *ACS Appl. Mater. Interfaces* **2014**, *6*, 20340–20349.
- (29) Lee, S.; Kapustin, E. A.; Yaghi, O. M. Coordinative Alignment of Molecules in Chiral Metal–Organic Frameworks. *Science* **2016**, *353*, 808–811.
- (30) Li, H.; Eddaoudi, M.; O’Keeffe, M.; Yaghi, O. M. Design and Synthesis of an Exceptionally Stable and Highly Porous Metal–Organic Framework. *Nature* **1999**, *402*, 276–279.
- (31) Moulton, B.; Zaworotko, M. J. From Molecules to Crystal Engineering: Supramolecular Isomerism and Polymorphism in Network Solids. *Chem. Rev.* **2001**, *101*, 1629–1658.
- (32) Mason, J. A.; Oktawiec, J.; Taylor, M. K.; Hudson, M. R.; Rodriguez, J.; Bachman, J. E.; Gonzalez, M. I.; Cervellino, A.; Guagliardi, A.; Brown, C. M.; Llewellyn, P. L.; Masciocchi, N.; Long, J. R. Methane Storage in Flexible Metal–Organic Frameworks with Intrinsic Thermal Management. *Nature* **2015**, *527*, 357–361.
- (33) Kajiwara, T.; Fujii, M.; Tsujimoto, M.; Kobayashi, K.; Higuchi, M.; Tanaka, K.; Kitagawa, S. Photochemical Reduction of Low Concentrations of CO₂ in a Porous Coordination Polymer with a Ruthenium(II)-CO Complex. *Angew. Chem., Int. Ed.* **2016**, *55*, 2697–2700.
- (34) Foo, M. L.; Matsuda, R.; Hijikata, Y.; Krishna, R.; Sato, H.; Horike, S.; Hori, A.; Duan, J. G.; Sato, Y.; Kubota, Y.; Takata, M.; Kitagawa, S. An Adsorbate Discriminatory Gate Effect in a Flexible Porous Coordination Polymer for Selective Adsorption of CO₂ over C₂H₂. *J. Am. Chem. Soc.* **2016**, *138*, 3022–3030.
- (35) Reboul, J.; Furukawa, S.; Horike, N.; Tsotsalas, M.; Hirai, K.; Uehara, H.; Kondo, M.; Louvain, N.; Sakata, O.; Kitagawa, S. Mesoscopic Architectures of Porous Coordination Polymers Fabricated by Pseudomorphic Replication. *Nat. Mater.* **2012**, *11*, 717–723.
- (36) Kitagawa, H.; Ohtsu, H.; Kawano, M. Kinetic Assembly of a Thermally Stable Porous Coordination Network Based on Labile CuI Units and the Visualization of I₂ Sorption. *Angew. Chem., Int. Ed.* **2013**, *52*, 12395–12399.
- (37) Park, J. Y.; Feng, D. W.; Zhou, H. C. Dual Exchange in PCN-333: A Facile Strategy to Chemically Robust Mesoporous Chromium Metal–Organic Framework with Functional Groups. *J. Am. Chem. Soc.* **2015**, *137*, 11801–11809.
- (38) Feng, D. W.; Liu, T. F.; Su, J.; Bosch, M.; Wei, Z. W.; Wan, W.; Yuan, D. Q.; Chen, Y. P.; Wang, X.; Wang, K. C.; Lian, X. Z.; Gu, Z. Y.; Park, J.; Zou, X. D.; Zhou, H. C. Stable Metal–Organic Frameworks Containing Single-Molecule Traps for Enzyme Encapsulation. *Nat. Commun.* **2015**, *6*, 5979.
- (39) Gascon, J.; Corma, A.; Kapteijn, F.; Llabres i Xamena, F. X. Metal Organic Framework Catalysis: Quo vadis? *ACS Catal.* **2014**, *4*, 361–378.
- (40) Cook, T. R.; Zheng, Y.-R.; Stang, P. J. Metal–Organic Frameworks and Self-Assembled Supramolecular Coordination Complexes: Comparing and Contrasting the Design, Synthesis, and Functionality of Metal–Organic Materials. *Chem. Rev.* **2013**, *113*, 734–777.
- (41) Yoon, M.; Srirambalaji, R.; Kim, K. Homochiral Metal–Organic Frameworks for Asymmetric Heterogeneous Catalysis. *Chem. Rev.* **2012**, *112*, 1196–1231.
- (42) Perry, J. J., IV; Perman, J. A.; Zaworotko, M. J. Design and Synthesis of Metal–Organic Frameworks Using Metal–Organic Polyhedra as Supermolecular Building Blocks. *Chem. Soc. Rev.* **2009**, *38*, 1400–1417.
- (43) Qiu, S.; Zhu, G. Molecular Engineering for Synthesizing Novel Structures of Metal–Organic Frameworks with Multifunctional Properties. *Coord. Chem. Rev.* **2009**, *253*, 2891–2911.
- (44) Zhang, J.; Bu, J. T.; Chen, S.; Wu, T.; Zheng, S.; Chen, Y.; Nieto, R. A.; Feng, P.; Bu, X. Urothermal Synthesis of Crystalline Porous Materials. *Angew. Chem., Int. Ed.* **2010**, *49*, 8876–8879.
- (45) Chen, Y.; Hong, S.; Fu, C. W.; Hoang, T.; Li, X.; Valencia, V.; Zhang, Z.; Perman, J. A.; Ma, S. Investigation of the Mesoporous Metal–Organic Framework as a New Platform to Study the Transport Phenomena of Biomolecules. *ACS Appl. Mater. Interfaces* **2017**, *9*, 10874–10881.
- (46) Zhou, H. C.; Long, J. R.; Yaghi, O. M. Introduction to Metal–Organic Frameworks. *Chem. Rev.* **2012**, *112*, 673–674.
- (47) Yuan, S.; Liu, T.-F.; Feng, D.; Tian, J.; Wang, K.; Qin, J.; Zhang, Q.; Chen, Y.-P.; Bosch, M.; Zou, L.; Teat, S. J.; Dalgarno, S. J.; Zhou, H.-C. A Single Crystalline Porphyrinic Titanium Metal–Organic Framework. *Chem. Sci.* **2015**, *6*, 3926–3930.
- (48) Tian, J.; Xu, Z. Y.; Zhang, D. W.; Wang, H.; Xie, S. H.; Xu, D. W.; Ren, Y. H.; Wang, H.; Liu, Y.; Li, Z. T. Supramolecular Metal–Organic Frameworks That Display High Homogeneous and Heterogeneous Photocatalytic Activity for H₂ Production. *Nat. Commun.* **2016**, *7*, 11580.
- (49) Corma, A.; Garcia, H.; Llabres i Xamena, F. X. L. I. Engineering Metal Organic Frameworks for Heterogeneous Catalysis. *Chem. Rev.* **2010**, *110*, 4606–4655.
- (50) Lu, Z.-Z.; Zhang, R.; Li, Y.-Z.; Guo, Z.-J.; Zheng, H.-G. Solvatochromic Behavior of a Nanotubular Metal–Organic Framework for Sensing Small Molecules. *J. Am. Chem. Soc.* **2011**, *133*, 4172–4174.
- (51) Li, D.-S.; Wu, Y.-P.; Zhao, J.; Zhang, J.; Lu, J. Y. Metal–Organic Frameworks Based upon Non-Zeotype 4-Connected Topology. *Coord. Chem. Rev.* **2014**, *261*, 1–27.
- (52) Zhang, J.; Chen, S.; Nieto, R. A.; Wu, T.; Feng, P.; Bu, X. A Tale of Three Carboxylates: Cooperative Asymmetric Crystallization of a Three-Dimensional Microporous Framework from Achiral Precursors. *Angew. Chem., Int. Ed.* **2010**, *49*, 1267–1270.
- (53) Du, D.-Y.; Qin, J.-S.; Li, S.-L.; Su, Z.-M.; Lan, Y.-Q. Recent Advances in Porous Polyoxometalate-Based Metal–Organic Framework Materials. *Chem. Soc. Rev.* **2014**, *43*, 4615–4632.
- (54) Qin, J.-S.; Du, D.-Y.; Li, M.; Lian, X.-Z.; Dong, L.-Z.; Bosch, M.; Su, Z.-M.; Zhang, Q.; Li, S.-L.; Lan, Y.-Q.; Yuan, S.; Zhou, H.-C. Derivation and Decoration of Nets with Trigonal-Prismatic Nodes: A Unique Route to Reticular Synthesis of Metal–Organic Frameworks. *J. Am. Chem. Soc.* **2016**, *138*, 5299–5307.
- (55) Qin, J.-X.; Tan, P.; Jiang, Y.; Liu, X.-Q.; He, Q.-X.; Sun, L.-B. Functionalization of Metal–Organic Frameworks with Cuprous Sites Using Vapor-Induced Selective Reduction: Efficient Adsorbents for Deep Desulfurization. *Green Chem.* **2016**, *18*, 3210–3215.
- (56) Tan, P.; Li, Y.-H.; Liu, X.-Q.; Jiang, Y.; Sun, L.-B. Core–Shell AgCl@SiO₂ Nanoparticles: Ag(I)-Based Antibacterial Materials with Enhanced Stability. *ACS Sustainable Chem. Eng.* **2016**, *4*, 3268–3275.
- (57) Farrusseng, D.; Aguado, S.; Pinel, C. Metal–Organic Frameworks: Opportunities for Catalysis. *Angew. Chem., Int. Ed.* **2009**, *48*, 7502–7513.
- (58) Lee, J.; Farha, O. K.; Roberts, J.; Scheidt, K. A.; Nguyen, S. T.; Hupp, J. T. Metal–Organic Framework Materials as Catalysts. *Chem. Soc. Rev.* **2009**, *38*, 1450–1459.
- (59) Horcajada, P.; Gref, R.; Baati, T.; Allan, P. K.; Maurin, G.; Couvreur, P.; Férey, G.; Morris, R. E.; Serre, C. Metal–Organic Frameworks in Biomedicine. *Chem. Rev.* **2012**, *112*, 1232–1268.
- (60) Dhakshinamoorthy, A.; Asiri, A. M.; Garcia, H. Metal–Organic Frameworks Catalyzed C–C and C–Heteroatom Coupling Reactions. *Chem. Soc. Rev.* **2015**, *44*, 1922–1947.
- (61) Li, Y.-X.; Jiang, W.-J.; Tan, P.; Liu, X.-Q.; Zhang, D.-Y.; Sun, L.-B. What Matters to the Adsorptive Desulfurization Performance of Metal–Organic Frameworks? *J. Phys. Chem. C* **2015**, *119*, 21969–21977.
- (62) Wang, C.; Liu, D.; Lin, W. Metal–Organic Frameworks as a Tunable Platform for Designing Functional Molecular Materials. *J. Am. Chem. Soc.* **2013**, *135*, 13222–13234.

- (63) Ding, N.; Li, H. W.; Feng, X.; Wang, Q. Y.; Wang, S.; Ma, L.; Zhou, J. W.; Wang, B. Partitioning MOF-5 into Confined and Hydrophobic Compartments for Carbon Capture under Humid Conditions. *J. Am. Chem. Soc.* **2016**, *138*, 10100–10103.
- (64) Huang, Y. B.; Wang, Q.; Liang, J.; Wang, X. S.; Cao, R. Soluble Metal-Nanoparticle-Decorated Porous Coordination Polymers for the Homogenization of Heterogeneous Catalysis. *J. Am. Chem. Soc.* **2016**, *138*, 10104–10107.
- (65) Luo, F.; Yan, C. S.; Dang, L. L.; Krishna, R.; Zhou, W.; Wu, H.; Dong, X. L.; Han, Y.; Hu, T. L.; O’Keeffe, M.; Wang, L. L.; Luo, M. B.; Lin, R. B.; Chen, B. L. UTSA-74: A MOF-74 Isomer with Two Accessible Binding Sites per Metal Center for Highly Selective Gas Separation. *J. Am. Chem. Soc.* **2016**, *138*, 5678–5684.
- (66) Tovar, T. M.; Zhao, J. J.; Nunn, W. T.; Barton, H. F.; Peterson, G. W.; Parsons, G. N.; Levan, M. D. Diffusion of CO₂ in Large Crystals of Cu-BTC MOF. *J. Am. Chem. Soc.* **2016**, *138*, 11449–11452.
- (67) Yang, H.; Bradley, S. J.; Chan, A.; Waterhouse, G. I. N.; Nann, T.; Kruger, P. E.; Telfer, S. G. Catalytically Active Bimetallic Nanoparticles Supported on Porous Carbon Capsules Derived From Metal-Organic Framework Composites. *J. Am. Chem. Soc.* **2016**, *138*, 11872–11881.
- (68) Zhang, M.; Feng, G. X.; Song, Z. G.; Zhou, Y. P.; Chao, H. Y.; Yuan, D. Q.; Tan, T. T. Y.; Guo, Z. G.; Hu, Z. G.; Tang, B. Z.; Liu, B.; Zhao, D. Two-Dimensional Metal-Organic Framework with Wide Channels and Responsive Turn-On Fluorescence for the Chemical Sensing of Volatile Organic Compounds. *J. Am. Chem. Soc.* **2014**, *136*, 7241–7244.
- (69) Chughtai, A. H.; Ahmad, N.; Younus, H. A.; Laypkov, A.; Verpoort, F. Metal-Organic Frameworks: Versatile Heterogeneous Catalysts for Efficient Catalytic Organic Transformations. *Chem. Soc. Rev.* **2015**, *44*, 6804–6849.
- (70) Lin, A. K.-Y.; Chang, H.-A.; Chen, B.-J. Multi-Functional MOF-Derived Magnetic Carbon Sponge. *J. Mater. Chem. A* **2016**, *4*, 13611–13625.
- (71) Zu, D.-D.; Lu, L.; Liu, X.-Q.; Zhang, D.-Y.; Sun, L.-B. Improving Hydrothermal Stability and Catalytic Activity of Metal-Organic Frameworks by Graphite Oxide Incorporation. *J. Phys. Chem. C* **2014**, *118*, 19910–19917.
- (72) Sun, L.-B.; Li, J.-R.; Lu, W.; Gu, Z.-Y.; Luo, Z.; Zhou, H.-C. Confinement of Metal-Organic Polyhedra in Silica Nanopores. *J. Am. Chem. Soc.* **2012**, *134*, 15923–15928.
- (73) Cohen, S. M. Postsynthetic Methods for the Functionalization of Metal-Organic Frameworks. *Chem. Rev.* **2012**, *112*, 970–1000.
- (74) Cohen, S. M. Modifying MOFs: New Chemistry, New Materials. *Chem. Sci.* **2010**, *1*, 32–36.
- (75) Kuppler, R. J.; Timmons, D. J.; Fang, Q.-R.; Li, J.-R.; Makal, T. A.; Young, M. D.; Yuan, D.; Zhao, D.; Zhuang, W.; Zhou, H.-C. Potential Applications of Metal-Organic Frameworks. *Coord. Chem. Rev.* **2009**, *253*, 3042–3066.
- (76) Chizallet, C.; Lazare, S.; Bazer-Bachi, D.; Bonnier, F.; Lecocq, V.; Soyer, E.; Quoineaud, A.-A.; Bats, N. Catalysis of Transesterification by a Nonfunctionalized Metal-Organic Framework: Acido-Basicity at the External Surface of ZIF-8 Probed by FTIR and ab Initio Calculations. *J. Am. Chem. Soc.* **2010**, *132*, 12365–12377.
- (77) Kim, J.; Kim, S. N.; Jang, H. G.; Seo, G.; Ahn, W. S. CO₂ Cycloaddition of Styrene Oxide over MOF Catalysts. *Appl. Catal., A* **2013**, *453*, 175–180.
- (78) Liu, C. J.; Wang, H. M.; Karim, A. M.; Sun, J. M.; Wang, Y. Catalytic Fast Pyrolysis of Lignocellulosic Biomass. *Chem. Soc. Rev.* **2014**, *43*, 7594–7623.
- (79) Van de Voorde, B.; Bueken, B.; Denayer, J.; De Vos, D. Adsorptive Separation on Metal-Organic Frameworks in the Liquid Phase. *Chem. Soc. Rev.* **2014**, *43*, 5766–5788.
- (80) Kreno, L. E.; Leong, K.; Farha, O. K.; Allendorf, M.; Van Duyne, R. P.; Hupp, J. T. Metal-Organic Framework Materials as Chemical Sensors. *Chem. Rev.* **2012**, *112*, 1105–1125.
- (81) Zhang, T.; Lin, W. Metal-Organic Frameworks for Artificial Photosynthesis and Photocatalysis. *Chem. Soc. Rev.* **2014**, *43*, 5982–5993.
- (82) de Lange, M. F.; Verouden, K. J. F. M.; Vlugt, T. J. H.; Gascon, J.; Kapteijn, F. Adsorption-Driven Heat Pumps: The Potential of Metal-Organic Frameworks. *Chem. Rev.* **2015**, *115*, 12205–12250.
- (83) He, Y.; Zhou, W.; Qian, G.; Chen, B. Methane Storage in Metal-Organic Frameworks. *Chem. Soc. Rev.* **2014**, *43*, 5657–5678.
- (84) Jiang, J.; Yaghi, O. M. Bronsted Acidity in Metal-Organic Frameworks. *Chem. Rev.* **2015**, *115*, 6966–6997.
- (85) Eddaoudi, M.; Kim, J.; Rosi, N.; Vodak, D.; Wachter, J.; O’Keeffe, M.; Yaghi, O. M. Systematic Design of Pore Size and Functionality in Isoreticular MOFs and Their Application in Methane Storage. *Science* **2002**, *295*, 469–472.
- (86) Gascon, J.; Aktay, U.; Hernandez-Alonso, M. D.; van Klink, G. P.; Kapteijn, F. Amino-Based Metal-Organic Frameworks as Stable, Highly Active Basic Catalysts. *J. Catal.* **2009**, *261*, 75–87.
- (87) Hwang, Y. K.; Hong, D. Y.; Chang, J. S.; Jhung, S. H.; Seo, Y. K.; Kim, J.; Vimont, A.; Daturi, M.; Serre, C.; Férey, G. Amine Grafting on Coordinatively Unsaturated Metal Centers of MOFs: Consequences for Catalysis and Metal Encapsulation. *Angew. Chem., Int. Ed.* **2008**, *47*, 4144–4148.
- (88) Sun, L. B.; Gu, F. N.; Chun, Y.; Yang, J.; Wang, Y.; Zhu, J. H. Attempt to Generate Strong Basicity on Silica and Titania. *J. Phys. Chem. C* **2008**, *112*, 4978–4985.
- (89) Zhu, L.; Lu, F.; Liu, X.-D.; Liu, X.-Q.; Sun, L.-B. A New Redox Strategy for Low-Temperature Formation of Strong Basicity on Mesoporous Silica. *Chem. Commun.* **2015**, *51*, 10058–10061.
- (90) Sun, L.-B.; Li, Y.-H.; Yin, Y.; Wu, X.-L.; Liu, X.-Q. A Water-Resistant Solid Superbase Derived from Calcium: Synthesis, Characterization and Catalytic Performance. *Curr. Org. Chem.* **2013**, *17*, 2249–2255.
- (91) Yan, Y. B.; Dai, Y. H.; Wang, S. C.; Jia, X. L.; Yu, H.; Yang, Y. H. Catalytic Applications of Alkali-Functionalized Carbon Nanospheres and Their Supported Pd Nanoparticles. *Appl. Catal., B* **2016**, *184*, 104–118.
- (92) Sun, L.-B.; Liu, X.-Q.; Zhou, H.-C. Design and Fabrication of Mesoporous Heterogeneous Basic Catalysts. *Chem. Soc. Rev.* **2015**, *44*, 5092–5147.
- (93) Keller, T. C.; Isabettoni, S.; Verboekend, D.; Rodrigues, E. G.; Perez-Ramirez, J. Hierarchical High-Silica Zeolites as Superior Base Catalysts. *Chem. Sci.* **2014**, *5*, 677–684.
- (94) Choudary, B. M.; Ranganath, K. V.; Pal, U.; Kantam, M. L.; Sreedhar, B. Nanocrystalline MgO for asymmetric Henry and Michael reactions. *J. Am. Chem. Soc.* **2005**, *127*, 13167–13171.
- (95) Sun, L. B.; Kou, J. H.; Chun, Y.; Yang, J.; Gu, F. N.; Wang, Y.; Zhu, J. H.; Zou, Z. G. New Attempt at Directly Generating Superbasicity on Mesoporous Silica SBA-15. *Inorg. Chem.* **2008**, *47*, 4199–4208.
- (96) She, L.; Li, J.; Wan, Y.; Yao, X.; Tu, B.; Zhao, D. Synthesis of Ordered Mesoporous MgO/Carbon Composites by a One-Pot Assembly of Amphiphilic Triblock Copolymers. *J. Mater. Chem.* **2011**, *21*, 795–800.
- (97) Simanjuntak, F. S. H.; Kim, T. K.; Lee, S. D.; Ahn, B. S.; Kim, H. S.; Lee, H. CaO-Catalyzed Synthesis of Glycerol Carbonate from Glycerol and Dimethyl Carbonate: Isolation and Characterization of an Active Ca Species. *Appl. Catal., A* **2011**, *401*, 220–225.
- (98) Thitsartarn, W.; Kawi, S. An Active and Stable CaO-CeO₂ Catalyst for Transesterification of Oil to Biodiesel. *Green Chem.* **2011**, *13*, 3423–3430.
- (99) Faungnawakij, K.; Yoosuk, B.; Namuangruk, S.; Krasae, P.; Viriya-empikul, N.; Puttasawat, B. Sr–Mg Mixed Oxides as Biodiesel Production Catalysts. *ChemCatChem* **2012**, *4*, 209–216.
- (100) Matsushashi, H.; Kawamura, A. Preparation of a Novel Solid Base Catalyst of CaO Covered with SiO₂. *Catal. Today* **2012**, *185*, 236–240.
- (101) Shen, W.; Tompsett, G. A.; Xing, R.; Curtis Conner, W., Jr; Huber, G. W. Vapor Phase Butanal Self-Condensation over

Unsupported and Supported Alkaline Earth Metal Oxides. *J. Catal.* **2012**, *286*, 248–259.

(102) Chen, L.; Zhao, J.; Yin, S.-F.; Au, C.-T. A Mini-Review on Solid Superbase Catalysts Developed in the Past Two Decades. *RSC Adv.* **2013**, *3*, 3799–3814.

(103) Fromm, K. M. Coordination Polymer Networks with s-Block Metal Ions. *Coord. Chem. Rev.* **2008**, *252*, 856–885.

(104) Platero-Prats, A. E.; Iglesias, M.; Snejko, N.; Monge, Á.; Gutiérrez-Puebla, E. From Coordinatively Weak Ability of Constituents to Very Stable Alkaline-Earth Sulfonate Metal–Organic Frameworks. *Cryst. Growth Des.* **2011**, *11*, 1750–1758.

(105) Britt, D.; Furukawa, H.; Wang, B.; Glover, T. G.; Yaghi, O. M. Highly Efficient Separation of Carbon Dioxide by a Metal–Organic Framework Replete with Open Metal Sites. *Proc. Natl. Acad. Sci. U. S. A.* **2009**, *106*, 20637–20640.

(106) Sen, R.; Saha, D.; Koner, S. Controlled Construction of Metal–Organic Frameworks: Hydrothermal Synthesis, X-ray Structure, and Heterogeneous Catalytic Study. *Chem. - Eur. J.* **2012**, *18*, 5979–5986.

(107) Platero Prats, A. E.; de la Peña-O’Shea, V. A.; Iglesias, M.; Snejko, N.; Monge, Á.; Gutiérrez-Puebla, E. Heterogeneous Catalysis with Alkaline-Earth Metal-Based MOFs: A Green Calcium Catalyst. *ChemCatChem* **2010**, *2*, 147–149.

(108) Pan, L.; Frydel, T.; Sander, M. B.; Huang, X.; Li, J. The Effect of pH on the Dimensionality of Coordination Polymers. *Inorg. Chem.* **2001**, *40*, 1271–1283.

(109) Brinkmann, C.; Barrett, A. G. M.; Hill, M. S.; Procopiou, P. A. Heavier Alkaline Earth Catalysts for the Intermolecular Hydroamination of Vinylarenes, Dienes, and Alkynes. *J. Am. Chem. Soc.* **2012**, *134*, 2193–2207.

(110) Zhu, H.-F.; Zhang, Z.-H.; Sun, W.-Y.; Okamura, T.-a.; Ueyama, N. Syntheses, Structures, and Properties of Two-Dimensional Alkaline Earth Metal Complexes with Flexible Tripodal Tricarboxylate Ligands. *Cryst. Growth Des.* **2005**, *5*, 177–182.

(111) Lee, D. W.; Jo, V.; Ok, K. M. $\text{Sr}_2[\text{C}_6\text{H}_3(\text{CO}_2)_3(\text{NO}_3)] \cdot \text{DMF}$: One-Dimensional Nano-Channel in a New Non-Centrosymmetric Strontium–Organic Framework with High Thermal Stability. *Cryst. Growth Des.* **2011**, *11*, 2698–2701.

(112) Pan, C.; Nan, J.; Dong, X.; Ren, X.-M.; Jin, W. A Highly Thermally Stable Ferroelectric Metal–Organic Framework and Its Thin Film with Substrate Surface Nature Dependent Morphology. *J. Am. Chem. Soc.* **2011**, *133*, 12330–12333.

(113) Foo, M. L.; Horike, S.; Inubushi, Y.; Kitagawa, S. An Alkaline Earth I^3O^0 Porous Coordination Polymer: $[\text{Ba}_2\text{TMA}(\text{NO}_3)(\text{DMF})]$. *Angew. Chem., Int. Ed.* **2012**, *51*, 6107–6111.

(114) Xiao, D.; Chen, H.; Zhang, G.; Sun, D.; He, J.; Yuan, R.; Wang, E. An Unprecedented (5,12)-Connected 3D Self-Penetrating Metal–Organic Framework Based on Dinuclear Barium Clusters as Building Blocks. *CrystEngComm* **2011**, *13*, 433–436.

(115) Maity, T.; Saha, D.; Das, S.; Koner, S. Barium Carboxylate Metal–Organic Framework-Synthesis, X-ray Crystal Structure, Photoluminescence and Catalytic Study. *Eur. J. Inorg. Chem.* **2012**, *2012*, 4914–4920.

(116) Liu, X.-Y.; Sun, L.-B.; Liu, X.-D.; Li, A.-G.; Lu, F.; Liu, X.-Q. Low-Temperature Fabrication of Mesoporous Solid Strong Bases by Using Multifunction of a Carbon Interlayer. *ACS Appl. Mater. Interfaces* **2013**, *5*, 9823–9829.

(117) Liu, X.-Y.; Sun, L.-B.; Lu, F.; Liu, X.-D.; Liu, X.-Q. Low-Temperature Generation of Strong Basicity via an Unprecedented Guest-Host Redox Interaction. *Chem. Commun.* **2013**, *49*, 8087–8089.

(118) Chevreau, H.; Devic, T.; Salles, F.; Maurin, G.; Stock, N.; Serre, C. Mixed-Linker Hybrid Superpolyhedra for the Production of a Series of Large-Pore Iron(III) Carboxylate Metal–Organic Frameworks. *Angew. Chem., Int. Ed.* **2013**, *52*, 5056–5060.

(119) Garibay, S. J.; Cohen, S. M. Isoreticular Synthesis and Modification of Frameworks with the UiO-66 Topology. *Chem. Commun.* **2010**, *46*, 7700–7702.

(120) Zhang, C.; Xiao, Y.; Liu, D.; Yang, Q.; Zhong, C. A Hybrid Zeolitic Imidazolate Framework Membrane by Mixed-Linker Synthesis for Efficient CO_2 Capture. *Chem. Commun.* **2013**, *49*, 600–602.

(121) Marx, S.; Kleist, W.; Huang, J.; Maciejewski, M.; Baiker, A. Tuning Functional Sites and Thermal Stability of Mixed-Linker MOFs Based on MIL-53 (Al). *Dalton Trans.* **2010**, *39*, 3795–3798.

(122) Deng, H.; Doonan, C. J.; Furukawa, H.; Ferreira, R. B.; Towne, J.; Knobler, C. B.; Wang, B.; Yaghi, O. M. Multiple Functional Groups of Varying Ratios in Metal–Organic Frameworks. *Science* **2010**, *327*, 846–850.

(123) Lee, W. R.; Ryu, D. W.; Phang, W. J.; Park, J. H.; Hong, C. S. Charge Effect of Foreign Metal Ions and the Crystal Growth Process in Hybridized Metal–Organic Frameworks. *Chem. Commun.* **2012**, *48*, 10847–10849.

(124) Wang, F.; Liu, Z. S.; Yang, H.; Tan, Y. X.; Zhang, J. Hybrid Zeolitic Imidazolate Frameworks with Catalytically Active TO_4 Building Blocks. *Angew. Chem., Int. Ed.* **2011**, *50*, 450–453.

(125) Botas, J. A.; Calleja, G.; Sánchez-Sánchez, M.; Orcajo, M. G. Effect of Zn/Co Ratio in MOF-74 Type Materials Containing Exposed Metal Sites on their Hydrogen Adsorption Behaviour and on their Band Gap Energy. *Int. J. Hydrogen Energy* **2011**, *36*, 10834–10844.

(126) Zhang, Q. J.; Cao, L. J.; Li, B. H.; Chen, L. Catalyzed Activation of CO_2 by a Lewis-Base Site in W-Cu-BTC Hybrid Metal Organic Frameworks. *Chem. Sci.* **2012**, *3*, 2708–2715.

(127) Kramer, M.; Schwarz, U.; Kaskel, S. Synthesis and Properties of the Metal–Organic Framework $\text{Mo}_3(\text{BTC})_2$ (TUDMOF-1). *J. Mater. Chem.* **2006**, *16*, 2245–2248.

(128) Murray, L. J.; Dinca, M.; Yano, J.; Chavan, S.; Bordiga, S.; Brown, C. M.; Long, J. R. Highly-Selective and Reversible O_2 Binding in $\text{Cr}_3(1,3,5\text{-benzenetricarboxylate})_2$. *J. Am. Chem. Soc.* **2010**, *132*, 7856–7857.

(129) Gotthardt, M. A.; Grosjean, S.; Brunner, T. S.; Kotzel, J.; Ganzler, A. M.; Wolf, S.; Brase, S.; Kleist, W. Synthesis and Post-Synthetic Modification of Amine-, Alkyne-, Azide- and Nitro-Functionalized Metal–Organic Frameworks Based on DUT-5. *Dalton Trans.* **2015**, *44*, 16802–16809.

(130) Aguilera-Sigalat, J.; Bradshaw, D. A Colloidal Water-Stable MOF as a Broad-Range Fluorescent pH Sensor via Post-Synthetic Modification. *Chem. Commun.* **2014**, *50*, 4711–4713.

(131) Dong, X.-W.; Liu, T.; Hu, Y.-Z.; Liu, X.-Y.; Che, C.-M. Urea Postmodified in a Metal–Organic Framework as a Catalytically Active Hydrogen-Bond-Donating Heterogeneous Catalyst. *Chem. Commun.* **2013**, *49*, 7681–7683.

(132) Jiang, D.; Keenan, L. L.; Burrows, A. D.; Edler, K. J. Synthesis and Post-Synthetic Modification of MIL-101(Cr)- NH_2 via a Tandem Diazotisation Process. *Chem. Commun.* **2012**, *48*, 12053–12055.

(133) Kleist, W.; Jutz, F.; Maciejewski, M.; Baiker, A. Mixed-Linker Metal–Organic Frameworks as Catalysts for the Synthesis of Propylene Carbonate from Propylene Oxide and CO_2 . *Eur. J. Inorg. Chem.* **2009**, *2009*, 3552–3561.

(134) Toyao, T.; Saito, M.; Horiuchi, Y.; Matsuoka, M. Development of a Novel One-Pot Reaction System Utilizing a Bifunctional Zr-Based Metal–Organic Framework. *Catal. Sci. Technol.* **2014**, *4*, 625–628.

(135) Long, J. L.; Wang, S. B.; Ding, Z. X.; Wang, S. C.; Zhou, Y. E.; Huang, L.; Wang, X. X. Amine-Functionalized Zirconium Metal–Organic Framework as Efficient Visible-Light Photocatalyst for Aerobic Organic Transformations. *Chem. Commun.* **2012**, *48*, 11656–11658.

(136) Vermoortele, F.; Ameloot, R.; Vimont, A.; Serre, C.; De Vos, D. An Amino-Modified Zr-Terephthalate Metal–Organic Framework as an Acid-Base Catalyst for Cross-Aldol Condensation. *Chem. Commun.* **2011**, *47*, 1521–1523.

(137) Shen, L. J.; Liang, S. J.; Wu, W. M.; Liang, R. W.; Wu, L. Multifunctional NH_2 -Mediated Zirconium Metal–Organic Framework as an Efficient Visible-Light-Driven Photocatalyst for Selective Oxidation of Alcohols and Reduction of Aqueous Cr(VI). *Dalton Trans.* **2013**, *42*, 13649–13657.

(138) Yang, Y.; Yao, H. F.; Xi, F. G.; Gao, E. Q. Amino-Functionalized Zr(IV) Metal–Organic Framework as Bifunctional

Acid-Base Catalyst for Knoevenagel Condensation. *J. Mol. Catal. A: Chem.* **2014**, *390*, 198–205.

(139) Timofeeva, M. N.; Panchenko, V. N.; Jun, J. W.; Hasan, Z.; Matrosova, M. M.; Jhung, S. H. Effects of Linker Substitution on Catalytic Properties of Porous Zirconium Terephthalate UiO-66 in Acetalization of Benzaldehyde with Methanol. *Appl. Catal., A* **2014**, *471*, 91–97.

(140) Srirambalaji, R.; Hong, S.; Natarajan, R.; Yoon, M.; Hota, R.; Kim, Y.; Ko, Y. H.; Kim, K. Tandem Catalysis with a Bifunctional Site-Isolated Lewis Acid-Bronsted Base Metal-Organic Framework, NH₂-MIL-101(Al). *Chem. Commun.* **2012**, *48*, 11650–11652.

(141) Hartmann, M.; Fischer, M. Amino-Functionalized Basic Catalysts with MIL-101 Structure. *Microporous Mesoporous Mater.* **2012**, *164*, 38–43.

(142) Wang, D. K.; Huang, R. K.; Liu, W. J.; Sun, D. R.; Li, Z. H. Fe-Based MOFs for Photocatalytic CO₂ Reduction: Role of Coordination Unsaturated Sites and Dual Excitation Pathways. *ACS Catal.* **2014**, *4*, 4254–4260.

(143) Wang, D.; Li, Z. Bi-Functional NH₂-MIL-101(Fe) for One-Pot Tandem Photo-Oxidation/Knoevenagel Condensation between Aromatic Alcohols and Active Methylene Compounds. *Catal. Sci. Technol.* **2015**, *5*, 1623–1628.

(144) Rodenas, T.; van Dalen, M.; Garcia-Perez, E.; Serra-Crespo, P.; Zornoza, B.; Kapteijn, F.; Gascon, J. Visualizing MOF Mixed Matrix Membranes at the Nanoscale: Towards Structure-Performance Relationships in CO₂/CH₄ Separation over NH₂-MIL-53(Al)@PI. *Adv. Funct. Mater.* **2014**, *24*, 249–256.

(145) Zhang, F.; Zou, X. Q.; Gao, X.; Fan, S. J.; Sun, F. X.; Ren, H.; Zhu, G. S. Hydrogen Selective NH₂-MIL-53(Al) MOF Membranes with High Permeability. *Adv. Funct. Mater.* **2012**, *22*, 3583–3590.

(146) Rodenas, T.; van Dalen, M.; Serra-Crespo, P.; Kapteijn, F.; Gascon, J. Mixed Matrix Membranes Based on NH₂-Functionalized MIL-Type MOFs: Influence of Structural and Operational Parameters on the CO₂/CH₄ Separation Performance. *Microporous Mesoporous Mater.* **2014**, *192*, 35–42.

(147) Chen, X. Y.; Hoang, V. T.; Rodrigue, D.; Kaliaguine, S. Optimization of Continuous Phase in Amino-Functionalized Metal-Organic Framework (MIL-53) Based co-Polyimide Mixed Matrix Membranes for CO₂/CH₄ Separation. *RSC Adv.* **2013**, *3*, 24266–24279.

(148) Sun, D. R.; Ye, L.; Li, Z. H. Visible-Light-Assisted Aerobic Photocatalytic Oxidation of Amines to Imines over NH₂-MIL-125(Ti). *Appl. Catal., B* **2015**, *164*, 428–432.

(149) Vaesen, S.; Guillerm, V.; Yang, Q. Y.; Wiersum, A. D.; Marszalek, B.; Gil, B.; Vimont, A.; Daturi, M.; Devic, T.; Llewellyn, P. L.; Serre, C.; Maurin, G.; De Weireld, G. A Robust Amino-Functionalized Titanium(IV) Based MOF for Improved Separation of Acid Gases. *Chem. Commun.* **2013**, *49*, 10082–10084.

(150) Tran, U. P. N.; Le, K. K. A.; Phan, N. T. S. Expanding Applications of Metal-Organic Frameworks: Zeolite Imidazolate Framework ZIF-8 as an Efficient Heterogeneous Catalyst for the Knoevenagel Reaction. *ACS Catal.* **2011**, *1*, 120–127.

(151) Jin, R. Z.; Bian, Z.; Li, J. Z.; Ding, M. X.; Gao, L. X. ZIF-8 Crystal Coatings on a Polyimide Substrate and their Catalytic Behaviours for the Knoevenagel Reaction. *Dalton Trans.* **2013**, *42*, 3936–3940.

(152) Wu, P.; Wang, J.; Li, Y.; He, C.; Xie, Z.; Duan, C. Luminescent Sensing and Catalytic Performances of a Multifunctional Lanthanide-Organic Framework Comprising a Triphenylamine Moiety. *Adv. Funct. Mater.* **2011**, *21*, 2788–2794.

(153) Hasegawa, S.; Horike, S.; Matsuda, R.; Furukawa, S.; Mochizuki, K.; Kinoshita, Y.; Kitagawa, S. Three-Dimensional Porous Coordination Polymer Functionalized with Amide Groups Based on Tridentate Ligand: Selective Sorption and Catalysis. *J. Am. Chem. Soc.* **2007**, *129*, 2607–2614.

(154) Xiao, J.; Chen, C. X.; Liu, Q. K.; Ma, J. P.; Dong, Y. B. Cd(II)-Schiff-Base Metal Organic Frameworks: Synthesis, Structure, and Reversible Adsorption and Separation of Volatile Chlorocarbons. *Cryst. Growth Des.* **2011**, *11*, S696–S701.

(155) Fang, Q.-R.; Yuan, D.-Q.; Sculley, J.; Li, J.-R.; Han, Z.-B.; Zhou, H.-C. Functional Mesoporous Metal–Organic Frameworks for the Capture of Heavy Metal Ions and Size-Selective Catalysis. *Inorg. Chem.* **2010**, *49*, 11637–11642.

(156) Park, J.; Li, J.-R.; Chen, Y.-P.; Yu, J.; Yakovenko, A. A.; Wang, Z. U.; Sun, L.-B.; Balbuena, P. B.; Zhou, H.-C. A Versatile Metal-Organic Framework for Carbon Dioxide Capture and Cooperative Catalysis. *Chem. Commun.* **2012**, *48*, 9995–9997.

(157) Vaidhyanathan, R.; Iremonger, S. S.; Dawson, K. W.; Shimizu, G. K. H. An Amine-Functionalized Metal Organic Framework for Preferential CO₂ Adsorption at Low Pressures. *Chem. Commun.* **2009**, 5230–5232.

(158) Sun, L.-B.; Li, J.-R.; Park, J.; Zhou, H.-C. Cooperative Template-Directed Assembly of Mesoporous Metal–Organic Frameworks. *J. Am. Chem. Soc.* **2012**, *134*, 126–129.

(159) Vinu, A.; Srinivasu, P.; Sawant, D. P.; Mori, T.; Ariga, K.; Chang, J.-S.; Jhung, S.-H.; Balasubramanian, V. V.; Hwang, Y. K. Three-Dimensional Cage Type Mesoporous CN-Based Hybrid Material with Very High Surface Area and Pore Volume. *Chem. Mater.* **2007**, *19*, 4367–4372.

(160) Chen, Y. Z.; Wang, C.; Wu, Z. Y.; Xiong, Y.; Xu, Q.; Yu, S. H.; Jiang, H. L. From Bimetallic Metal-Organic Framework to Porous Carbon: High Surface Area and Multicomponent Active Dopants for Excellent Electrocatalysis. *Adv. Mater.* **2015**, *27*, S010–S016.

(161) Jiang, H.-L.; Feng, D.; Liu, T.-F.; Li, J.-R.; Zhou, H.-C. Pore Surface Engineering with Controlled Loadings of Functional Groups via Click Chemistry in Highly Stable Metal–Organic Frameworks. *J. Am. Chem. Soc.* **2012**, *134*, 14690–14693.

(162) Jiang, H.-L.; Makal, T. A.; Zhou, H.-C. Interpenetration Control in Metal–Organic Frameworks for Functional Applications. *Coord. Chem. Rev.* **2013**, *257*, 2232–2249.

(163) Phan, A.; Doonan, C. J.; Uribe-Romo, F. J.; Knobler, C. B.; O’Keeffe, M.; Yaghi, O. M. Synthesis, Structure, and Carbon Dioxide Capture Properties of Zeolitic Imidazolate Frameworks. *Acc. Chem. Res.* **2010**, *43*, 58–67.

(164) Banerjee, R.; Phan, A.; Wang, B.; Knobler, C.; Furukawa, H.; O’Keeffe, M.; Yaghi, O. M. High-Throughput Synthesis of Zeolitic Imidazolate Frameworks and Application to CO₂ Capture. *Science* **2008**, *319*, 939–943.

(165) Galvelis, R.; Slater, B.; Chaudret, R.; Creton, B.; Nieto-Draghi, C.; Mellot-Draznieks, C. Impact of Functionalized Linkers on the Energy Landscape of ZIFs. *CrystEngComm* **2013**, *15*, 9603–9612.

(166) Huang, X. C.; Lin, Y. Y.; Zhang, J. P.; Chen, X. M. Ligand-Directed Strategy for Zeolite-Type Metal–Organic Frameworks: Zinc(II) Imidazolates with Unusual Zeolitic Topologies. *Angew. Chem.* **2006**, *118*, 1587–1589.

(167) Venna, S. R.; Jasinski, J. B.; Carreon, M. A. Structural Evolution of Zeolitic Imidazolate Framework-8. *J. Am. Chem. Soc.* **2010**, *132*, 18030–18033.

(168) Bernt, S.; Guillerm, V.; Serre, C.; Stock, N. Direct Covalent Post-Synthetic Chemical Modification of Cr-MIL-101 Using Nitrating Acid. *Chem. Commun.* **2011**, *47*, 2838–2840.

(169) Dietzel, P. D. C.; Morita, Y.; Blom, R.; Fjellvåg, H. An In Situ High-Temperature Single-Crystal Investigation of a Dehydrated Metal–Organic Framework Compound and Field-Induced Magnetization of One-Dimensional Metal–Oxygen Chains. *Angew. Chem., Int. Ed.* **2005**, *44*, 6354–6358.

(170) Dietzel, P. D.; Panella, B.; Hirscher, M.; Blom, R.; Fjellvåg, H. Hydrogen Adsorption in a Nickel Based Coordination Polymer with Open Metal Sites in the Cylindrical Cavities of the Desolvated Framework. *Chem. Commun.* **2006**, 959–961.

(171) Rosi, N. L.; Kim, J.; Eddaoudi, M.; Chen, B.; O’Keeffe, M.; Yaghi, O. M. Rod Packings and Metal–Organic Frameworks Constructed from Rod-Shaped Secondary Building Units. *J. Am. Chem. Soc.* **2005**, *127*, 1504–1518.

(172) Zhou, W.; Wu, H.; Yildirim, T. Enhanced H₂ Adsorption in Isostructural Metal–Organic Frameworks with Open Metal Sites: Strong Dependence of the Binding Strength on Metal Ions. *J. Am. Chem. Soc.* **2008**, *130*, 15268–15269.

- (173) Xiang, S.; Zhou, W.; Zhang, Z.; Green, M. A.; Liu, Y.; Chen, B. Open Metal Sites within Isostructural Metal–Organic Frameworks for Differential Recognition of Acetylene and Extraordinarily High Acetylene Storage Capacity at Room Temperature. *Angew. Chem., Int. Ed.* **2010**, *49*, 4615–4618.
- (174) Geier, S. J.; Mason, J. A.; Bloch, E. D.; Queen, W. L.; Hudson, M. R.; Brown, C. M.; Long, J. R. Selective Adsorption of Ethylene over Ethane and Propylene over Propane in the Metal–Organic Frameworks M2(dobdc) (M = Mg, Mn, Fe, Co, Ni, Zn). *Chem. Sci.* **2013**, *4*, 2054–2061.
- (175) Liu, J.; Tian, J.; Thallapally, P. K.; McGrail, B. P. Selective CO₂ Capture from Flue Gas Using Metal–Organic Frameworks—A Fixed Bed Study. *J. Phys. Chem. C* **2012**, *116*, 9575–9581.
- (176) Remy, T.; Peter, S. A.; Van der Perre, S.; Valvekens, P.; De Vos, D. E.; Baron, G. V.; Denayer, J. F. M. Selective Dynamic CO₂ Separations on Mg–MOF-74 at Low Pressures: A Detailed Comparison with 13X. *J. Phys. Chem. C* **2013**, *117*, 9301–9310.
- (177) Bloch, E. D.; Queen, W. L.; Krishna, R.; Zadrozny, J. M.; Brown, C. M.; Long, J. R. Hydrocarbon Separations in a Metal–Organic Framework with Open Iron(II) Coordination Sites. *Science* **2012**, *335*, 1606–1610.
- (178) Valvekens, P.; Vandichel, M.; Waroquier, M.; Van Speybroeck, V.; De Vos, D. Metal–Dioxidoterephthalate MOFs of The MOF-74 Type: Microporous Basic Catalysts with Well-Defined Active Sites. *J. Catal.* **2014**, *317*, 1–10.
- (179) Hatano, M.; Horibe, T.; Ishihara, K. Chiral Magnesium(II) Binaphtholates as Cooperative Brønsted/Lewis Acid–Base Catalysts for the Highly Enantioselective Addition of Phosphorus Nucleophiles to α,β -Unsaturated Esters and Ketones. *Angew. Chem., Int. Ed.* **2013**, *52*, 4549–4553.
- (180) Li, B.; Chrzanowski, M.; Zhang, Y.; Ma, S. Applications of Metal–Organic Frameworks Featuring Multi-Functional Sites. *Coord. Chem. Rev.* **2016**, *307*, 106–129.
- (181) Fracaroli, A. M.; Siman, P.; Nagib, D. A.; Suzuki, M.; Furukawa, H.; Toste, F. D.; Yaghi, O. M. Seven Post-synthetic Covalent Reactions in Tandem Leading to Enzyme-like Complexity within Metal–Organic Framework Crystals. *J. Am. Chem. Soc.* **2016**, *138*, 8352–8355.
- (182) Marshall, R. J.; Forgan, R. S. Postsynthetic Modification of Zirconium Metal–Organic Frameworks. *Eur. J. Inorg. Chem.* **2016**, *2016*, 4310–4331.
- (183) Couck, S.; Gobechiya, E.; Kirschhock, C. E.; Serra-Crespo, P.; Juan-Alcañiz, J.; Martinez Joaristi, A.; Stavitski, E.; Gascon, J.; Kapteijn, F.; Baron, G. V. Adsorption and Separation of Light Gases on an Amino-Functionalized Metal–Organic Framework: An Adsorption and In Situ XRD Study. *ChemSusChem* **2012**, *5*, 740–750.
- (184) Babarao, R.; Dai, S.; Jiang, D.-e. Functionalizing Porous Aromatic Frameworks with Polar Organic Groups for High-Capacity and Selective CO₂ Separation: A Molecular Simulation Study. *Langmuir* **2011**, *27*, 3451–3460.
- (185) Banerjee, R.; Furukawa, H.; Britt, D.; Knobler, C.; O’Keeffe, M.; Yaghi, O. M. Control of Pore Size and Functionality in Isorecticular Zeolitic Imidazolate Frameworks and their Carbon Dioxide Selective Capture Properties. *J. Am. Chem. Soc.* **2009**, *131*, 3875–3877.
- (186) McDonald, T. M.; Lee, W. R.; Mason, J. A.; Wiers, B. M.; Hong, C. S.; Long, J. R. Capture of Carbon Dioxide from Air and Flue Gas in the Alkylamine-Appended Metal–Organic Framework mmen-Mg₂(dobpdc). *J. Am. Chem. Soc.* **2012**, *134*, 7056–7065.
- (187) Ahmed, I.; Hasan, Z.; Khan, N. A.; Jhung, S. H. Adsorptive Denitrogenation of Model Fuels with Porous Metal–Organic Frameworks (MOFs): Effect of Acidity and Basicity of MOFs. *Appl. Catal., B* **2013**, *129*, 123–129.
- (188) Demessence, A.; D’Alessandro, D. M.; Foo, M. L.; Long, J. R. Strong CO₂ Binding in a Water-Stable, Triazolate-Bridged Metal–Organic Framework Functionalized with Ethylenediamine. *J. Am. Chem. Soc.* **2009**, *131*, 8784–8786.
- (189) Kasinathan, P.; Seo, Y.-K.; Shim, K.-E.; Hwang, Y. K.; Lee, U.-H.; Hwang, D. W.; Hong, D.-Y.; Halligudi, S. B.; Chang, J.-S. Effect of Diamine in Amine-Functionalized MIL-101 for Knoevenagel Condensation. *Bull. Korean Chem. Soc.* **2011**, *32*, 2073–2075.
- (190) Chen, J. Z.; Liu, R. L.; Gao, H.; Chen, L. M.; Ye, D. Q. Amine-Functionalized Metal–Organic Frameworks for the Transesterification of Triglycerides. *J. Mater. Chem. A* **2014**, *2*, 7205–7213.
- (191) Shi, T.; Guo, Z. W.; Yu, H. X.; Xie, J. W.; Zhong, Y. J.; Zhu, W. D. Atom-Economic Synthesis of Optically Active Warfarin Anticoagulant over a Chiral MOF Organocatalyst. *Adv. Synth. Catal.* **2013**, *355*, 2538–2543.
- (192) Banerjee, M.; Das, S.; Yoon, M.; Choi, H. J.; Hyun, M. H.; Park, S. M.; Seo, G.; Kim, K. Postsynthetic Modification Switches an Achiral Framework to Catalytically Active Homochiral Metal–Organic Porous Materials. *J. Am. Chem. Soc.* **2009**, *131*, 7524–7525.
- (193) Kim, S.-N.; Yang, S.-T.; Kim, J.; Park, J.-E.; Ahn, W.-S. Post-Synthesis Functionalization of MIL-101 Using Diethylenetriamine: A Study on Adsorption and Catalysis. *CrystEngComm* **2012**, *14*, 4142–4147.
- (194) Choi, S.; Watanabe, T.; Bae, T. H.; Sholl, D. S.; Jones, C. W. Modification of the Mg/DOBDC MOF with Amines to Enhance CO₂ Adsorption from Ultradilute Gases. *J. Phys. Chem. Lett.* **2012**, *3*, 1136–1141.
- (195) Gu, J. M.; Kim, W. S.; Huh, S. Size-Dependent Catalysis by Dabco-Functionalized Zn–MOF with One-Dimensional Channels. *Dalton Trans.* **2011**, *40*, 10826–10829.
- (196) Gu, J.-M.; Kwon, T.-H.; Park, J.-H.; Huh, S. DABCO-Functionalized Metal–Organic Framework Bearing a C_{2h}-Symmetric Terphenyl Dicarboxylate Linker. *Dalton Trans.* **2010**, *39*, 5608–5610.
- (197) Férey, G.; Mellot-Draznieks, C.; Serre, C.; Millange, F.; Dutour, J.; Surlblé, S.; Margiolaki, I. A Chromium Terephthalate-Based Solid with Unusually Large Pore Volumes and Surface Area. *Science* **2005**, *309*, 2040–2042.
- (198) Yokoi, T.; Kubota, Y.; Tatsumi, T. Amino-Functionalized Mesoporous Silica as Base Catalyst and Adsorbent. *Appl. Catal., A* **2012**, *421–422*, 14–37.
- (199) Cheng, L.; Jiang, Y.; Yan, N.; Shan, S.-F.; Liu, X.-Q.; Sun, L.-B. Smart Adsorbents with Photoregulated Molecular Gates for Both Selective Adsorption and Efficient Regeneration. *ACS Appl. Mater. Interfaces* **2016**, *8*, 23404–23411.
- (200) Jiang, W.-J.; Yin, Y.; Liu, X.-Q.; Yin, X.-Q.; Shi, Y.-Q.; Sun, L.-B. Fabrication of Supported Cuprous Sites at Low Temperatures: An Efficient, Controllable Strategy Using Vapor-Induced Reduction. *J. Am. Chem. Soc.* **2013**, *135*, 8137–8140.
- (201) Jiang, Y.; Tan, P.; Cheng, L.; Shan, S.-F.; Liu, X.-Q.; Sun, L.-B. Selective adsorption and efficient regeneration via smart adsorbents possessing thermo-controlled molecular switches. *Phys. Chem. Chem. Phys.* **2016**, *18*, 9883–9887.
- (202) Wu, L. Y.; Wang, H. J.; Lan, H. C.; Liu, H. J.; Qu, J. H. Adsorption of Cu(II)-EDTA Chelates on Tri-Ammonium-Functionalized Mesoporous Silica from Aqueous Solution. *Sep. Purif. Technol.* **2013**, *117*, 118–123.
- (203) Acharya, S. A.; Maheshwari, N.; Tatikondewar, L.; Kshirsagar, A.; Kulkarni, S. K. Ethylenediamine-Mediated Wurtzite Phase Formation in ZnS. *Cryst. Growth Des.* **2013**, *13*, 1369–1376.
- (204) Gee, W. J.; Cadman, L. K.; Amer Hamzah, H.; Mahon, M. F.; Raithby, P. R.; Burrows, A. D. Furnishing Amine-Functionalized Metal–Organic Frameworks with the β -Amidoketone Group by Postsynthetic Modification. *Inorg. Chem.* **2016**, *55*, 10839–10842.
- (205) Lian, X.; Yan, B. A Postsynthetic Modified MOF Hybrid as Heterogeneous Photocatalyst for α -Phenethyl Alcohol and Reusable Fluorescence Sensor. *Inorg. Chem.* **2016**, *55*, 11831–11838.
- (206) Ma, W.; Xu, L.; Li, Z.; Sun, Y.; Bai, Y.; Liu, H. Post-Synthetic Modification of an Amino-Functionalized Metal–Organic Framework for Highly Efficient Enrichment of N-Linked Glycopeptides. *Nanoscale* **2016**, *8*, 10908–10912.
- (207) Song, Y. F.; Cronin, L. Postsynthetic Covalent Modification of Metal–Organic Framework (MOF) Materials. *Angew. Chem., Int. Ed.* **2008**, *47*, 4635–4637.
- (208) Morris, W.; Doonan, C. J.; Furukawa, H.; Banerjee, R.; Yaghi, O. M. Crystals as Molecules: Postsynthesis Covalent Functionalization

of Zeolitic Imidazolate Frameworks. *J. Am. Chem. Soc.* **2008**, *130*, 12626–12627.

(209) Luan, Y.; Qi, Y.; Gao, H.; Andriamitantoa, R. S.; Zheng, N.; Wang, G. A General Post-Synthetic Modification Approach of Amino-Tagged Metal-Organic Frameworks to Access Efficient Catalysts for the Knoevenagel Condensation Reaction. *J. Mater. Chem. A* **2015**, *3*, 17320–17331.

(210) Mulfort, K. L.; Farha, O. K.; Stern, C. L.; Sarjeant, A. A.; Hupp, J. T. Post-Synthesis Alkoxide Formation within Metal–Organic Framework Materials: A Strategy for Incorporating Highly Coordinatively Unsaturated Metal Ions. *J. Am. Chem. Soc.* **2009**, *131*, 3866–3868.

(211) Hanna, T. A.; Liu, L. H.; Angeles-Boza, A. M.; Kou, X. D.; Gutsche, C. D.; Ejsmont, K.; Watson, W. H.; Zakharov, L. N.; Incarvito, C. D.; Rheingold, A. L. Synthesis, Structures, and Conformational Characteristics of Calixarene Monoanions and Dianions. *J. Am. Chem. Soc.* **2003**, *125*, 6228–6238.

(212) Li, T.-T.; Sun, L.-B.; Liu, X.-Y.; Sun, Y.-H.; Song, X.-L.; Liu, X.-Q. Isolated Lithium Sites Supported on Mesoporous Silica: A Novel Solid Strong Base with High Catalytic Activity. *Chem. Commun.* **2012**, *48*, 6423–6425.

(213) Li, B. Y.; Zhang, Y. M.; Ma, D. X.; Li, L.; Li, G. H.; Li, G. D.; Shi, Z.; Feng, S. H. A Strategy Toward Constructing a Bifunctionalized MOF Catalyst: Post-Synthetic Modification of MOFs on Organic Ligands and Coordinatively Unsaturated Metal Sites. *Chem. Commun.* **2012**, *48*, 6151–6153.

(214) Li, B.; Ma, D.; Li, Y.; Zhang, Y.; Li, G.; Shi, Z.; Feng, S.; Zaworotko, M. J.; Ma, S. Dual Functionalized Cages in Metal–Organic Frameworks via Stepwise Postsynthetic Modification. *Chem. Mater.* **2016**, *28*, 4781–4786.

(215) Shiju, N. R.; Alberts, A. H.; Khalid, S.; Brown, D. R.; Rothenberg, G. Mesoporous Silica with Site-Isolated Amine and Phosphotungstic Acid Groups: A Solid Catalyst with Tunable Antagonistic Functions for One-Pot Tandem Reactions. *Angew. Chem., Int. Ed.* **2011**, *50*, 9615–9619.

(216) Hinde, C. S.; Webb, W. R.; Chew, B. K. J.; Tan, H. R.; Zhang, W.-H.; Hor, T. S. A.; Raja, R. Utilisation of Gold Nanoparticles on Amine-Functionalised UiO-66 (NH₂-UiO-66) Nanocrystals for Selective Tandem Catalytic Reactions. *Chem. Commun.* **2016**, *52*, 6557–6560.

(217) Zhang, Y.; Li, B.; Ma, S. Dual Functionalization of Porous Aromatic Frameworks as a New Platform for Heterogeneous Cascade Catalysis. *Chem. Commun.* **2014**, *50*, 8507–8510.

(218) Llabrés i Xamena, F. X.; Cirujano, F. G.; Corma, A. An Unexpected Bifunctional Acid Base Catalysis in IRMOF-3 for Knoevenagel Condensation Reactions. *Microporous Mesoporous Mater.* **2012**, *157*, 112–117.

(219) Tanabe, K. K.; Cohen, S. M. Postsynthetic Modification of Metal–Organic Frameworks—A Progress Report. *Chem. Soc. Rev.* **2011**, *40*, 498–519.

(220) Goto, Y.; Sato, H.; Shinkai, S.; Sada, K. Clickable” Metal–Organic Framework. *J. Am. Chem. Soc.* **2008**, *130*, 14354–14355.

(221) Wang, Z.; Cohen, S. M. Postsynthetic Modification of Metal–Organic Frameworks. *Chem. Soc. Rev.* **2009**, *38*, 1315–1329.

(222) Kumar, A.; Madden, D. G.; Lusi, M.; Chen, K.-J.; Daniels, E. A.; Curtin, T.; Perry, J. J.; Zaworotko, M. J. Direct Air Capture of CO₂ by Physisorbent Materials. *Angew. Chem., Int. Ed.* **2015**, *54*, 14372–14377.

(223) Zhou, Z.; Mei, L.; Ma, C.; Xu, F.; Xiao, J.; Xia, Q.; Li, Z. A Novel Bimetallic MIL-101(Cr, Mg) with High CO₂ Adsorption Capacity and CO₂/N₂ Selectivity. *Chem. Eng. Sci.* **2016**, *147*, 109–117.

(224) Liu, X.-Y.; Sun, L.-B.; Lu, F.; Li, T.-T.; Liu, X.-Q. Constructing mesoporous solid superbases by a dualcoating strategy. *J. Mater. Chem. A* **2013**, *1*, 1623–1631.

(225) Hill, I. M.; Hanspal, S.; Young, Z. D.; Davis, R. J. DRIFTS of Probe Molecules Adsorbed on Magnesia, Zirconia, and Hydroxyapatite Catalysts. *J. Phys. Chem. C* **2015**, *119*, 9186–9197.

(226) Vimont, A.; Travert, A.; Bazin, P.; Lavalley, J.-C.; Daturi, M.; Serre, C.; Férey, G.; Bourrelly, S.; Llewellyn, P. L. Evidence of CO₂

Molecule Acting as an Electron Acceptor on a Nanoporous Metal–Organic-Framework MIL-53 or Cr³⁺(OH)(O₂C-C₆H₄-CO₂). *Chem. Commun.* **2007**, 3291–3293.

(227) Teh, L. P.; Triwahyono, S.; Jalil, A. A.; Mukti, R. R.; Aziz, M. A. A.; Shishido, T. Mesoporous ZSM5 Having both Intrinsic Acidic And Basic Sites for Cracking and Methanation. *Chem. Eng. J.* **2015**, *270*, 196–204.

(228) Murphy, D.; Massiani, P.; Franck, R.; Barthomeuf, D. Basic Site Heterogeneity and Location in Alkali Cation Exchanged EMT Zeolite. An IR Study Using Adsorbed Pyrrole. *J. Phys. Chem.* **1996**, *100*, 6731–6738.

(229) Dietzel, P. D.; Besikiotis, V.; Blom, R. Application of Metal–Organic Frameworks with Coordinatively Unsaturated Metal Sites in Storage and Separation of Methane and Carbon Dioxide. *J. Mater. Chem.* **2009**, *19*, 7362–7370.

(230) Binet, C.; Jadi, A.; Lamotte, J.; Lavalley, J. Use of pyrrole as an IR spectroscopic molecular probe in a surface basicity study of metal oxides. *J. Chem. Soc., Faraday Trans.* **1996**, *92*, 123–129.

(231) Michalska, A.; Daturi, M.; Saussey, J.; Nowak, I.; Ziolk, M. The Role of MCM-41 Composition in the Creation of Basicity by Alkali Metal Impregnation. *Microporous Mesoporous Mater.* **2006**, *90*, 362–369.

(232) Moulin, B.; Salles, F.; Bourrelly, S.; Llewellyn, P. L.; Devic, T.; Horcajada, P.; Serre, C.; Clet, G.; Lavalley, J. C.; Daturi, M.; Maurin, G.; Vimont, A. Effect of the Ligand Functionalization on the Acid-Base Properties of Flexible MOFs. *Microporous Mesoporous Mater.* **2014**, *195*, 197–204.

(233) Devic, T.; Horcajada, P.; Serre, C.; Salles, F.; Maurin, G.; Moulin, B.; Heurtaux, D.; Clet, G.; Vimont, A.; Grenèche, J.-M.; Ouay, B. L.; Moreau, F.; Magnier, E.; Filinchuk, Y.; Marrot, J.; Lavalley, J.-C.; Daturi, M.; Férey, G. Functionalization in Flexible Porous Solids: Effects on the Pore Opening and the Host–Guest Interactions. *J. Am. Chem. Soc.* **2010**, *132*, 1127–1136.

(234) Sun, L. B.; Sun, Y. H.; Liu, X. D.; Zhu, L.; Liu, X. Q. Preparation of Mesoporous Solid Superbases by Using Metal Oxide Interlayers. *Curr. Org. Chem.* **2014**, *18*, 1296–1304.

(235) Li, T.-T.; Sun, L.-B.; Gong, L.; Liu, X.-Y.; Liu, X.-Q. In Situ Generation of Superbasic Sites on Mesoporous Ceria and their Application in Transesterification. *J. Mol. Catal. A: Chem.* **2012**, *352*, 38–44.

(236) Gong, L.; Sun, L.-B.; Sun, Y.-H.; Li, T.-T.; Liu, X.-Q. Exploring in Situ Functionalization Strategy in a Hard Template Process: Preparation of Sodium-Modified Mesoporous Tetragonal Zirconia with Superbasicity. *J. Phys. Chem. C* **2011**, *115*, 11633–11640.

(237) Nørskov, J. K.; Abild-Pedersen, F.; Studt, F.; Bligaard, T. Density Functional Theory in Surface Chemistry and Catalysis. *Proc. Natl. Acad. Sci. U. S. A.* **2011**, *108*, 937–943.

(238) Fang, H.; Kamakoti, P.; Zang, J.; Cundy, S.; Paur, C.; Ravikovitch, P. I.; Sholl, D. S. Prediction of CO₂ Adsorption Properties in Zeolites Using Force Fields Derived from Periodic Dispersion-Corrected DFT Calculations. *J. Phys. Chem. C* **2012**, *116*, 10692–10701.

(239) Xu, J.; Krüger, P.; Natoli, C. R.; Hayakawa, K.; Wu, Z.; Hatada, K. X-Ray Absorption Spectra of Graphene and Graphene Oxide by Full-Potential Multiple Scattering Calculations with Self-Consistent Charge Density. *Phys. Rev. B: Condens. Matter Mater. Phys.* **2015**, *92*, 125408.

(240) Ye, J.-y.; Liu, C.-j. Cu₃(BTC)₂: CO Oxidation over MOF Based Catalysts. *Chem. Commun.* **2011**, *47*, 2167–2169.

(241) Liu, D. H.; Zhong, C. L. Characterization of Lewis Acid Sites in Metal–Organic Frameworks Using Density Functional Theory. *J. Phys. Chem. Lett.* **2010**, *1*, 97–101.

(242) Kale, S. R.; Kahandal, S. S.; Burange, A. S.; Gawande, M. B.; Jayaram, R. V. A Benign Synthesis of 2-Amino-4H-Chromene in Aqueous Medium Using Hydrotalcite (HT) as a Heterogeneous Base Catalyst. *Catal. Sci. Technol.* **2013**, *3*, 2050–2056.

(243) Sun, L.-B.; Tian, W.-H.; Liu, X.-Q. Magnesia-Incorporated Mesoporous Alumina with Crystalline Frameworks: A Solid Strong

- Base Derived from Direct Synthesis. *J. Phys. Chem. C* **2009**, *113*, 19172–19178.
- (244) Sun, L. B.; Gu, F. N.; Chun, Y.; Kou, J. H.; Yang, J.; Wang, Y.; Zhu, J. H.; Zou, Z. G. Adjusting the Host-Guest Interaction to Promote KNO_3 Decomposition and Strong Basicity Generation on Zeolite NaY. *Microporous Mesoporous Mater.* **2008**, *116*, 498–503.
- (245) Liu, P.; Derchi, M.; Hensen, E. J. Promotional Effect of Transition Metal Doping on the Basicity and Activity of Calcined Hydroxalcite Catalysts for Glycerol Carbonate Synthesis. *Appl. Catal., B* **2014**, *144*, 135–143.
- (246) Parameswaram, G.; Srinivas, M.; Babu, B. H.; Prasad, P. S.; Lingaiah, N. Transesterification of Glycerol with Dimethyl Carbonate for the Synthesis of Glycerol Carbonate over Mg/Zr/Sr Mixed Oxide Base Catalysts. *Catal. Sci. Technol.* **2013**, *3*, 3242–3249.
- (247) Sun, Y.-H.; Sun, L.-B.; Li, T.-T.; Liu, X.-Q. Modulating the Host Nature by Coating Alumina: A Strategy to Promote Potassium Nitrate Decomposition and Superbasicity Generation on Mesoporous Silica SBA-15. *J. Phys. Chem. C* **2010**, *114*, 18988–18995.
- (248) Opanasenko, M.; Dhakshinamoorthy, A.; Shamzhy, M.; Nachtigall, P.; Horáček, M.; Garcia, H.; Čejka, J. Comparison of the Catalytic Activity of MOFs and Zeolites in Knoevenagel Condensation. *Catal. Sci. Technol.* **2013**, *3*, 500–507.
- (249) Opanasenko, M.; Dhakshinamoorthy, A.; Čejka, J.; Garcia, H. Deactivation Pathways of the Catalytic Activity of Metal–Organic Frameworks in Condensation Reactions. *ChemCatChem* **2013**, *5*, 1553–1561.
- (250) Dhakshinamoorthy, A.; Opanasenko, M.; Čejka, J.; Garcia, H. Metal Organic Frameworks as Heterogeneous Catalysts for the Production of Fine Chemicals. *Catal. Sci. Technol.* **2013**, *3*, 2509–2540.
- (251) Saravanamurugan, S.; Palanichamy, M.; Hartmann, M.; Murugesan, V. Knoevenagel Condensation over β and Y Zeolites in Liquid Phase under Solvent Free Conditions. *Appl. Catal., A* **2006**, *298*, 8–15.
- (252) Su, F.; Antonietti, M.; Wang, X. mpg- C_3N_4 as a Solid Base Catalyst for Knoevenagel Condensations and Transesterification Reactions. *Catal. Sci. Technol.* **2012**, *2*, 1005–1009.
- (253) Burgoyne, A. R.; Meijboom, R. Knoevenagel Condensation Reactions Catalysed by Metal–Organic Frameworks. *Catal. Lett.* **2013**, *143*, 563–571.
- (254) Hartmann, M.; Fischer, M. Amino-functionalized basic catalysts with MIL-101 structure. *Microporous Mesoporous Mater.* **2012**, *164*, 38–43.
- (255) Serra-Crespo, P.; Ramos-Fernandez, E. V.; Gascon, J.; Kapteijn, F. Synthesis and Characterization of an Amino Functionalized MIL-101(Al): Separation and Catalytic Properties. *Chem. Mater.* **2011**, *23*, 2565–2572.
- (256) Ernst, S.; Hartmann, M.; Sauerbeck, S.; Bongers, T. A Novel Family of Solid Basic Catalysts Obtained by Nitridation of Crystalline Microporous Aluminosilicates and Aluminophosphates. *Appl. Catal., A* **2000**, *200*, 117–123.
- (257) McKittrick, M. W.; Jones, C. W. Toward Single-Site Functional Materials-Preparation of Amine-Functionalized Surfaces Exhibiting Site-Isolated Behavior. *Chem. Mater.* **2003**, *15*, 1132–1139.
- (258) Rodriguez, I.; Sastre, G.; Corma, A.; Iborra, S. Catalytic Activity of Proton Sponge: Application to Knoevenagel Condensation Reactions. *J. Catal.* **1999**, *183*, 14–23.
- (259) Sakthivel, K.; Notz, W.; Bui, T.; Barbas, C. F. Amino Acid Catalyzed Direct Asymmetric Aldol Reactions: A Bioorganic Approach to Catalytic Asymmetric Carbon–Carbon Bond-Forming Reactions. *J. Am. Chem. Soc.* **2001**, *123*, S260–S267.
- (260) Nair, V.; Menon, R. S.; Biju, A. T.; Sinu, C.; Paul, R. R.; Jose, A.; Sreekumar, V. Employing Homoionolates Generated by NHC Catalysis in Carbon–Carbon Bond-Forming Reactions: State of the Art. *Chem. Soc. Rev.* **2011**, *40*, S336–S346.
- (261) Saha, D.; Maity, T.; Das, S.; Koner, S. A Magnesium-Based Multifunctional Metal–Organic Framework: Synthesis, Thermally Induced Structural Variation, Selective Gas Adsorption, Photoluminescence and Heterogeneous Catalytic Study. *Dalton Trans.* **2013**, *42*, 13912–13922.
- (262) Angelici, C.; Velthoen, M. E.; Weckhuysen, B. M.; Bruijninx, P. C. Influence of Acid–Base Properties on the Lebedev Ethanol-to-Butadiene Process Catalyzed by SiO_2 -MgO Materials. *Catal. Sci. Technol.* **2015**, *5*, 2869–2879.
- (263) Banon-Caballero, A.; Guillena, G.; Najera, C. Solvent-Free Enantioselective Organocatalyzed Aldol Reactions. *Mini-Rev. Org. Chem.* **2014**, *11*, 118–128.
- (264) Saha, D.; Sen, R.; Maity, T.; Koner, S. Porous Magnesium Carboxylate Framework: Synthesis, X-Ray Crystal Structure, Gas Adsorption Property and Heterogeneous Catalytic Aldol Condensation Reaction. *Dalton Trans.* **2012**, *41*, 7399–7408.
- (265) Choudary, B. M.; Chakrapani, L.; Ramani, T.; Kumar, K. V.; Kantam, M. L. Direct Asymmetric Aldol Reaction Catalyzed by Nanocrystalline Magnesium Oxide. *Tetrahedron* **2006**, *62*, 9571–9576.
- (266) Izquierdo, J.; Orue, A.; Scheidt, K. A. A Dual Lewis Base Activation Strategy for Enantioselective Carbene-Catalyzed Annulations. *J. Am. Chem. Soc.* **2013**, *135*, 10634–10637.
- (267) Li, Y.; Li, X.; Cheng, J. P. Catalytic Asymmetric Synthesis of Chiral Benzofuranones. *Adv. Synth. Catal.* **2014**, *356*, 1172–1198.
- (268) Mather, B. D.; Viswanathan, K.; Miller, K. M.; Long, T. E. Michael Addition Reactions in Macromolecular Design for Emerging Technologies. *Prog. Polym. Sci.* **2006**, *31*, 487–531.
- (269) Świderek, K.; Pabis, A.; Moliner, V. A Theoretical Study of Carbon–Carbon Bond Formation by a Michael-Type Addition. *Biomol. Chem.* **2012**, *10*, 5598–5605.
- (270) Kopylovich, M. N.; Mizar, A.; Guedes da Silva, M. F. C.; MacLeod, T. C.; Mahmudov, K. T.; Pombeiro, A. J. Template Syntheses of Copper (II) Complexes from Arylhydrazones of Malononitrile and their Catalytic Activity towards Alcohol Oxidations and the Nitroaldol Reaction: Hydrogen Bond-Assisted Ligand Liberation and E/Z Isomerisation. *Chem. - Eur. J.* **2013**, *19*, 588–600.
- (271) Jin, Y.; Yu, C.; Denman, R. J.; Zhang, W. Recent Advances in Dynamic Covalent Chemistry. *Chem. Soc. Rev.* **2013**, *42*, 6634–6654.
- (272) Shi, L.-X.; Wu, C.-D. A Nanoporous Metal–Organic Framework with Accessible Cu^{2+} Sites for the Catalytic Henry Reaction. *Chem. Commun.* **2011**, *47*, 2928–2930.
- (273) Corma, A. Inorganic Solid Acids and Their Use in Acid-Catalyzed Hydrocarbon Reactions. *Chem. Rev.* **1995**, *95*, 559–614.
- (274) Mizuno, N.; Misono, M. Heterogeneous Catalysis. *Chem. Rev.* **1998**, *98*, 199–218.
- (275) Capelot, M.; Unterlass, M. M.; Tournilhac, F.; Leibler, L. Catalytic Control of the Vitrimers Glass Transition. *ACS Macro Lett.* **2012**, *1*, 789–792.
- (276) Savonnet, M.; Aguado, S.; Ravon, U.; Bazer-Bachi, D.; Lecocq, V.; Bats, N.; Pinel, C.; Farrusseng, D. Solvent Free Base Catalysis and Transesterification over Basic Functionalised Metal–Organic Frameworks. *Green Chem.* **2009**, *11*, 1729–1732.
- (277) Zhou, F.; Lu, N.; Fan, B.; Wang, H.; Li, R. Zirconium-Containing UiO-66 as an Efficient and Reusable Catalyst for Transesterification of Triglyceride with Methanol. *J. Energy Chem.* **2016**, *25*, 874–879.
- (278) Saeedi, M.; Fazaeli, R.; Aliyan, H. Nanostructured Sodium–Zeolite Imidazolate Framework (ZIF-8) Doped with Potassium by Sol–Gel Processing for Biodiesel Production from Soybean Oil. *J. Sol-Gel Sci. Technol.* **2016**, *77*, 404–415.
- (279) Otera, J. Transesterification. *Chem. Rev.* **1993**, *93*, 1449–1470.
- (280) Savonnet, M.; Camarata, A.; Canivet, J.; Bazer-Bachi, D.; Bats, N.; Lecocq, V.; Pinel, C.; Farrusseng, D. Tailoring Metal–Organic Framework Catalysts by Click Chemistry. *Dalton Trans.* **2012**, *41*, 3945–3948.
- (281) Kou, J.; Sun, L.-B. Fabrication of Nitrogen-Doped Porous Carbons for Highly Efficient CO_2 Capture: Rational Choice of a Polymer Precursor. *J. Mater. Chem. A* **2016**, *4*, 17299–17307.
- (282) Kou, J.; Sun, L.-B. Nitrogen-Doped Porous Carbons Derived from Carbonization of a Nitrogen-Containing Polymer: Efficient Adsorbents for Selective CO_2 Capture. *Ind. Eng. Chem. Res.* **2016**, *55*, 10916–10925.

- (283) Geng, J.-C.; Xue, D.-M.; Liu, X.-Q.; Shi, Y.-Q.; Sun, L.-B. *N*-Doped Porous Carbons for CO₂ Capture: Rational Choice of *N*-Containing Polymer with High Phenyl Density as Precursor. *AIChE J.* **2017**, *63*, 1648–1658.
- (284) Li, X.-Y.; Zhang, D.-Y.; Liu, X.-Q.; Shi, L.-Y.; Sun, L.-B. A Tandem Demetalization–Desilication Strategy to Enhance the Porosity of Attapulgite for Adsorption and Catalysis. *Chem. Eng. Sci.* **2016**, *141*, 184–194.
- (285) Shi, Y.-L.; Zhang, P.; Liu, D.-H.; Zhou, P.-F.; Sun, L.-B. Homogenous Dual-Ligand Zinc Complex Catalysts for Chemical Fixation of CO₂ to Propylene Carbonate. *Catal. Lett.* **2015**, *145*, 1673–1682.
- (286) Miralda, C. M.; Macias, E. E.; Zhu, M.; Ratnasamy, P.; Carreon, M. A. Zeolitic Imidazole Framework-8 Catalysts in the Conversion of CO₂ to Chloropropene Carbonate. *ACS Catal.* **2012**, *2*, 180–183.
- (287) Ugale, B.; Dhankhar, S. S.; Nagaraja, C. M. Construction of 3-Fold-Interpenetrated Three-Dimensional Metal–Organic Frameworks of Nickel(II) for Highly Efficient Capture and Conversion of Carbon Dioxide. *Inorg. Chem.* **2016**, *55*, 9757–9766.
- (288) Beyzavi, M. H.; Klet, R. C.; Tussupbayev, S.; Borycz, J.; Vermeulen, N. A.; Cramer, C. J.; Stoddart, J. F.; Hupp, J. T.; Farha, O. K. A Hafnium-Based Metal–Organic Framework as an Efficient and Multifunctional Catalyst for Facile CO₂ Fixation and Regioselective and Enantioselective Epoxide Activation. *J. Am. Chem. Soc.* **2014**, *136*, 15861–15864.
- (289) Ema, T.; Miyazaki, Y.; Shimonishi, J.; Maeda, C.; Hasegawa, J.-y. Bifunctional Porphyrin Catalysts for the Synthesis of Cyclic Carbonates from Epoxides and CO₂: Structural Optimization and Mechanistic Study. *J. Am. Chem. Soc.* **2014**, *136*, 15270–15279.
- (290) Li, P.-Z.; Wang, X.-J.; Liu, J.; Lim, J. S.; Zou, R.; Zhao, Y. A Triazole-Containing Metal–Organic Framework as a Highly Effective and Substrate Size-Dependent Catalyst for CO₂ Conversion. *J. Am. Chem. Soc.* **2016**, *138*, 2142–2145.
- (291) He, H.; Perman, J. A.; Zhu, G.; Ma, S. Metal–Organic Frameworks for CO₂ Chemical Transformations. *Small* **2016**, *12*, 6309–6324.
- (292) Babu, R.; Roshan, R.; Kathalikkattil, A. C.; Kim, D. W.; Park, D.-W. Rapid, Microwave-Assisted Synthesis of Cubic, Three-Dimensional, Highly Porous MOF-205 for Room Temperature CO₂ Fixation via Cyclic Carbonate Synthesis. *ACS Appl. Mater. Interfaces* **2016**, *8*, 33723–33731.
- (293) De, D.; Pal, T. K.; Neogi, S.; Senthilkumar, S.; Das, D.; Gupta, S. S.; Bharadwaj, P. K. A Versatile CuII Metal–Organic Framework Exhibiting High Gas Storage Capacity with Selectivity for CO₂: Conversion of CO₂ to Cyclic Carbonate and Other Catalytic Abilities. *Chem. - Eur. J.* **2016**, *22*, 3387–3396.
- (294) Liu, L.; Zhang, J.; Fang, H.; Chen, L.; Su, C.-Y. Metal–Organic Gel Material Based on UiO-66-NH₂ Nanoparticles for Improved Adsorption and Conversion of Carbon Dioxide. *Chem. - Asian J.* **2016**, *11*, 2278–2283.
- (295) Zhang, G.; Wei, G.; Liu, Z.; Oliver, S. R. J.; Fei, H. A Robust Sulfonate-Based Metal–Organic Framework with Permanent Porosity for Efficient CO₂ Capture and Conversion. *Chem. Mater.* **2016**, *28*, 6276–6281.
- (296) Babu, R.; Kathalikkattil, A. C.; Roshan, R.; Tharun, J.; Kim, D.-W.; Park, D.-W. Dual-Porous Metal Organic Framework for Room Temperature CO₂ Fixation via Cyclic Carbonate Synthesis. *Green Chem.* **2016**, *18*, 232–242.
- (297) Han, Y.-H.; Zhou, Z.-Y.; Tian, C.-B.; Du, S.-W. A Dual-Walled Cage MOF as an Efficient Heterogeneous Catalyst for the Conversion of CO₂ Under Mild and co-Catalyst Free Conditions. *Green Chem.* **2016**, *18*, 4086–4091.
- (298) Ma, J.; Sun, N.; Zhang, X.; Zhao, N.; Xiao, F.; Wei, W.; Sun, Y. A Short Review of Catalysis for CO₂ Conversion. *Catal. Today* **2009**, *148*, 221–231.
- (299) Tu, M.; Davis, R. J. Cycloaddition of CO₂ to Epoxides over Solid Base Catalysts. *J. Catal.* **2001**, *199*, 85–91.
- (300) Paull, D. H.; Abraham, C. J.; Scerba, M. T.; Alden-Danforth, E.; Lectka, T. Bifunctional Asymmetric Catalysis: Cooperative Lewis Acid/Base Systems. *Acc. Chem. Res.* **2008**, *41*, 655–663.
- (301) Nicolaou, K.; Edmonds, D. J.; Bulger, P. G. Cascade Reactions in Total Synthesis. *Angew. Chem., Int. Ed.* **2006**, *45*, 7134–7186.
- (302) Allen, A. E.; MacMillan, D. W. Synergistic Catalysis: A Powerful Synthetic Strategy for New Reaction Development. *Chem. Sci.* **2012**, *3*, 633–658.
- (303) Huang, C.; Ding, R.; Song, C.; Lu, J.; Liu, L.; Han, X.; Wu, J.; Hou, H.; Fan, Y. Template-Induced Diverse Metal–Organic Materials as Catalysts for the Tandem Acylation–Nazarov Cyclization. *Chem. - Eur. J.* **2014**, *20*, 16156–16163.
- (304) Huang, Y.-B.; Shen, M.; Wang, X.; Shi, P.-C.; Li, H.; Cao, R. Hierarchically Micro- and Mesoporous Metal–Organic Framework-Supported Alloy Nanocrystals as Bifunctional Catalysts: Toward Cooperative Catalysis. *J. Catal.* **2015**, *330*, 452–457.
- (305) He, H.; Sun, F.; Aguila, B.; Perman, J. A.; Ma, S.; Zhu, G. A Bifunctional Metal–Organic Framework Featuring the Combination of Open Metal Sites and Lewis Basic Sites for Selective Gas Adsorption and Heterogeneous Cascade Catalysis. *J. Mater. Chem. A* **2016**, *4*, 15240–15246.
- (306) Sun, Q.; Aguila, B.; Ma, S. A Bifunctional Covalent Organic Framework as an Efficient Platform for Cascade Catalysis. *Mater. Chem. Front.* **2017**, DOI: 10.1039/C6QM00363J.
- (307) Dhakshinamoorthy, A.; Garcia, H. Cascade Reactions Catalyzed by Metal Organic Frameworks. *ChemSusChem* **2014**, *7*, 2392–2410.
- (308) Liu, H.; Xi, F.-G.; Sun, W.; Yang, N.-N.; Gao, E.-Q. Amino- and Sulfo-Bifunctionalized Metal–Organic Frameworks: One-Pot Tandem Catalysis and the Catalytic Sites. *Inorg. Chem.* **2016**, *55*, 5753–5755.
- (309) Yuan, B.; Yin, X.-Q.; Liu, X.-Q.; Li, X.-Y.; Sun, L.-B. Enhanced Hydrothermal Stability and Catalytic Performance of HKUST-1 by Incorporating Carboxyl-Functionalized Attapulgite. *ACS Appl. Mater. Interfaces* **2016**, *8*, 16457–16464.
- (310) Lu, L.; Li, X.-Y.; Liu, X.-Q.; Wang, Z.-M.; Sun, L.-B. Enhancing the Hydrostability and Catalytic Performance of Metal–Organic Frameworks by Hybridizing with Attapulgite, a Natural Clay. *J. Mater. Chem. A* **2015**, *3*, 6998–7005.
- (311) Kang, Y.-H.; Liu, X.-D.; Yan, N.; Jiang, Y.; Liu, X.-Q.; Sun, L.-B.; Li, J.-R. Fabrication of Isolated Metal–Organic Polyhedra in Confined Cavities: Adsorbents/Catalysts with Unusual Dispersity and Activity. *J. Am. Chem. Soc.* **2016**, *138*, 6099–6102.
- (312) Feng, D.; Chung, W.-C.; Wei, Z.; Gu, Z.-Y.; Jiang, H.-L.; Chen, Y.-P.; Darensbourg, D. J.; Zhou, H.-C. Construction of Ultrastable Porphyrin Zr Metal–Organic Frameworks through Linker Elimination. *J. Am. Chem. Soc.* **2013**, *135*, 17105–17110.
- (313) Feng, D.; Wang, K.; Su, J.; Liu, T.-F.; Park, J.; Wei, Z.; Bosch, M.; Yakovenko, A.; Zou, X.; Zhou, H.-C. A Highly Stable Zeotype Mesoporous Zirconium Metal–Organic Framework with Ultralarge Pores. *Angew. Chem., Int. Ed.* **2015**, *54*, 149–154.
- (314) Wang, B.; Lv, X.-L.; Feng, D.; Xie, L.-H.; Zhang, J.; Li, M.; Xie, Y.; Li, J.-R.; Zhou, H.-C. Highly Stable Zr(IV)-Based Metal–Organic Frameworks for the Detection and Removal of Antibiotics and Organic Explosives in Water. *J. Am. Chem. Soc.* **2016**, *138*, 6204–6216.
- (315) Cui, R.; Lin, Y.; Qian, J.; Zhu, Y.; Xu, N.; Chen, F.; Liu, C.; Wu, Z.; Chen, Z.; Zhou, X. Two-Dimensional Porous SiO₂ Nanostructures Derived from Renewable Petal Cells with Enhanced Adsorption Efficiency for Removal of Hazardous Dye. *ACS Sustainable Chem. Eng.* **2017**, *5*, 3478–3487.
- (316) Wu, Z.; Lu, Q.; Fu, W. H.; Wang, S.; Liu, C.; Xu, N.; Wang, D.; Wang, Y. M.; Chen, Z. Fabrication of Mesoporous Al-SBA-15 as a Methylene Blue Capturer via a Spontaneous Infiltration Route. *New J. Chem.* **2015**, *39*, 985–993.
- (317) Kang, Y.-H.; Yan, N.; Gao, Z.-Y.; Tan, P.; Jiang, Y.; Liu, X.-Q.; Sun, L.-B. Controllable Construction of Metal–Organic Polyhedra in Confined Cavities via In Situ Site-Induced Assembly. *J. Mater. Chem. A* **2017**, *5*, 5278–5282.

(318) Editorial. Frameworks for Commercial Success. *Nat. Chem.* **2016**, *8*, 987–987.

(319) Furukawa, H.; Müller, U.; Yaghi, O. M. Heterogeneity within Order” in Metal–Organic Frameworks. *Angew. Chem., Int. Ed.* **2015**, *54*, 3417–3430.